THESIS

ADVANCED CONTROL TECHNIQUES AND SENSORS FOR GAS ENGINES WITH NSCR

Submitted by

John Gattoni

Department of Mechanical Engineering

In partial fulfillment of the requirements

For the Degree of Master of Science

Colorado State University

Fort Collins, Colorado

Spring 2012

Master's Committee:

Advisor: Daniel Olsen

Anthony Marchese
Peter Young

ABSTRACT

ADVANCED CONTROL TECHNIQUES AND SENSORS FOR GAS ENGINES WITH NSCR

High exhaust emissions reduction efficiency from an Internal Combustion Engine (ICE) utilizing a Non Selective Catalyst Reduction (NSCR) catalyst system requires complex fuel control strategies. The allowable equivalence ratio operating range is very narrow where NSCR systems achieve simultaneous reduction of Carbon Monoxide (CO), Nitrogen Oxides (NOx), Total Hydrocarbons (THC), Volatile Organic Compounds (VOC's), and formaldehyde (CH_2O). This range is difficult to maintain as transients are introduced into the system. Current fuel control technologies utilizing lambda sensor feedback are reported to be unable to sustain these demands for extended operation periods. Lambda sensor accuracy is the critical issue with current fuel controllers.

The goal of this project was to develop a minimization control algorithm utilizing a Continental NOx sensor installed downstream of the NSCR catalyst system for feedback air/fuel ratio control. When the engine is operated under lean conditions, NOx is produced in the engine out exhaust emissions and the NOx sensor responds accordingly. When the engine is operated under rich burn conditions, the NSCR catalyst system produces Ammonia (NH_3). NOx sensors have a cross sensitivity to NH_3 and will respond as though it has been exposed to NOx. This behavior provides a unique control strategy that allows lambda sensor calibration to be ignored. Testing was performed on a Cummins-Onan Generator Set, model GGHD 60HZ, capable of a power output of 100kW at standard ambient air conditions. The engine was

reconfigured to operate utilizing an electronic gas carburetor (EGC2) with lambda sensor feedback, manufactured by Continental Controls Corporation (CCC) and a high reduction efficiency NSCR catalyst system manufactured by DCL International. A Data Acquisition (DAQ) system manufactured by National Instruments (NI) acquired the NOx sensor output. The control algorithm was programmed utilizing a LabVIEW interface and a feed forward command was executed through the NI DAQ system to the CCC EGC2 where the fuel trim adjustment was physically made.

Exhaust gas species measurements were acquired via a Rosemount 5-gas analyzer and a Nicolet 6700 FTIR. Fuel composition was acquired utilizing a Varian CP-4900 Micro GC and Air Fuel Ratio (AFR) was obtained with an ECM AFRecorder 4800R. Results utilizing NOx sensor feedback control revealed that under steady state operating conditions, improvements in emissions reduction efficiency of CO, NOx, and THC were significant. The system was also evaluated during load and fuel composition transients.

ACKNOWLEDGEMENTS

Many people were involved throughout the project by providing guidance, technical support and help with various portions of the developmental process. First and foremost, I would like to send many thanks to my advisor Dr. Daniel Olsen who I immediately worked with on a regular basis to achieve all tasks of the project. His expertise and patience was of great value and a wealth of knowledge was passed onto me, aiding towards the successful completion within the desired time period. Additional thanks to Dr. Anthony Marchese and Dr. Peter Young for serving on the thesis committee for this project.

Kirk Evans, Engineering Manager at the Engines and Energy Conversion Lab (EECL) performed the LabVIEW programming for the NOx sensor control algorithm and exhaust emissions measurements. He also provided technical support as needed throughout the project during all phases. Research Engineer at the EECL Cory Kreutzer was available for technical support and control room assistance. Research Engineer Philip Bacon provided guidance during the engine reconfiguration process. Post graduate student Christian L-Orange was indispensable as he provided guidance in many areas including instrumentation selection, control room operations, and thesis writing advice. Undergraduate student Cory Degroot provided additional engine emissions testing support. Undergraduate students Benjamin Neuner and Darryl Beemer aided with the installation of the catalyst assembly and tap water plumbing for the intercooler setup, respectively.

The main funding source for the project was the California Energy Commission (CEC) with additional funding from Pipeline Research Counsil International (PRCI). Donations in kind

for the EGC2 electronic fuel control system and required hardware, and the NSCR catalyst system were provided from Continental Controls Corporation (CCC) and DCL International, respectively. Additional technical assistance was provided from Continental Controls Corporation. Vice President Rick Fisher and Electrical Engineer Hillary Grimes were nice enough to fly out to the EECL to personally see through the installation of the CCC EGC2 electronic carburetor. Hillary performed a large portion of the wiring required for their hardware to operate correctly. He was also very patient and enthusiastic to answer all technical questions we had throughout the project. Joe Aleixo from DCL International provided technical assistance in regards to the NSCR catalyst assembly.

TABLE OF CONTENTS

LIST OF FIGURES

LIST OF TABLES

LIST OF ABBREVIATIONS

AFR – Air Fuel Ratio

BSE – Brake Specific Emissions

BHP – Brake Horsepower

CCC – Continental Controls Corporation

CH_2O – Formaldehyde

CI – Compression Ignition

CM – Chemiluminescence Method

CO – Carbon Monoxide

CO_2 – Carbon Dioxide

DAQ – Data Acquisition

DG – Distributed Generation

ECU – Electronic Control Unit

ECM – Engine Controls and Monitoring

EECL – Engines and Energy Conversion Laboratory

EGC – Electronic Gas Carburetor

FID – Flame Ionization Detection

GUI – Graphical User Interface

H_2O – Water

HAP – Hazardous Air Pollutant

ICE – Internal Combustion Engine

IR – Infrared Radiation

MAP – Manifold Absolute Pressure

NESHAP – National Emissions Standards for Hazardous Air Pollutants

NH_3 – Ammonia

NI – National Instruments

NO – Nitric Oxide

NO_2 – Nitrogen Dioxide

NOx – Nitric Oxides

NSCR – Non Selective Catalyst Reduction

NSPS – New Source Performance Standards

O_2 – Oxygen

O_3 – Ozone

PID – Proportional Integral Derivative

SEGO – Simulated Exhaust Gas Oxygen

SI – Spark Ignition

SOx – Sulfuric Oxides

STP – Standard Temperature and Pressure

THC – Total Hydrocarbons

VOC – Volatile Organic Compound

VRSS – Variable Reluctor Speed Sensor

YSZ – Yttria Stabilized Zirconia

ZrO_2 – Zirconium Dioxide

1. Introduction

1.1 Motivation for Research

Stationary reciprocating Internal Combustion Engines (ICE's) are used in a variety of applications including electrical power generation, gas compression, and liquid pumping. These systems require regular system calibration in order to meet exhaust emissions regulations. In order to accomplish this, expensive mobile exhaust emissions testing equipment must be transported to the site and setup. The engine is run and the fuel delivery system is adjusted until an optimum equivalence ratio (Φ) is achieved, minimizing exhaust emissions for the given application. Non Selective Catalyst Reduction (NSCR) catalyst systems are employed on stoichiometric, stationary ICE's. These systems are most effective in stoichiometric Spark Ignited (SI) engines. When controlled properly they simultaneously reduce Nitric Oxides (NOx), Carbon Monoxide (CO), Total Hydrocarbons (THC), Volatile Organic Compounds (VOC's), and formaldehyde (CH_2O) (DCL International 2009).

Proper NSCR catalyst system functionality requires that the equivalence ratio (Φ) be precisely controlled within a narrow range near stoichiometric conditions (Amadu and Olsen 2008). As emissions regulations are lowered, fuel control technologies must evolve accordingly. Long term stability of air/fuel ratio (AFR) control systems to maintain the required equivalence ratio range has not been established for stationary ICE's. Two aspects that make long term stability difficult are requirements for continuous operation and variable fuel quality. Many

control systems utilize lambda sensor feedback for equivalence ratio control; however, research suggests that the lambda sensor calibration drifts, leading to a shift outside of the narrow control range (Nuss-Warren and Hohn 2011). The use of additional instrumentation for feedback fuel control such as a NOx sensor has been investigated (Vronay et al. 2010), leading to the evolution of this project.

1.2 Spark-Ignition Natural Gas Exhaust Emissions

Natural gas, which is primarily composed of methane (CH_4), is considered one of the most promising alternative fuels to meet strict engine emission regulations in many countries. Natural gas has relatively wide flammability limits, allowing natural gas engines to be operated in a large range of lean, stoichiometric, and rich burn conditions. The operating equivalence ratio and exhaust after treatment system employed generally characterizes the engine exhaust emissions (Cho and He 2007). The main engine out exhaust pollutants are NOx, CO, and VOC's. Other pollutants, such as Sulfuric Oxides and Particulate Matter (PM) are not a concern for SI natural gas engines. The sulfur content of the fuel dictates emissions of sulfur compounds and is predominantly in the form of SO_2. PM is emitted mainly in compression Ignition (CI) engines using liquid fuels (Energy and Environmental Analysis 2008).

NOx emissions are primarily composed of Nitric Oxide (NO) and Nitrogen Dioxide (NO_2). NOx is typically reported either as parts per million (ppm), as a mass flow rate (lbs/hr), or in reference to engine power (g/bhp-hr or g/bkW-hr). NOx levels vary based on equivalence ratio and combustion temperature, which are related to each other. The lowest engine out NOx emissions in SI natural gas engines occur when operating under extreme lean burn conditions

($\Phi < 1$), close to the flammability limit, due to the low combustion chamber temperatures (Korakianitis 2009). The tradeoff is an increase in engine out CO and THC emissions due to slower flame initiation and propagation at extreme lean burn conditions (Cho and He 2007).

High CO and THC engine out exhaust emissions are produced under rich burn conditions ($\Phi > 1$) due to insufficient oxygen to fully oxidize the fuel. Exhaust residence time, reaction quenching in the exhaust process, and cooling at the combustion chamber walls also contribute to incomplete combustion and increased CO and THC concentration (Energy and Environmental Analysis 2008), (Cho and He 2007). At the same equivalence ratio, natural gas SI engines can produce CO_2 levels lower than that of diesel engines. Natural gas can also produce more than 20% lower CO_2 levels than gasoline engines at equal power due to basic stoichiometry (Korakianitis 2009). The typical trends of NOx, THC, and CO with respect to equivalence ratio are displayed in Figure 1-1. This is based on a SI engine running standard gasoline fuel, however, the trends are very similar for natural gas.

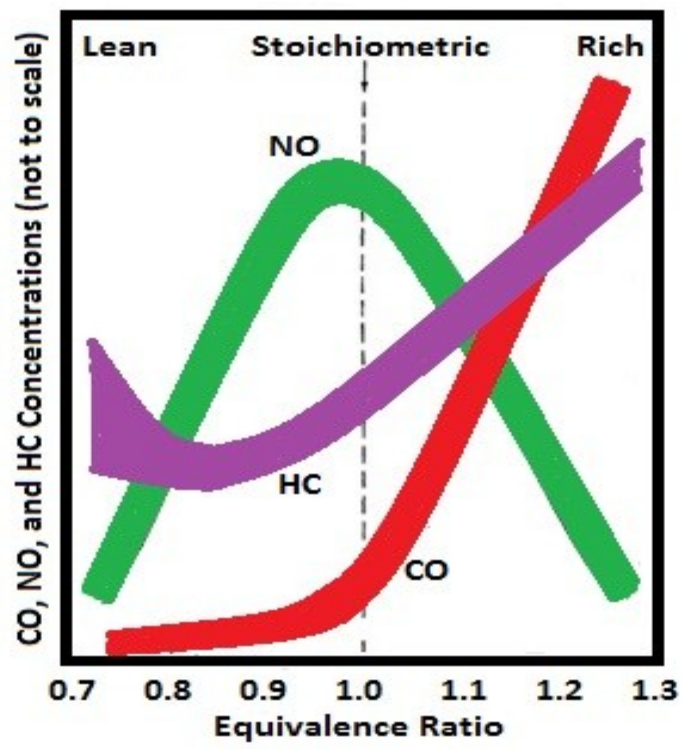

Figure 1-1: Typical NOx, HC, and CO trends with respect to equivalence ratio in a gasoline SI engine (Heywood 1998)

1.3 Spark-Ignition Natural Gas Emissions Regulations

Air quality has been a concern in the US for over 50 years. Emissions standards for automobiles were introduced initially in California and then nationwide in the United States shortly after, starting in the early 1960s (Heywood 1998). Growing concern with internal combustion engine exhaust emissions has resulted in the implementation of strict emission regulations in many automotive and industrial fields in the United States and Europe. There are separate emissions regulations corresponding to engine type and size, application and fuel being used. National Emission Standards for Hazardous Air Pollutants (NESHAP) for Reciprocating Internal Combustion Engines (RICE's) are described by the Environmental

Protection Agency (EPA). Docket ID No. EPA-HQ-OAR-2008-0708, FRL-9277-3 details the new RICE emissions requirements for Hazardous Air Pollutants (HAP's) set forth on March 9th, 2011 (US EPA 2011). New Source Performance Standards (NSPS) describes the national emissions standards for stationary SI ICE's with regards to NOx, CO, and VOC's. Docket ID No. EPA–HQ–OAR–2005–0030, FRL-8512-4 details the emissions standards which were made effective as of March 18th, 2008 (US EPA 2011).

The California Air Resources Board (CARB) also imposes their own set of emissions standards for various ICE platforms in the state of California. In particular, the CARB 2007 distributed generation (DG) certification program requires manufacturers of electrical generation technologies to meet specific emission standards before they can be sold in California starting on or after January 1, 2007. Any DG unit subject to this regulation burning a fossil fuel source must be certified pursuant to section 94204 to the following set of standards shown in Table 1-1 (CEPA ARB 2007).

Table 1-1: CARB 2007 Fossil Fuel Emission Standards

Pollutant Emission Standard	(lb/MW-hr)	g/bhp-hr	g/kW-hr
NOx	0.07	0.024	0.032
CO	0.1	0.034	0.045
VOC's	0.02	0.007	0.009

1.4 Response to Emissions Regulations

The emissions signature of natural gas SI engines has improved significantly over the last 10 years by improved design and control of the combustion process and advancements in catalyst systems. Controlling the fuel delivery to a specified equivalence ratio is the best

approach to tailoring the engine out exhaust emissions; however, there are tradeoffs to each approach. The 1st approach is to adjust to extreme lean burn conditions to achieve the lowest NOx concentration, with the possibility of increased CO and THC emissions. The 2nd approach is to find an optimal balance between emissions and efficiency. The 3rd approach is to design for the highest efficiency and use an exhaust after treatment system. The 3rd approach is widely accepted as the most effective way of reducing exhaust emissions without sacrificing thermal efficiency (Energy and Environmental Analysis 2008).

The exhaust after treatment system is typically coupled to the application based on if the engine operates under lean burn or stoichiometric burn. In order to meet extremely low emissions regulations, like CARB 2007, with lean burn engines, a rather complex NOx reduction after treatment system is required, such as a Selective Catalyst Reduction (SCR) method or a NOx trap system (Energy and Environmental Analysis 2008). Lean burn operating limits are dependent on ignition timing and energy, combustion chamber geometry, and turbulence. The addition of an Exhaust Gas Recirculation (EGR) system not only reduces combustion temperatures leading to a decrease in NOx concentration, but results in better fuel economy at stoichiometric SI operating conditions.

Stoichiometric SI natural gas engines equipped with a NSCR catalyst can meet future emissions demands, but requires very precise AFR control strategies and highly efficient catalyst systems. A heated O_2 sensor is used as feedback to maintain precise AFR control, promoting high NSCR catalyst activity, ultimately leading to high emissions reduction of NOx, CO, and VOC's (Korakianitis 2009).

2. Literature Review

2.1 Current Fuel Control Techniques

Many forms of fuel delivery control exist and commonly are characterized as mechanical or electronic. Fuel delivery techniques, both mechanical and electronic, using carburetors and injectors are found on all types of engines including, SI, CI, 2-stroke, lean burn, rich burn, and stoichiometric burn engines. Mechanical carburetors and fuel injectors are installed on all of the above mentioned platforms of nearly any engine displacement, for various fuel types, and in both automotive and industrial applications. Both mechanical fuel delivery devices are incorporated onto engines as a single component, providing fuel to all cylinders by distributing the air/fuel mixture accordingly through an intake manifold. Furthermore, a carburetor or injector can be placed at the intake runner of each cylinder to provide individual fuel delivery.

Small scale (<100 kW) Stationary natural gas SI internal combustion engines typically utilize a simplistic mechanical carburetor fuel delivery system. The fuel is quantified using a venturi that air passes through, creating a vacuum and drawing the fuel into the air stream. There is no feedback control but rather the air/fuel is manually adjusted via a needle jet screw located on the carburetor. As fuel composition and ambient air conditions change, exhaust emissions output will change and many times emissions compliance can no longer be met. This becomes especially apparent with NSCR catalyst systems that require stoichiometric operation. Passive, mechanical systems are incapable of controlling AFR in the narrow range required for

NSCR operation. Electronic carburetors with lambda feedback, such as the Continental Controls Corporation (CCC) Electronic Gas Carburetor (EGC) 2 incorporate a pre catalyst lambda sensor for feedback control (Continental Controls Corporation 2008). These systems will often operate at stoichiometric burn conditions, unless the system has the support for the user to designate the air/fuel ratio. The application operating AFR is typically coupled with the type of exhaust after treatment that will be used.

The lambda sensor, originally invented in 1976 by Bosch, has revolutionized the way in which fuel delivery is controlled. All automobiles today utilize at least 1, if not 2 lambda sensors and are coupled with a NSCR system. It provides feedback to the electronic control unit (ECU) based on the O_2% contained in the exhaust gas, which then determines the amount of fuel to be delivered to the engine to maintain an air/fuel ratio as close to stoichiometric burn as possible (Bosch 2006). Automotive systems with an ECU and lambda feedback are equipped with electronic fuel delivery systems either using a distributed fuel injector on an intake manifold (throttle body injection) or fuel injectors at each cylinder head intake port (tuned port injection).

Recent developments in direct injection SI gasoline engines use a NOx sensor as feedback fuel control in lean burn engines. A NOx storage catalyst system is employed to adsorb the high levels of NOx produced when the engine is operated lean. Once the catalyst is saturated, the NOx sensor, installed downstream of the catalyst, communicates to the ECU. The ECU then operates the engine at a rich condition for approximately 2 seconds, effectively reducing NOx into harmless N_2 (NGK 2012).

2.2 Exhaust Gas Treatment

Many forms of exhaust gas after treatment exist for applications of spark ignition (SI) engines, compression ignition (CI) engines, and various fuels. This includes oxidation catalysts, SCR systems, NSCR systems, thermal reactors, EGR systems, and particulate and NOx traps. All catalyst systems are designed to operate in a specified temperature range and are ineffective until temperature has risen above a designated value. The term "light-off temperature" is used to describe this minimum temperature where the catalyst operates at a reduction efficiency of 50% or greater. An example of a typical light-off curve for a NSCR catalyst is shown in Figure 2-1.

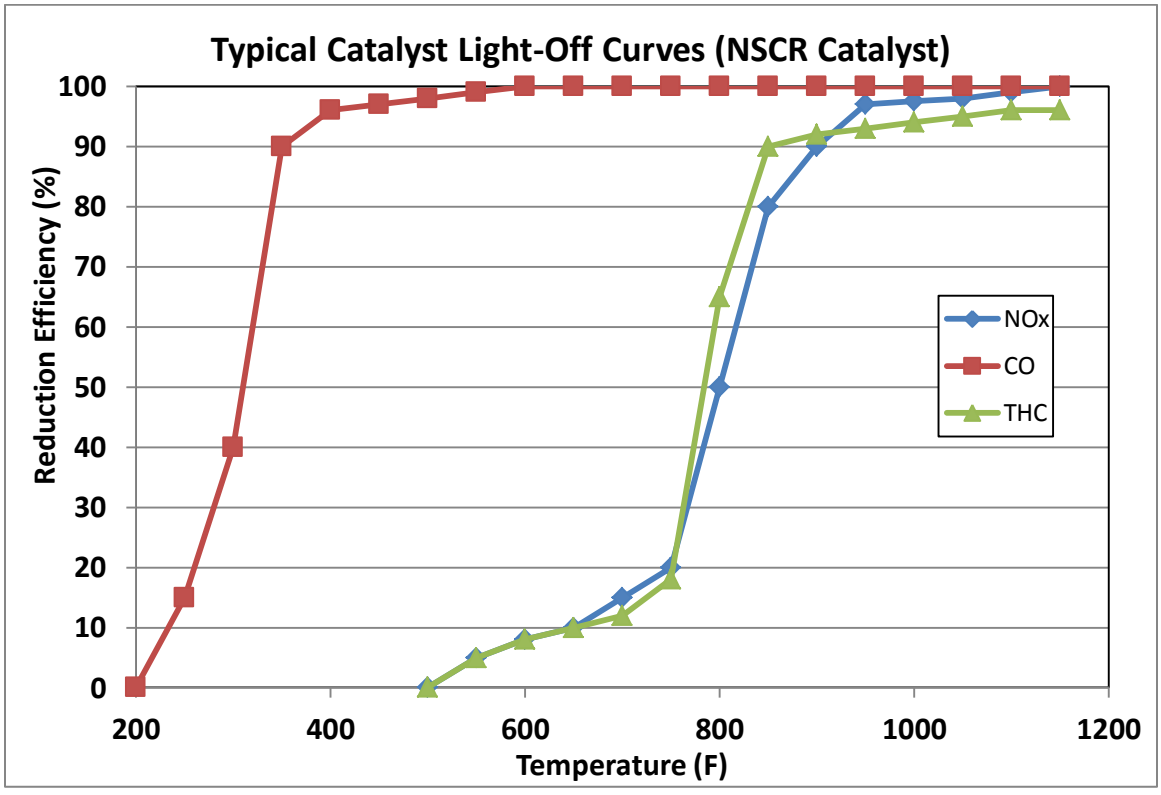

Figure 2-1: Typical NSCR catalyst light off curves (Johnson Matthey Catalysts)

Catalyst reduction efficiency is determined by equation 2.1 below, where $\dot{m}_{i,IN}$ represents the mass flow of a given species measured prior to entering the catalyst and $\dot{m}_{i,OUT}$ is the mass flow of a given species exiting the catalyst. Table 2-1 describes exhaust after treatment systems.

$$\eta_{CAT} = 1 - \frac{\dot{m}_{i,OUT}}{\dot{m}_{i,IN}} \qquad (2.1)$$

Table 2-1: Major components in regards to construction and functionality of exhaust gas treatment systems (BASF Corporation), (DCL International 2009), (Heywood 1998), (Navarro 2008), (Pulkrabek 2004), (Schmitt 2010)

Oxidation Catalyst	• Oxidizes THC and CO into CO_2 and H_2O • O_2 introduced by lean burn or stoichiometric operation • Air pump can be used to provide additional O_2 • Catalyst bed constructed of noble metals (Platinum and palladium)
SCR	• Involves injection of reagent (urea, NH_3) in the exhaust upstream of the catalyst • Reduces NOx into chemically benign diatomic nitrogen and water • Designed to operate in CI and lean burn SI engines
NSCR	• Simultaneously reduces NOx and oxidizes THC and CO • Narrow range of air/fuel ratios near stoichiometric required for high reduction efficiency (~0.1 air/fuel ratios) • Close loop control via an O_2 sensor is required • Cyclic variation (~1 Hz) of fuel flow (dithering) widens this range • Rich operating conditions produces NH_3 across catalyst • Catalyst bed constructed of Rhodium (Rh) and Platinum (Pt)
Thermal Reactors	• Oxidizes CO and THC, typically in an enlarged exhaust manifold • Designed to operate with rich burn engines and air injection • Effectiveness depends on temperature, available oxygen and residence time
EGR	• Designed to primarily reduce NOx emissions • Recirculates exhaust gases back into the intake manifold • Effectively reduces maximum combustion temperature
NOx Traps	• Designed to reduce NOx on lean burn SI and CI engines • System contains oxidation catalyst (Pt), adsorbent (Barium), and reduction catalyst (Rh) • NO is oxidized to NO2, adsorbs onto Barium surface, then engine is operated at rich condition, reducing NOx
Particulate Traps	• Designed to reduce particulate emissions in CI engine systems • Filter like systems made of ceramic in a mat or mesh structure • Traps typically remove 60-90% of particulates in exhaust stream • Requires oxidation regeneration periodically

Currently for stationary reciprocating SI stoichiometric natural gas engines, NSCR catalytic converters are the primary focus for exhaust after treatment. They are designed to simultaneously reduce NOx, CO, and THC concentrations while also having an impact on the reduction of VOC's and HAP's. These systems are only used in SI internal combustion engines and not CI, two-stroke, or other lean burn engines because the catalyst is required to operate at stoichiometric air/fuel ratios. Table 2-2 describes the dominant chemical reactions that occur within a NSCR catalyst including the 2 major reactions that occur within a NSCR catalyst that produce NH_3.

Table 2-2: Main chemical kinetic reactions that occur across a 3-way catalyst (DCL International 2009)

Oxidation reactions with O_2:
$CO + ½\ O_2 \rightarrow CO_2$
$HC + ½\ O_2 \rightarrow CO_2 + H_2O$
$HC + ½\ O_2 \rightarrow CO + H_2O$
$H_2 + ½\ O_2 \rightarrow H_2O$
Oxidation/reduction reactions with NO:
$CO + NO \rightarrow ½\ N_2 + CO_2$
$HC + NO \rightarrow N_2 + H_2O + CO_2$
$HC + NO \rightarrow N_2 + H_2O + CO$
$H_2 + NO \rightarrow ½\ N_2 + H_2O$
$H_2 + 2\ NO \rightarrow N_2O + H_2O$
$5/2\ H_2 + NO \rightarrow NH_3 + H_2O$
$2\ NO + 2\ NH_3 + ½\ O_2 \rightarrow 2N_2 + 3\ H_2O$
Water-gas shift reaction:
$CO + H_2O \rightarrow CO_2 + H_2$
Reforming reactions:
$HC + H_2O \rightarrow CO_2 + H_2$
$HC + H_2O \rightarrow CO + H_2$

2.3 NOx Sensor Construction and Operation

NOx sensor technology dates back to the late 1980's, with the initial designs being constructed from various forms of ceramic type metal oxides including yttria stabilized zirconia (YSZ). Material selection was adopted from lambda sensor technology which had been developed previous to the NOx sensor. Improved models such as the dual chamber Zirconium Dioxide (ZrO_2) have been developed and continue to be an area of active engineering research. Requirements of a robust NOx sensor include a wide operating temperature range, sensitivity, accuracy, lifetime, and appropriate material selection to avoid degradation by gases such as CO_2 and SO_2 (Woo 2010).

The ZrO_2 dual cavity NOx sensor operates in the following sequence: (a) Exhaust gases including NOx, HC, CO, O2, H2, etc. enter the 1st cavity of the sensor, (b) O2 concentration is maintained to a constant concentration within a few ppm of NOx via the main O2 pumping cell and the rest are oxidized at the Pt pumping electrode, (c) The new concentrated gas of NOx and O2 enter the 2nd cavity of the sensor, (d) The auxiliary pump completely removes gaseous O2 in the 2nd cavity, (e) At the measuring electrode, the equilibrium of $2NO \leftrightarrow N2 + O2$ is changed by removing the generated oxygen from the reduction of NO, (f) The measuring pump extracts and measures this generated oxygen , which represents the NOx concentration of the exhaust gas. The zirconia electrolyte acquires an amperometric measurement. An ECU is required to provide power control in order to heat and maintain the temperature of the sensor (Continental 2008), (Inagaki et al. 1998). Figure 2-2 displays the operation and construction of a ZrO_2 NOx sensor.

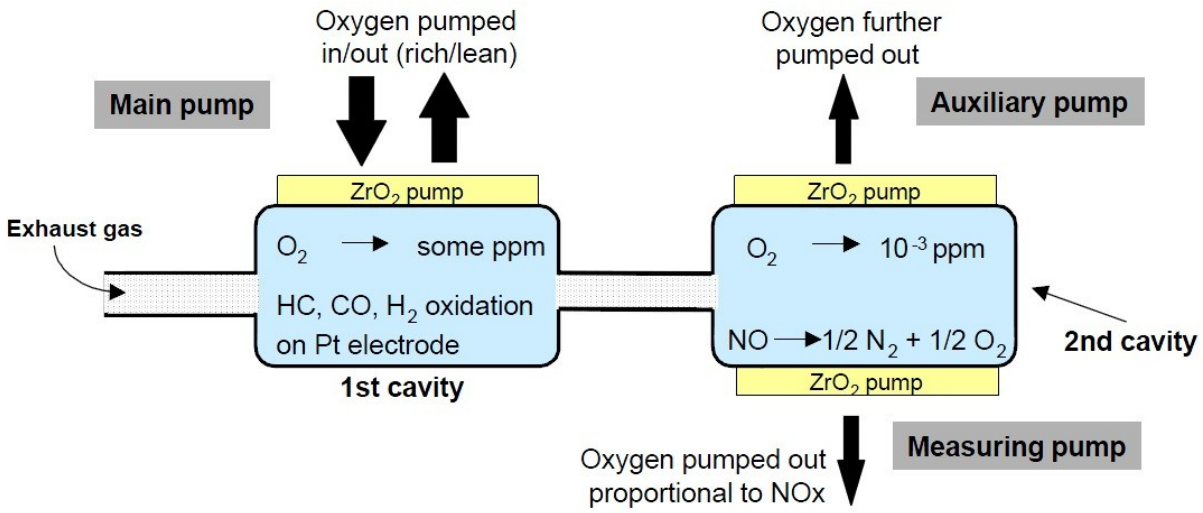

Figure 2-2: ZrO2 NOx sensor construction and operation (Continental 2008)

There are multiple uses for implementing a NOx sensor into a combustion system such as an ICE. These range from monitoring NOx levels to feedback control. NOx sensors have a cross sensitivity to NH3, which is produced across a NSCR catalyst when the ICE is operated in a rich condition ($\phi \geq 1$). SCR systems on both spark ignition and compression ignition engines often are coupled with NOx sensor feedback to control the injection concentration of chemicals such as urea and NH3 (Schmitt 2010), (Marquis 2001). With a NSCR system, engine out emissions do not include NH3, rather it is produced across the catalyst (Vronay et al. 2010). NOx sensors are primarily designed to be utilized in stoichiometric or lean burn engines ($\phi \leq 1$) where NOx is prevalent. To make gasoline engines more environmentally friendly and consume less fuel, manufacturers are focusing on direct injection engines that operate at lean conditions when run at partial load. The result is a decrease of fuel consumption by 12-20%; however, it requires a NOx storage catalytic converter and a NOx sensor (NGK 2012).

2.4 Minimization Control Algorithms

Techniques to drive a feedback signal to a minimum are available in many forms and complexities. The most basic form is to acquire 2 consecutive samples of data, evaluate if the 2nd sample has decreased or increased, and then make a feed forward command to drive it in the same or opposite direction, respectively. Slightly more advanced algorithms would include the Golden Section Algorithm and the Brent Minimization Algorithm.

The Golden Section Algorithm is a search method used for unimodial concave or convex curves when trying to find a minimum or maximum point. An interval of uncertainty is designated between 2 points (A, B) with length B-A. Two points, (X_1, X_2) are chosen between this interval and the function is evaluated for $f(X_1)$ and $f(X_2)$. For determining a minimum point, whichever evaluated point is higher in magnitude, becomes the upper bound. For example if $f(X_1) > f(X_2)$ as shown in Figure 2-3, the function is decreasing in the range of [X_1, X_2], therefore the minimum cannot be greater than X_1 and $f(X_1)$ and the new interval now becomes (X_1, B] (Cheney and Kincaid 1994), (Gerald and Wheatley 2004).

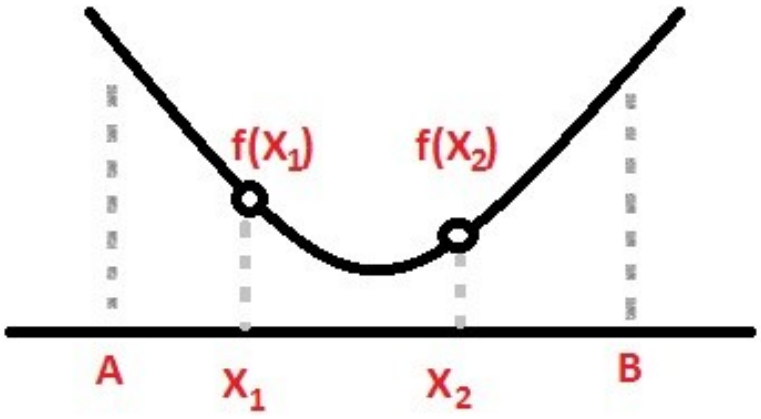

Figure 2-3: Golden section algorithm example

The values of X_1 and X_2 are chosen such that each point divides the interval of uncertainty [A, B] into 2 separate fractions where:

$$\frac{Length\ of\ Whole\ Line}{Length\ of\ Larger\ Fraction} = \frac{Length\ of\ Larger\ Fraction}{Length\ of\ Smaller\ Fraction}$$

$$\frac{B-A}{F} = \frac{F}{(B-A)-F} \tag{2.2}$$

The length of the larger fraction (F) is solved for by taking the positive root of the quadratic. To solve for X_1 and X_2, the fraction multiplied by the initial interval of uncertainty is subtracted from the opposite end of the interval:

$$X_1 = B - F*(B-A) \tag{2.3}$$

$$X_2 = A + F*(B-A) \tag{2.4}$$

By dividing the line segment up in this manner, the interval of uncertainty is updated every iteration and one of the previous test points can be used in the following iteration. It is not referred to as the most efficient search method, but can work well with complicated unimodal curves and can be modified to compliment other types of functions (Cheney and Kincaid 1994), (Gerald and Wheatley 2004).

The Brent Minimization Algorithm combines the Golden Section Algorithm with a parabolic interpolation producing a faster algorithm that still remains robust and improves convergence. When iterations are performed, the Brent Minimization Algorithm approximates a function by interpolating a parabola through 3 existing points acquired on the curve. The

parabolas minimum point is used as the estimate for the minimum point of the function. If this point is within the range of the current interval, then it is accepted and used to generate a smaller interval of uncertainty. If the point is not within the range, then the algorithm reverts back to the standard Golden Section Algorithm (Gonnet 2002).

3. Experimental Setup and Procedures

3.1 Generator Set Specifications

The platform utilized is a Cummins-Onan Generator Set, model GGHD 60HZ, assembled in 1999. This system contains a rugged 4-cycle industrial ICE manufactured by Ford, model LSG-875, that can operate on various gaseous fuels including propane and natural gas. This particular model chosen for testing had been previously installed in the Engines and Energy Conversion Laboratory (EECL), providing an ample opportunity for an engine configuration for testing.

Displacement of the engine is 7.5 liters or 460 cubic inches. It utilizes a cast iron block and heads in a 90 degree V-8 configuration, and operates at approximately 1800rpm. Engine parameters in tabularized format are shown in Table 3-1 (Onan Corporation 2001a).

Table 3-1: Engine specifications

Base Engine	LSG-875, Turbocharged
Displacement in^3 (L)	460.0 (7.5)
Gross Engine Power Output, bhp (kWm)	173.0 (129.1)
BMEP, psi (kPa)	150.0 (1034.2)
Bore, in. (mm)	4.36 (110.7)
Stroke, in. (mm)	3.85 (97.8)
Piston Speed, ft/min (m/s)	1155.0 (5.9)
Compression Ratio	8.6:1
Lube Oil Capacity, qt. (L)	10.0 (9.5)
Exhaust Gas Flow (Full Load), cfm (m3/min)	760.0 (21.5)

Natural Gas had been originally plumbed at the EECL into the mechanical carburetor installed on the engine. Engine rotational speed is monitored via an electronic governor manufactured by Woodward Governor. Mechanically it operates the throttle body valve position, ultimately controlling the amount of air/fuel mixture required to maintain the generator load at 1800rpm. A variable reluctor speed sensor (VRSS) installed in the bell housing surrounding the flywheel gives feedback to the governor module as a reference to execute an adjustment to the throttle body. Figure 3-1 is an image of the original engine configuration of the generator set.

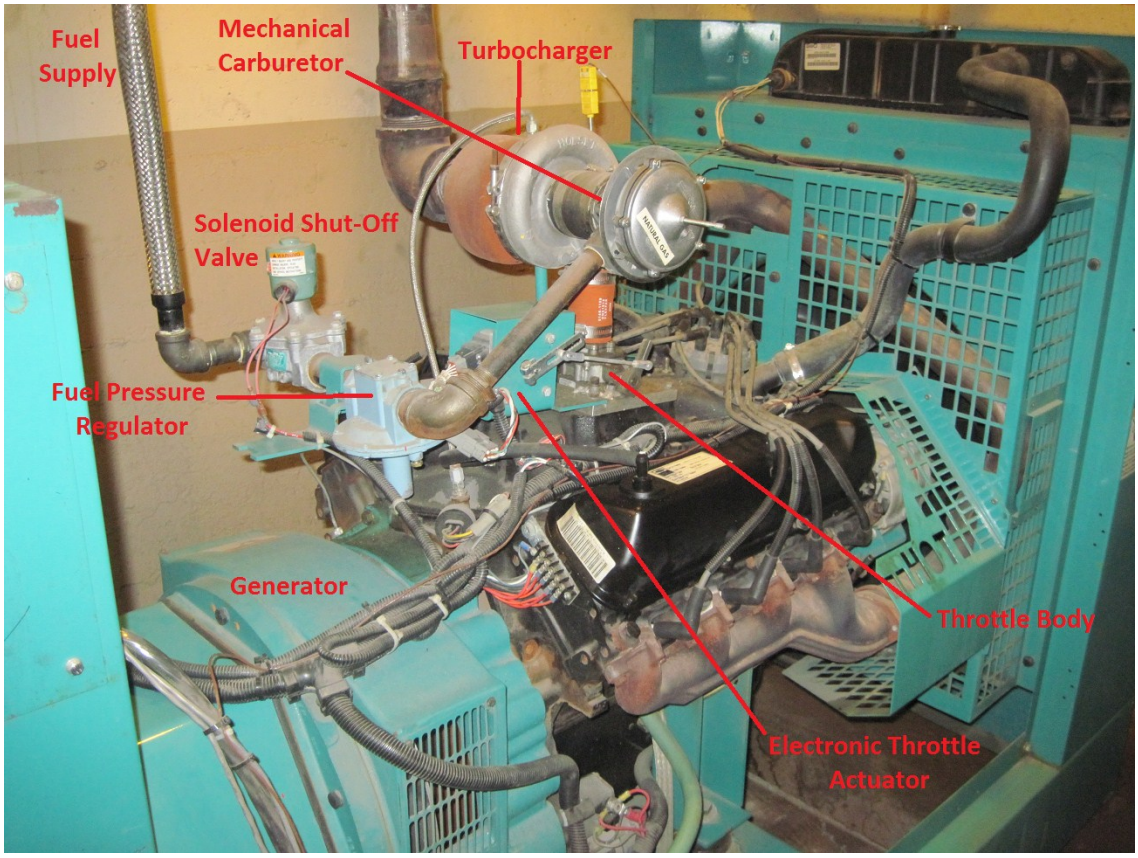

Figure 3-1: Original engine configuration

Additionally, the engine is equipped with a non wastegated turbocharger manufactured by Holset, model number H1C, which provides additional air/fuel mixture at higher loads. The turbocharger is located shortly upstream of the throttle body and does not have any type of air after-cooler to control the temperatures of the intake charge seen at the intake manifold. There is no exhaust after treatment installed on this engine either.

The engine is coupled to an electric alternator or generator, model UCF3. Maximum power output rating of the generator set on natural gas at STP air conditions is 100kW, however, at the elevation of approximately 5000 feet, the maximum power output or 100% load was derated to 80KW. The electrical power output can be supplied to the main city electrical grid system or to load bank. The generator was operated at 480 Volts, 60 Hertz, and a power factor of 1, meaning no reactive power (Onan Corporation 2001b).

3.2 Continental Controls EGC2 Carburetor

From the factory this generator set was equipped with a mechanical carburetor manufactured my IMPCO, which operates at a zero gage fuel pressure that is regulated upstream by an IMPCO fuel pressure regulator as seen in Figure 3-1. The carburetor and regulator were removed and a state of the art electronically controlled carburetor with lambda feedback, manufactured by CCC, EGC2 was installed and the fuel system was plumbed accordingly. A manufacturer drawing of the EGC2 is provided in Appendix I. The carburetor location was retained as before in the pre-compressor location, drawing air and fuel through the compressor inlet of the turbocharger promoting further air and natural gas mixing via the compressor wheel.

With the upstream fuel pressure regulator removed, the CCC EGC2 receives natural gas at a pressure of approximately 15 inches of water column. The EGC2 precisely controls the air to fuel ratio using the patented advanced mixing venturi designed for natural gas, variable pressure control, and wideband oxygen sensor feedback control. This system coupled with a 3-way catalyst yields high emissions reduction efficiency and improved engine fuel efficiency.

The venturi mixer is precisely shaped to produce a lower pressure in the throat, drawing the fuel through the injection ports and into the air stream where it is mixed. The injection ports and venturi mixer produce an optimal air to fuel ratio under all engine load and speed conditions at steady state operation when setup correctly by the user. A pressure transducer is located in the carburetor surrounding the gas injection holes in the venturi mixer. It measures the gas injection pressure and gives feedback in order to adjust the pressure set point within the carburetor just upstream of the gas injection holes. A wideband oxygen sensor located before the 3-way catalyst provides additional feedback to the carburetor. The air to fuel ratio is trimmed by adjusting the electronic pressure regulator inside of the carburetor (Continental Controls Corporation 2008). Figure 3-2 is an image of the CCC EGC2 installed on the engine.

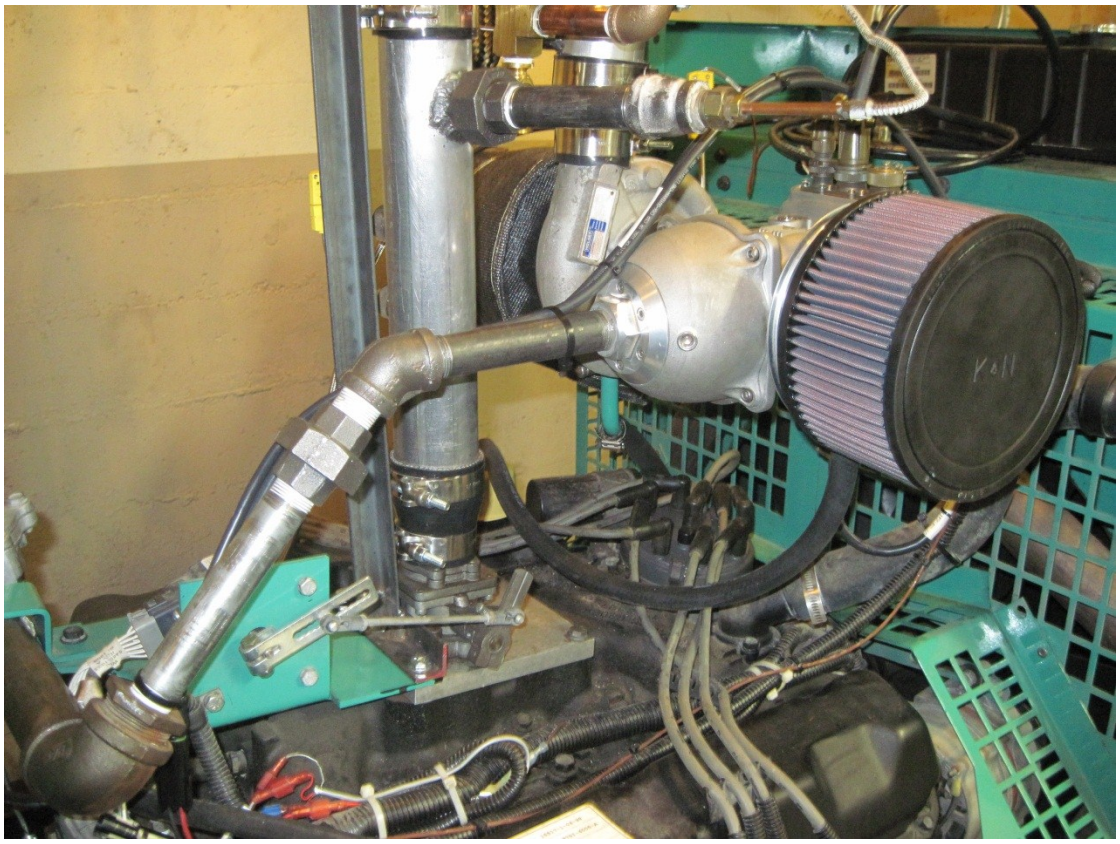

Figure 3-2: CCC EGC2 installed

Additional wiring and sensors were needed in order to successfully install this carburetor. The carburetor required two power sources both of which are 12VDC, one for the power control board as well as the electronic pressure regulator, fused individually at 1 amp and 6 amps, respectively. This particular carburetor has a built in manifold absolute pressure (MAP) sensor plumbed into the intake manifold just beneath the throttle body. Additionally, the carburetor needs a speed signal to control fuel delivery start and stop commands. A VRSS manufactured by Magnetic Sensors Corporation, secondary to the one installed for the engine speed governor, was installed into the bell housing. This provides feedback directly to the CCC EGC2. Refer to Appendix I for additional VRSS details.

3.3 Continental Controls Catalyst Monitor

In addition to the CCC EGC2 and all of the hardware previously discussed in Section 3.2, Continental Controls also provided a catalyst monitor which interacts with the fuel delivery and data acquisition (DAQ) systems. The main intention of this device is to monitor various sensors, including 2 thermocouples, differential pressure across the catalyst, 2 wideband O2 sensors, 2 NOx sensors, a single 4-20mA input, and 2 CAN Bus inputs if the NOx sensor inputs are not used. This provides a means of monitoring the aging and degradation of the catalyst. There are 2 programmable safeguards built into the system that can be activated to provide engine shutdown upon specific conditions for instance a high temperature condition above the maximum operating temperature of the catalyst. High temperatures can sinter precious metals located on the catalyst. Another example would be increased differential pressure across the catalyst, which may indicate masking and fouling of the catalyst sites (Continental Controls Corporation 2010).

All models of the catalyst monitor have a built in standalone data logger to acquire data for post processing. The catalyst monitor has the ability to receive feedback from a NOx sensor located downstream of the catalyst and use this feedback loop for further air/fuel ratio trim adjustments performed by the carburetor. The catalyst monitor communicates with the CCC EGC2 via CAN Bus communications to feed forward the desired air/fuel ratio increment adjustment. The adjustment is calculated utilizing a minimization control algorithm, which is the major focus of this work. One common CAN Bus is shared by the catalyst monitor, EGC2, Continental NOx sensor and NI Hardware. Figure 3-3 is a flow diagram that represents the logic performed by the catalyst monitor system.

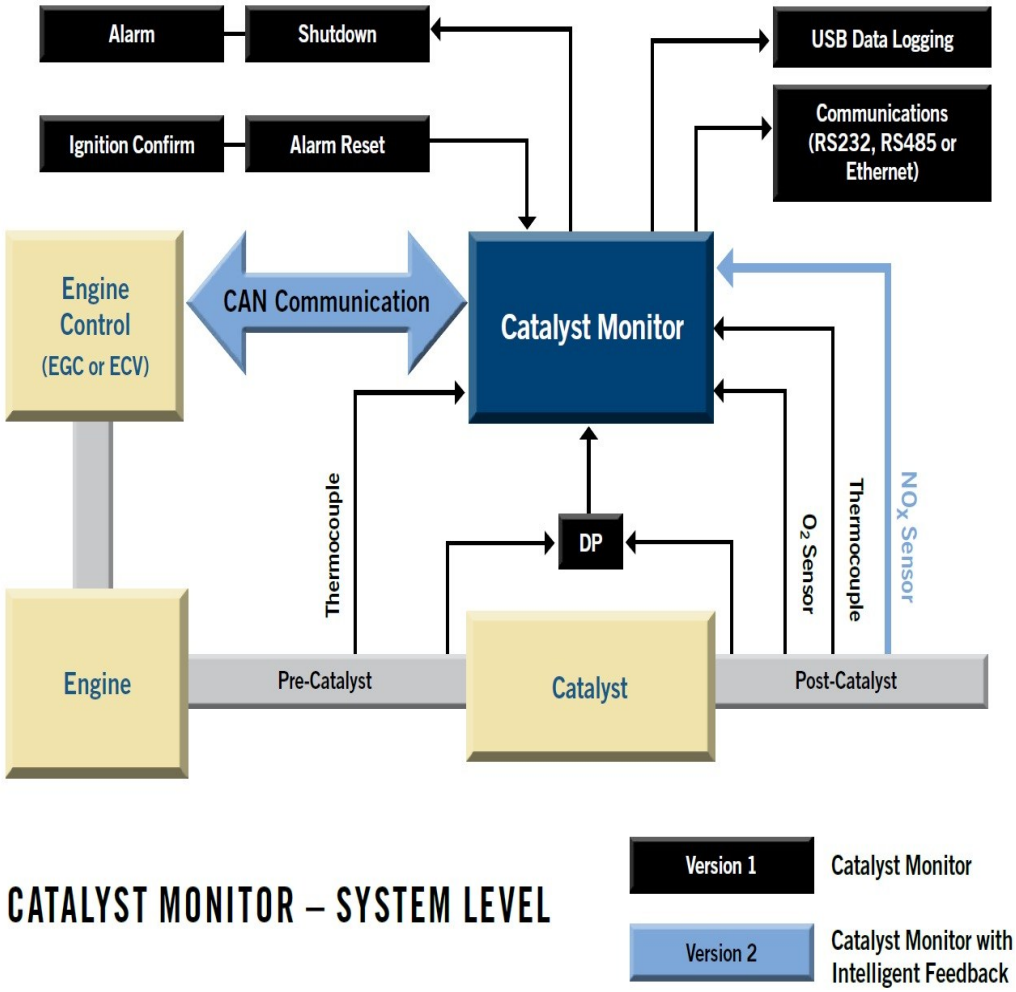

Figure 3-3: CCC Catalyst Monitor control logic (Continental Controls Corporation 2010)

3.4 DCL Catalyst

The catalyst used for the project was a NSCR, or 3-way, catalyst designed to reduce exhaust emissions including CO, THC, NOx, and aldehydes. It is manufactured by DCL International and was sized accordingly for the engine specifications. The MINE-X model catalytic converters from DCL International are designed with reliability and long life operation in mind and come with an emissions performance guarantee. The manufacturer guarantees a reduction efficiency of 90-99% for NOx and CO, 50-90% for THC, and 80-95% for CH2O and

HAP's. HAP's are a specific category of pollutants designated by the EPA. Typically the only species emitted about regulatory limits is CH2O.

NSCR catalysts are universal to many applications as they can accompany various fuels including natural gas, propane, and gasoline. Additionally, the catalyst has a modular design and can be easily modified to complement a different application. The assembly has removable catalyst inserts that can be stacked to meet the engine exhaust flow rate and emissions requirements. It is designed with a stainless steel structure and brazed metal substrate (DCL International 2009). The catalyst that was provided for the project can be seen in Figure 3-4.

Figure 3-4: DCL International catalyst chosen for the project

The catalyst was sized for the project by DCL to have 3 catalyst inserts, with a volume of 4560 (cm^3) each and an active area of 24.8 (cm^2/cm^3). It is also equipped with 4 threaded fittings, 2 pre and 2 post catalyst, located in the end caps where the catalyst is flanged. Pre and Post catalyst thermocouple measurements as well as the plumbing required to the differential pressure transducer, logged by the CCC catalyst monitor consumed these available threaded ports. The catalyst assembly arrived with 3 inch, 4 bolted ANSI companion flanges. The catalyst was placed in a location with flow characteristics in mind. It was also installed as close as possible to the engine to maximize catalyst temperature and reduction efficiency. In order to achieve high exhaust gas temperatures entering the catalyst, heavy insulation of the exhaust between the engine exhaust manifolds and catalyst outlet was performed. This resulted in temperatures just less than the catalysts maximum temperature and the highest emissions reduction efficiencies.

3.5 Turbocharger After-cooler

Previous testing performed by Southern California Gas Company and CCC, using the CCC EGC2 revealed that temperature fluctuations in the ambient air (mass air flow) around the intake filter due to radiator and engine heat were resulting in inconsistent engine exhaust emissions (Vronay Engineering Services Corp. 2011). To address this issue, their team plumbed the air filter away from the engine environment to try and maintain steady state air properties entering the engine.

To address the issue for this project, a water to air intercooler was installed between the turbocharger compressor outlet and the throttle body. The intercooler also compensates for

slow changes in air properties throughout the day. The intercooler is manufactured by Frozen Boost, who builds intercoolers primarily for automotive applications. It is rated up to 350 HP, has a pressure drop less than 0.1psig, and recommended for flow rates up to 450 CFM. Thus, the intercooler is oversized for the Cummins-Onan Genset. The finished intercooler setup installed and plumbed is displayed in Figure 3-5.

Figure 3-5: Intercooler installed and plumbed for air and water

3.6 NOx Sensor Systems

During initial engine re-configuration, there were 2 different NOx sensors installed downstream of the catalyst with their corresponding signal conditioners. The first system is manufactured by CCC, utilizes a Continental brand NOx sensor, and came with the EGC2 and

Catalyst Monitor. The second system was a standalone system manufactured by Engine Controls and Monitoring (ECM), model number NOx 5210. There are differences between both systems and comparison of their output values will be further investigated in Chapter 4. For the sake of this project, the Continental NOx sensor became the only system retained in the latter part of the project. Both NOx sensors were positioned in the exhaust stream according to manufacturer recommendations. Additionally, the driving technology for both sensors is a specialized thick film ZrO_2 standalone smart sensor that uses integrated in-connector control electronics.

The ECM NOx 5210 system is a much more versatile unit and can be easily implemented in the field to nearly any application. There are 2 sensor options including the NGK and the NTK sensor, with the main difference being their error tolerance of plus/minus 15 ppm for NGK and plus/minus 30 ppm for NTK. The NTK sensor was used during baseline testing. It returns values for NOx, Lambda, Equivalence Ratio, Air/Fuel Ratio (AFR), and % O_2. It also has the option for a secondary channel in which 2 sensors can be monitored simultaneously and logged (Engine Control and Monitoring 2008).

The Continental Smart NOx sensor "Uninox_12V" goes through a NOx sensor module manufactured by CCC that processes this raw signal and returns a signal in units of ppm onto the CAN Bus. This particular sensor is designed to operate between the range of 0 and 1500 ppm. The system returns an updated value to the CAN Bus every 50ms, or at a rate of 20Hz (Continental 2008). The Continental sensor is a thick film ZrO_2 dual cavity construction with in-connector control electronics, shown in Figure 3-6.

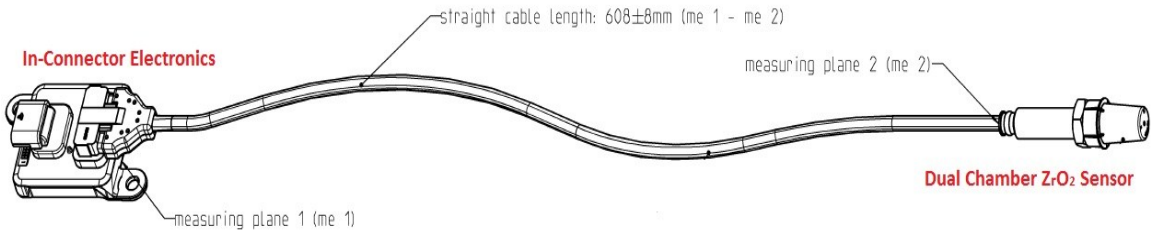

Figure 3-6: Continental Smart NOx sensor (Continental 2008)

3.7 Data Acquisition

Various measurement sensors were installed throughout the engine and its plumbing systems in order to monitor and record all necessary engine parameters. All sensor outputs were wired into the appropriate National Instruments (NI) module through conduit surrounding the engine platform. Each NI module plugs directly into a cRIO 9076 NI chassis that communicates to the LabVIEW data acquisition interface on the main floor of the EECL in the control room via Ethernet connection. All of the NI hardware was powered using a 24VDC power supply from the generator set control box. Multiple screen shots of the LabVIEW interface are shown in Appendix I.

Thermocouple measurements were wired using K-Type thermocouple wire and ran into a NI 9213 16-channel capable thermocouple input module. Analog inputs were wired into a wiring block fastened inside of the control box and then into a NI 9205 32-channel capable 0-5V input module. Parameters from the CCC EGC2, CCC Catalyst Monitor, and Continental NOx sensor system were wired onto one CAN Bus and the ECM 5210 NOx sensor system was wired onto its own designated CAN Bus. Each CAN Bus then communicates to a NI 9853 2-channel CAN Bus module. A list of instrumentation and sensors is provided in Table 3-2.

Table 3-2: Instrumentation list of all sensors installed to monitor and provide feedback from the engine configuration and the corresponding NI module

Measurement	Instrumentation	Data Collection System
Pre-Intercooler Temp	1/8" Type K thermocouple	NI-9213, LabVIEW
Post-Intercooler Temp	1/8" Type K thermocouple	NI-9213, LabVIEW
Pre-Turbine Temp	1/4" Type K thermocouple	NI-9213, LabVIEW
Pre-Catalyst Temp	1/4" Type K thermocouple	NI-9853, LabVIEW
Post-Catalyst Temp	1/4" Type K thermocouple	NI-9853, LabVIEW
Fuel Inlet Temp	1/4" Type K thermocouple	NI-9213, LabVIEW
Post-Intercooler Pressure	Omega PX309-050A5V pressure transducer	NI-9205, LabVIEW
Pre-Turbine Pressure	Omega PX309-050A5V pressure transducer	NI-9205, LabVIEW
Fuel Inlet Pressure	Omega PX309-030GI pressure transducer	NI-9205, LabVIEW
Catalyst Differential Pressure	Rosemount 0-15 inH2O pressure transducer	NI-9853, LabVIEW
Fuel Inlet Flow	Omega FTB938 flow meter	NI-9205, LabVIEW
Fuel Inlet Flow	Omega FLSC-62A signal conditioner	NI-9205, LabVIEW
Engine Speed	Magnetic Sensors Corporation VRSS	NI-9853, LabVIEW
Carburetor Fuel Pressure	CCC EGC2 Carburetor	NI-9853, LabVIEW
Intake Manifold Pressure	CCC EGC2 Carburetor	NI-9853, LabVIEW
Lambda (O2%)	Bosch LSU 4.2 Sensor	NI-9853, LabVIEW
Continental NOx System	Continental NOx Sensor	NI-9853, LabVIEW
ECM NOx System	ECM NOx 5210 with NTK Sensor	NI-9853, LabVIEW

3.8 CCC EGC2 and Catalyst Monitor Calibration and Software

In addition to the ability to log all CCC EGC2 and Catalyst Monitor parameters via CAN Bus communications, there is also the option to view the data live time using the software provided with the product. It offers a graphical user interface (GUI) with the ability to log and adjust parameters through the use of a laptop that communicates with both the CCC EGC2 and

Catalyst Monitor via serial communications. This provides a full engine on board diagnostics tool.

The EGC2 parameters including O_2 sensor set point, fuel pressure range limits, dithering options, initial cranking conditions, O_2 sensor and fuel pressure gain values can be set utilizing their "Valve Viewer" software. When the carburetor is in operation and connected to a laptop via the serial communications connector, the software provides a GUI feedback that updates at a rate of 1 Hz. Data logging can be enabled within the software as well. Figure 3-7 shows a screen shot of the Valve Viewer software.

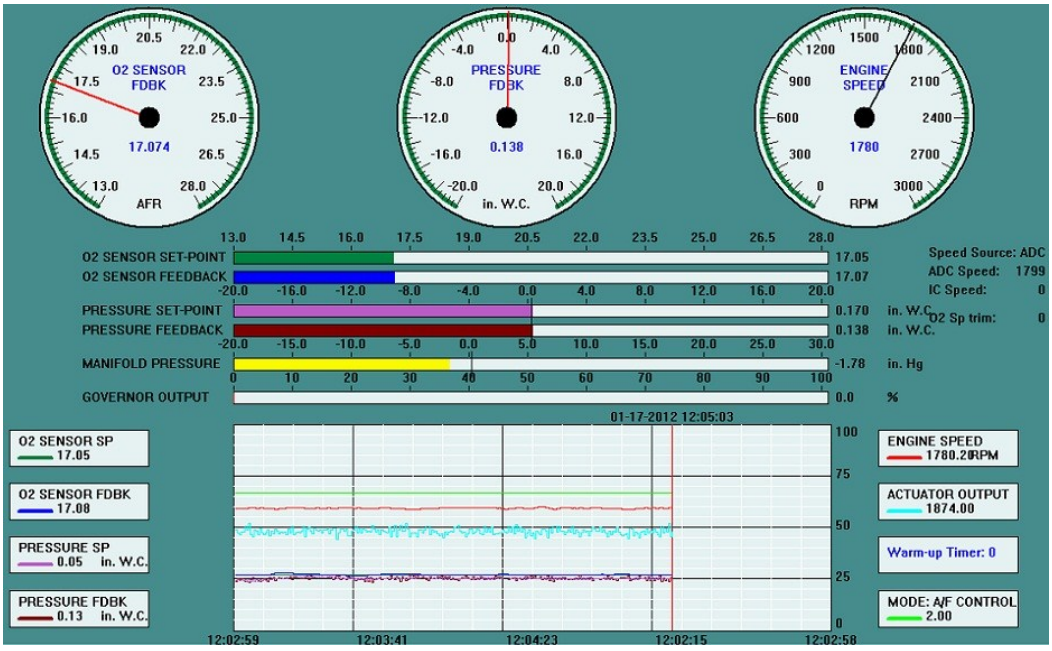

Figure 3-7: Valve Viewer software graphical user interface

Catalyst Monitor parameters including range adjustments of inputs and alarm settings can be modified using the secondary software provided referred to as "Catalyst Monitor

Viewer." Additionally the software provides a GUI that displays pre and post catalyst temperatures, Continental NOx sensor output (ppm), and catalyst differential pressure. These parameters can be logged for post processing as well. The EGC2 carburetor and Catalyst Monitor require a serial connection to communicate to their respective software. Figure 3-8 is a screen shot of the Catalyst Monitor Viewer software.

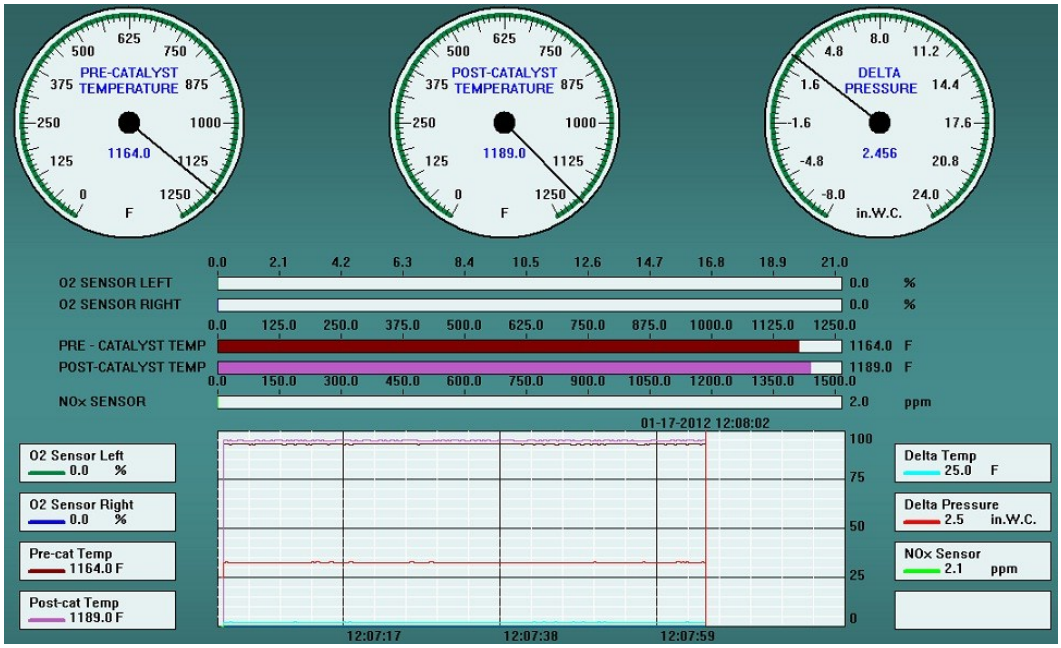

Figure 3-8: Catalyst Monitor Viewer software graphical user interface

Parameters that can be set within the CCC EGC2 include O_2 sensor set point, fuel pressure set point and range limits, dithering settings, initial conditions, O_2 sensor and fuel pressure gain values. In order to optimize these values, the engine was operated through a series of tests over the course of multiple days to determine the ideal settings needed to achieve maximum emissions reduction. Emissions feedback was provided using the Rosemount

5-gas analyzer rack. Table 3-3 compares the factory EGC2 carburetor settings to the new values found to provide the best engine out emissions results under steady state and transient conditions.

Table 3-3: CCC EGC2 carburetor settings

Setting	Previous Value	Optimal Value
Target AFR	17.2	17.053
O2 Sensor Gain	100	700
Pressure Proportional Gain	1600	1600
Pressure Integral Gain	600	200
Dithering Amplitude	1800	600
Dithering Period	667 (~1 s)	667

When dithering was enabled, the engine out emissions tended to be more stable and produce overall lower concentrations. Dithering is an operation performed by the EGC2 where it oscillates the AFR above and below the target AFR set point at a designated amplitude and frequency (period). Dithering was incorporated into the system initially by CCC due to previous research suggesting that it widened the narrow equivalence ratio operating range (Vronay et al. 2010). The O_2 sensor gain, dithering amplitude, and dithering period are all a function of one another and the actual AFR amplitude created by dithering depends on all 3 parameters.

Initially under load transients, the O_2 sensor gain was not high enough to keep up with the demands of the fuel adjustment required to maintain the desired AFR. After this value was increased, the ramp rate at which dithering occurred increased and started to make the engine speed lope up and down. To compensate, the dithering amplitude had to be lowered to keep the actual AFR amplitude within a practical range for steady engine operation. The dithering period of 667 corresponds to 1 second, meaning the dither will go above and then below the

target AFR set point in that period of time. This value was retained as this is a common frequency at which dithering occurs in automotive applications. Additionally, it was found that by lowering the pressure integral gain, the rate at which the fuel pressure changed internal to the EGC2 to ultimately change the AFR was appropriate under steady state and transient conditions.

3.9 Test Procedure (Steady State and Transient)

A test procedure was developed to accurately compare baseline testing to that using a NOx sensor feedback control algorithm. Various steady state and transient conditions were created in order to evaluate the system's ability to maintain high 3-way engine emissions reduction efficiency. When the engine was operated at 100% load for only a short period of time, overheating occurred due to the generator set being located in an area of the facility with poor air circulation. It was decided that 80% load (64 kW electric power) would be the maximum load.

5 test procedures were developed for the study:

1. Equivalence Ratio Sweep Steady State
2. Load Sweep Steady State
3. Load Transient
4. Propane Blending (Steady State and Transient)
5. Exhaust Back Pressure Transient

All testing, other than the load sweep and load transient tests, was performed at 60% load (48 kW electric power). For all testing, other than the equivalence ratio sweep, the optimal AFR was used. The equivalence ratio sweep is where the optimal AFR was obtained. During steady state testing, any time a test change was made, the engine was allowed to run until the Rosemount 5-gas emissions were stable (about 15 minutes). Shortly after, a 5 minute period of test data was recorded via LabVIEW, which included all inputs from the engine configuration shown in Table 3-2, the Rosemount 5-gas analyzer rack, Nicolet 6700 FTIR, and ECM AFRecorder 4800R.

The equivalence ratio sweep was among the most important test procedures that had to be executed because it determined the optimal AFR for all other tests performed. Additionally, the response of the NOx sensors with respect to the AFR can be accurately evaluated, which is critical for NOx sensor control. The target AFR in the CCC EGC2 was changed in both lean and rich directions so that a wide range of AFR's were captured in order to see the effects on the engine exhaust emissions output and NOx sensor response.

The load sweep consisted of operating the engine at steady state generator load settings of 20, 40, 60, and 80%. The effects of catalyst temperature and its relation to the required AFR set point were evaluated, as well as NOx sensor correlations. The load transient in test was conducted to evaluate the ability of the control system to maintain emissions compliance as load changes. The load transient test consisted of the following sequence: (a) zero load for 2 minutes, (b) step load up to 20% (16KW electric power) at a rate of approximately 1.5KW per second, (c) hold for 15 minutes, (d) step up load to 40% (32KW

electric power), (e) hold for 15 minutes, and (f) repeat through load steps of 60, 80, 60, 40, 20, and 0%.

In order to execute the propane blending testing, a propane injection system plumbed into the natural gas fuel feed line was developed using a standard propane holding tank, appropriate propane safe pressure valve, rota-flow meter and needle control valve. Flow rates of 25, 50, 75, and 100 SCFH were targeted and the Gas Chromatograph (GC) was used to determine the actual concentration (molar %). To be sure that satisfactory propane and natural gas mixing would occur before the Varian CP-4900 Micro GC sampling line, the propane was introduced approximately 2 feet upstream. For the transient test, propane blending was introduced instantly at a designated time and flow rate.

The last test developed was an exhaust back pressure transient. This was chosen with the understanding that a large amount of exhaust backpressure across the catalyst and lambda sensor, introduced instantaneously would compromise the calibration of the sensor and correct AFR lambda feedback control would not operate in the targeted range. A manual exhaust back pressure valve, manufactured by Apexi was installed downstream of the catalyst, exhaust sensors and emissions probes. A pressure gage was used to monitor exhaust backpressure. The 4 available exhaust back pressure settings the engine could operate at were 1, 5, 9, and 10 psig which corresponded to the valve manual set points.

3.10 Control Room Analyzers and Preparation

A total of 8 instruments characterized gaseous engine exhaust emissions and fuel composition. Included is a Rosemount 5-gas analyzer rack with 5 individual instruments to

monitor NOx, CO, THC, CO_2, and O_2 concentration. A Nicolet 6700 Fourier Transform Infra-Red (FTIR) spectrometer was used to acquire HAP's including NH3. A Varian CP-4900 Micro GC evaluated the fuel composition and an ECM AFRecorder model 4800R acquired the AFR.

A condenser removes water from the exhaust sample prior to entering the 5-gas analyzers rack. NOx concentration is measured using the chemiluminescence method (CM). NO2 is reduced into NO across the catalyst and then NO reacts with generated ozone (O3), forming an electronically excited NO2 molecule. The excited molecule immediately reverts to the ground state emitting photons, which is directly measured by a photodiode. The intensity is proportional to the NOx concentration. CO and CO2 concentration is measured by each respective analyzer using Infrared radiation (IR) adsorption. Total hydrocarbon compounds are detected using a flame ionization detection (FID) method. The sample exhaust gas flow is regulated and passes through a flame that is combusted by a fuel gas and air that is regulated as well. The flame produces electrons and positive ions, which are collected by an electrode that creates a current through the circuit which is proportional to the number of carbon atoms. O2 concentration is determined by measuring the magnetic susceptibility of the exhaust sample gas, referred to as paramagnetic detection (PD). O2 is strongly paramagnetic, and accounts for nearly all of the exhaust sample gas magnetic susceptibility. Figure 3-9 is an image of the Rosemount 5-gas analyzer rack with its corresponding devices.

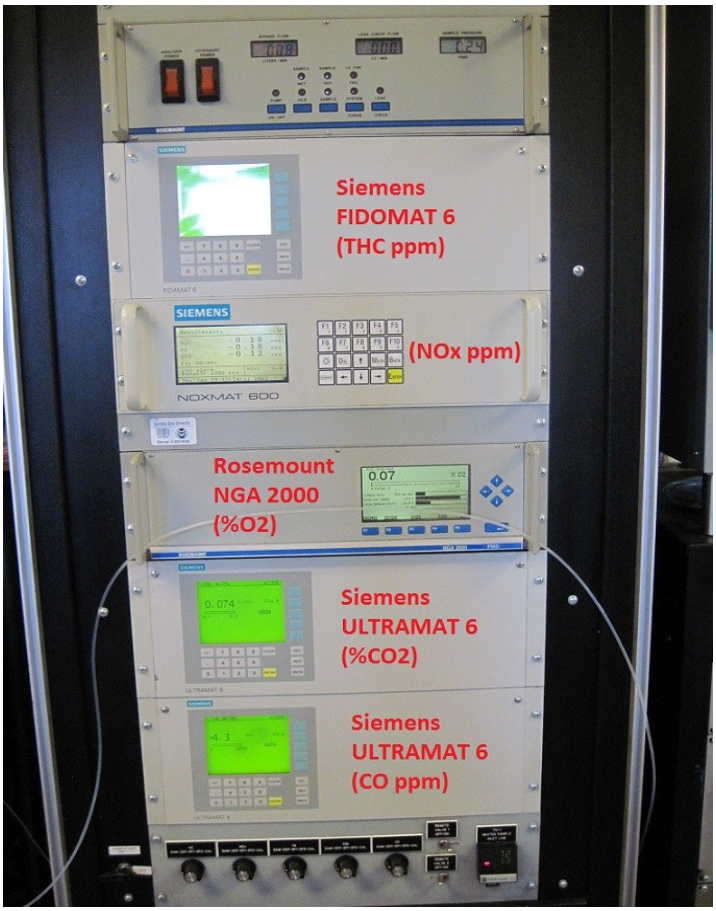

Figure 3-9: Rosemount 5-gas analyzer rack

Other gaseous components and Hazardous Air Pollutants (HAPs), defined by the EPA, are characterized using a FTIR spectrometer. The FTIR can be used to measure any polar molecule below a molecular weight of approximately 45. It uses an infrared light absorption (ILA) method by measuring the entire infrared spectrum of light in the exhaust gas sample using an interferometer. This pattern is then analyzed using a Fourier Transformation, resulting in a plot of absorbance magnitude versus wavelength. The absorbance plot is used to determine the species and their concentrations in the exhaust gas sample. Figure 3-10 is an image of the Nicolet 6700 FTIR.

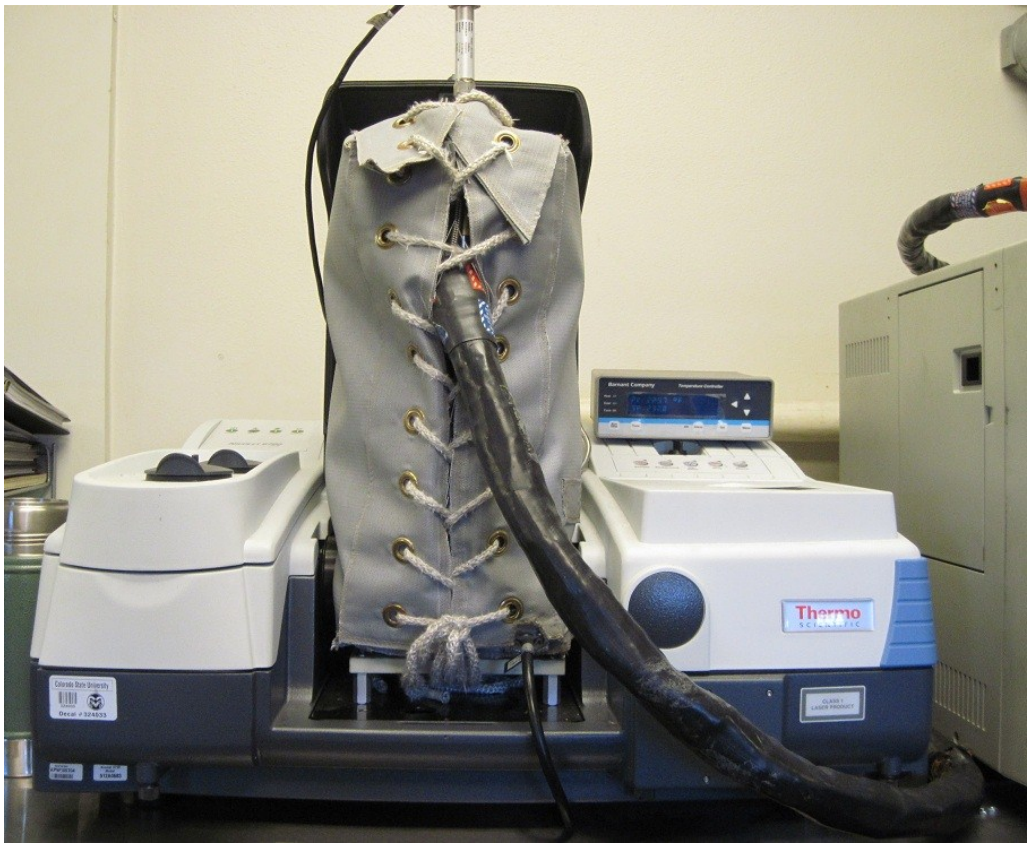

Figure 3-10: Nicolet 6700 FTIR

The Varian CP-4900 Micro GC was used to analyze fuel gas composition. A continuous sample was acquired just upstream of the engine and flowed to the GC located in the control room, where an analysis was carried out every 2 minutes. This analyzer utilizes a split-sample technique to achieve very fast analysis times (~50 seconds). Gas species are separated with packed columns and detected using a thermal conductivity detector. Typically the analysis is set up to determine fuel gas composition up through C6. Figure 3-11 is an image of the Varian CP-4900 Micro GC.

Figure 3-11: Varian CP-4900 Micro GC

The AFR is accurately determined by entering a series of calibration constants into the ECM AFRecorder 4800R that are provided specific to the SEGO wide range O2 sensor sent by the manufacturer. Furthermore, once a GC sample of the fuel gas composition has been acquired, the fuel Hydrogen, Oxygen, and Nitrogen to Carbon ratios can be entered into the device in order to record accurate AFR and/or equivalence ratio. The Simulated Exhaust Gas Oxygen (SEGO) sensor is mounted in the exhaust stream of the engine pre-catalyst configuration. A cable is then routed directly from the sensor up into the ECM AFRecorder located in the control room. Figure 3-12 is an image of the device.

Figure 3-12: ECM AFRecorder 4800R

The Rosemount 5-gas analyzer rack, Nicolet 6700 FTIR, and Varian CP-4900 Micro GC all went through a calibration process previous to testing and periodically throughout testing to ensure that consistent results were being acquired without concern for instrumentation error. All devices were calibrated using zero and span gases per EPA methods. The sampling probes were developed according to EPA AGA method 1. It is required that the pre catalyst sampling probe be located 2 pipe diameters up stream of any disturbance, which for this project was the catalyst. The post catalyst sampling probe is required to be located 8 pipe diameters downstream of any disturbance which was the bend directly off the catalyst output. Each emissions probe was plumbed into a stainless steel 3-way valve using stainless steel tubing to reduce the chance of corrosion and leaking. The lines leading up to the 3-way valve were insulated. A heated and insulated emissions filter was attached directly to the 3-way valve. The filter assembly, which has a separate temperature control module, is connected to a heated sample line that goes to the control room exhaust analyzers. The temperature of the sample line is maintained at a constant 100 °C.

Table 3-4 describes the instrumentation, the corresponding components that were characterized, and the methods used.

Table 3-4: Exhaust gas species characterized, methods, and devices used

Measurement	Method	Device
NOx concentration	CM	Siemens NOXMAT 600
CO concentration	IR	Siemens ULTRAMAT 6
THC concentration	FID	Siemens FIDAMAT 6
CO2 concentration	IR	Siemens ULTRAMAT 6
O2 concentration	PD	Rosemount NGA 2000
NH3 concentration	ILA	Nicolet 6700 FTIR
Other gaseous HAP's concentration	ILA	Nicolet 6700 FTIR
Fuel composition	Carbon	Varian CP-4900 Micro GC
Air Fuel Ratio	O2%	ECM AFRecorder 4800R with SEGO O2 Sensor

Additional images and technical information on test setup and hardware can be seen in Appendix I.

4. Baseline NSCR Control Results

One of the primary tasks for this work was to perform thorough baseline testing in order to accurately compare latter data using NOx sensor minimization control algorithm feedback. The 5 tests performed over the course of 3 days yielded a generous amount of data with ample opportunity for improvement utilizing NOx sensor feedback control.

4.1 Gas Chromatograph Analysis

During each steady state test that was performed, a fuel sample was acquired via the Varian CP-4900 Micro GC. For transient tests, a sample was taken before and after the transient test procedure. The species concentration is reported in percentages and includes: Methane (CH_4), Ethane (C_2H_6), Propane (C_3H_8), Iso-butane and n-butane (C_4H_{10}), Hydrogen (H_2), Nitrogen (N_2), Oxygen (O_2), and Carbon Dioxide (CO_2).

Using these concentration fractions of the fuel gas composition, properties of the fuel can be acquired including the molecular weight ($\dot{m}_f$), stoichiometric AFR, gas fuel molar quantities (α, β, Υ, ξ), and hydrogen, oxygen, nitrogen to carbon ratios. Gas fuel molar quantities represent the following: $C\alpha H_\beta O_\Upsilon N_\xi$. These values were quantified using methods described by Urban and Sharp (1994). The gas analysis was performed using Microsoft Excel and a screen shot example of a single processed GC sample is shown in Appendix II. In between each individual test, the ECM AFRecorder 4800R was reprogrammed using the hydrogen, oxygen,

nitrogen to carbon ratios calculated by the previous gas analysis. This ensured that the AFR being reported to LabVIEW for recording was consistent. With a stoichiometric AFR value and gas fuel molecular weight determined for each individual steady state and transient test, averaging for that specific test was performed.

For the equivalence ratio sweep test, an overall average stoichiometric AFR was determined from all tested points across the sweep. The molecular weight of the fuel was also averaged and found to be 17.212 g/mol. Brake specific emissions (g/bhp*hr) required the use of the calculated fuel carbon number (α) which was an average value of 1.019 moles. Detail on why this value was needed will be discussed further in Section 4.2. For the test procedures following the equivalence ratio sweep, the averaged stoichiometric AFR, gas fuel molecular weight, and fuel carbon number remained nearly constant.

Acquiring gas fuel composition samples for the propane blending tests at each target flow rate (SCFH) was also of high priority. Knowing the molar percentage of propane in the fuel composition was important to acquire rather than just knowing the target propane blending flow rate. To be certain the samples were correct and that proper mixing was occurring, 2 samples at each target flow rate were performed, and then averaged during post processing. Table 4-3 displays the relationship between target flow rates and averaged GC calculated propane (C_3H_8) molar %.

4.2 Brake Specific Emissions

Exhaust gas species concentrations recorded by the Rosemount 5-gas analyzer rack and Nicolet 6700 FTIR are reported in either percentage or ppm on a dry basis. In order to represent

the data with respect to brake horsepower (BHP), additional calculations must be performed using raw data from instrumentation installed throughout the engine system. BHP was acquired by knowing the electrical power output of the generator as well as the efficiency curve of the generator based on the power (kVA), frequency (Hz), and power factor. Considering a frequency of 60 Hz, voltage of 480 V, and power factor of 1.0 is used during all testing of the project, the electrical power (kVA) is the only variable needed to determine the efficiency of the generator. The generator set at sea level is rated at 100 KW which equates to 125 kVA. Generator efficiency (%) versus power (kVA) is displayed in Figure 4-1. The top line, representing a power factor equal to 1.0 is the efficiency curve of interest.

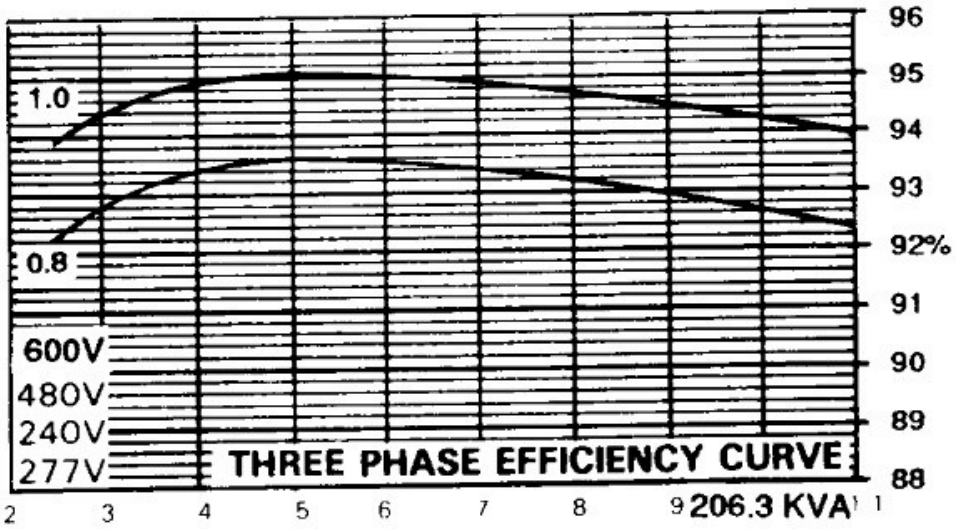

Figure 4-1: Generator Efficiency vs. Electrical Power Output (Onan Corporation 2001b)

The upper limit of 10 represents this maximum power output of 125 kVA. The elevation of the EECL limits the generators ability to create more than 80 kW electrical power. With the exception of load testing, all other tests were performed at 60% (48kW) generator load, with

respect to an 80 kW peak power. This means the point on the graph for the corresponding efficiency would occur at 4.8, resulting in a generator efficiency of approximately 95.1%.

The variables included in calculating brake specific emissions (BSE) are species concentrations reported by the Rosemount 5-gas analyzer rack, fuel properties acquired by the Varian CP-4900 Micro GC, and inputs acquired by the NI DAQ system. Table 4-1 describes the variables and their corresponding notation.

Table 4-1: Variables for BSE calculations

Notation	Description
BSE_i	Brake specific emissions of individual species (g/bhp*hr)
$\dot{m}_i$	Mass flow of individual species (g/hr)
$\dot{m}_f$	Mass flow of fuel (g/hr)
$\dot{V}_f$	Volumetric flow of fuel (m^3/hr)
P_f	Fuel pressure (Pa)
R	Universal gas constant (8.314 J/mol*K)
T_f	Fuel temperature (K)
ρ_f	Density of fuel (g/m^3)
α	Fuel carbon number
α_i	Species i carbon number
Y_i	Species i mole fraction
M_i	Molecular mass of species i (g/mol)
M_f	Molecular mass of fuel (g/mol)
$\sum(Y_i\alpha_i)$	Sum of all exhaustcarbon containing species
Molecular Mass (g/mol)	**Species**
46.00	NOx (molecular weight for NO_2)
28.01	CO
16.04	THC (molecular weight for CH_4)
32.00	O_2
44.00	CO_2

The Siemens NOXMAT 600 NOx measures the sum of NO and NO_2 as NOx. NO_2 is used as the molecular weight for the calculations performed below to be consistent with regulatory NOx limits. The Siemens FIDOMAT 6 THC concentration is based on methane calibration, which is why the molecular weight used for THC for these calculations is CH_4. Converting the species concentration returned by the Rosemount 5-gas analyzer rack to mole fraction requires that the species concentration in ppm (NOx, CO, THC) be divided by 10E6 and the species in

concentration % (CO_2, O_2) be divided by 100, which is shown in Equation 4.5. The following equations were exercised in order to acquire BSE:

$$BSE_i = \frac{\dot{m}_i}{BHP} \tag{4.1}$$

$$\dot{m}_i = \frac{\dot{m}_f * \alpha * Y_i * M_i}{M_f * \sum(Y_i \alpha_i)} \tag{4.2}$$

$$\rho = \frac{P}{\frac{R}{M_f} * T} \tag{4.3}$$

$$\dot{m}_f = \dot{V} * \rho \tag{4.4}$$

$$\sum(Y_i \alpha_i) = \frac{Y_{THC}(ppm)}{10E6} + \frac{Y_{CO}(ppm)}{10E6} + \frac{Y_{CO2}(\%)}{100} \tag{4.5}$$

4.3 Equivalence Ratio Sweep

In order to acquire the optimal AFR for the remaining tests as well as see the response of exhaust emissions species and the NOx sensor, a range of equivalence ratio values had to be tested. Each target value was recorded at steady state over a 5 minute time period. The tests were started after the Rosemount 5-gas analyzer displayed exhaust gas species stability. After the average stoichiometric AFR value was determined from the GC data, it was then compared to each steady state 5 minute averaged AFR (AFR_{avg_n}) obtained from the ECM AFRecorder. Equivalence ratio (Φ) was then calculated as:

$$\Phi = \frac{AFR_{stoich\_avg}}{AFR_{avg\_n}} \quad (4.6)$$

Table 4-2 describes the relationship between the target AFR and the resulting equivalence ratio. The target AFR is entered into CCC Valve Viewer software which is then stored in the CCC EGC2 carburetors internal memory.

Table 4-2: CCC EGC2 carburetor target AFR, calculated recorded AFR via ECM AFRecorder 4800R, and corresponding equivalence ratio

Target AFR (EGC2)	AFR (ECM AFRecorder)	Equivalence Ratio (Φ)
17.228	15.825	1.0081
17.128	15.777	1.0111
17.113	15.761	1.0121
17.098	15.752	1.0127
17.083	15.732	1.0140
17.068	15.716	1.0150
17.053	15.686	1.0170
17.038	15.647	1.0195
17.023	15.636	1.0202
17.008	15.622	1.0211
16.928	15.567	1.0248
16.828	15.519	1.0279
16.728	15.457	1.0321
16.428	15.319	1.0475
16.000	15.034	1.0673
15.500	14.640	1.0960

Figure 4-3 and Figure 4-3 displays pre and post catalyst exhaust emissions concentrations (ppm) for NOx, CO, and VOC's as well as NOx sensor response (ppm) with respect to equivalence ratio.

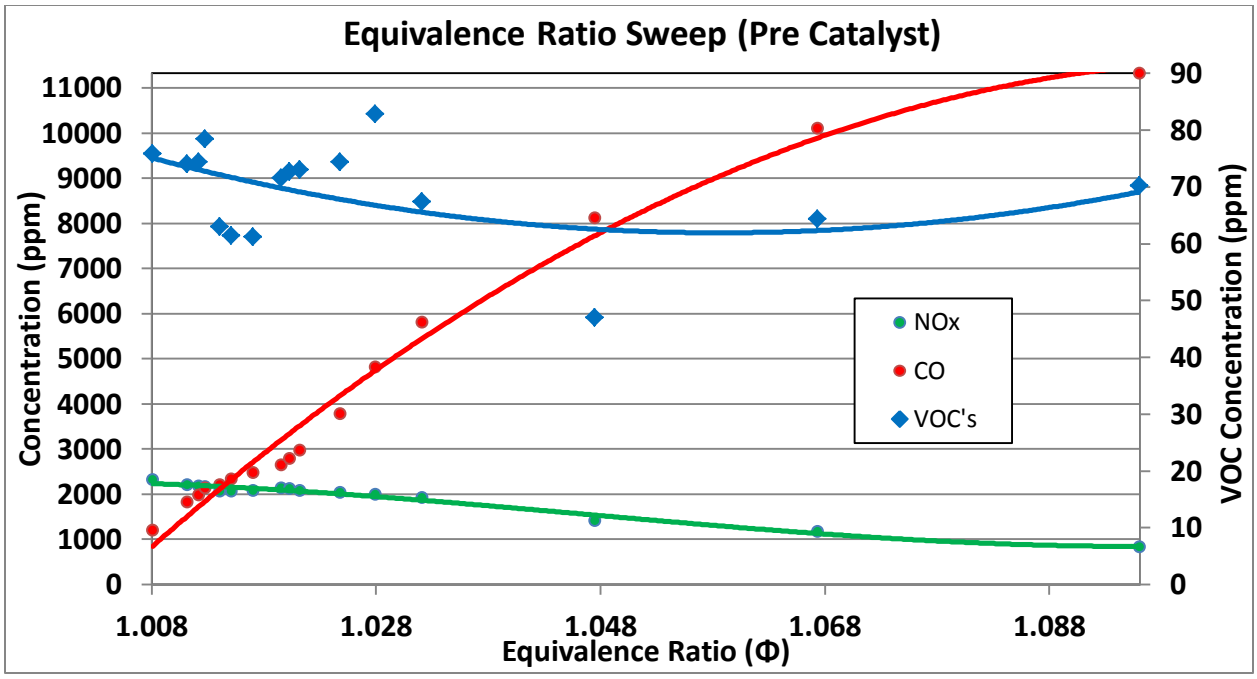

Figure 4-2: Pre catalyst exhaust emissions concentrations (ppm) with respect to equivalence ratio

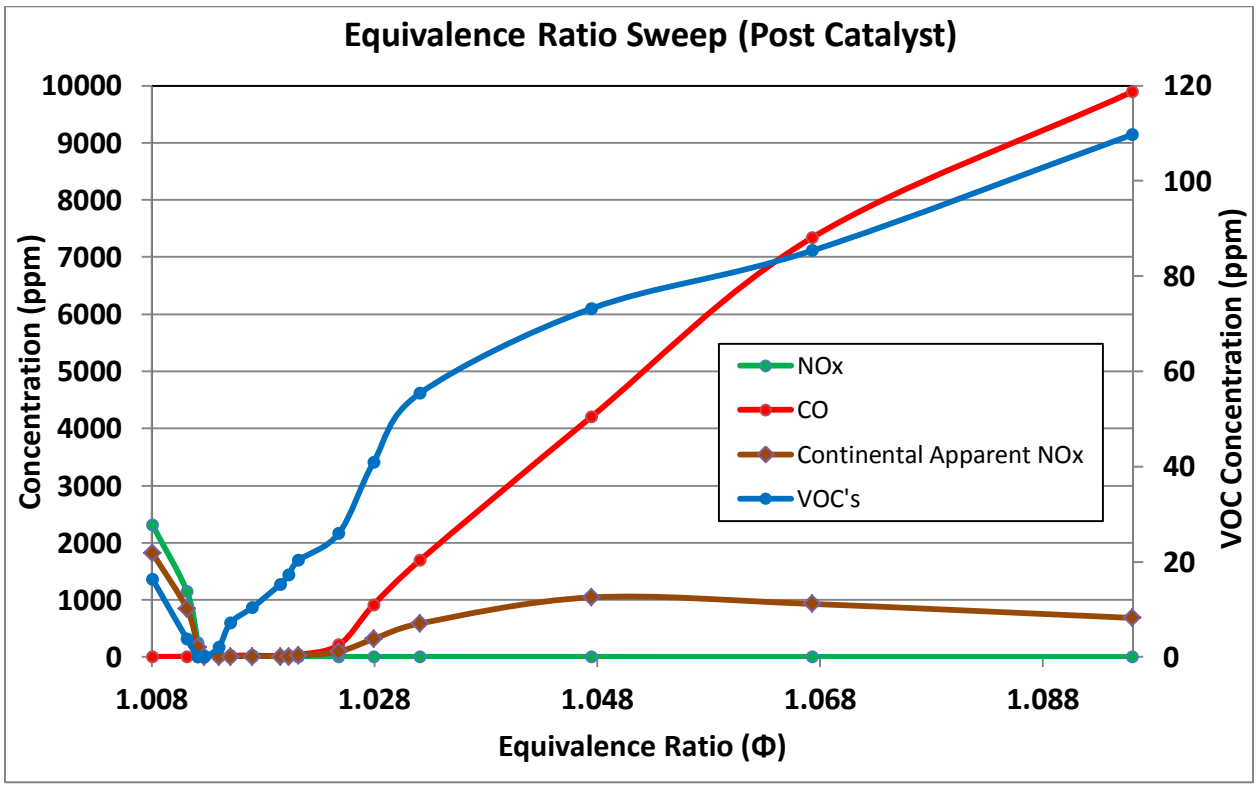

Figure 4-3: Post catalyst exhaust emissions concentrations (ppm) with respect to equivalence ratio

The result is a narrow equivalence ratio operating range to achieve high reduction efficiency of all exhaust pollutant species. When a shift in equivalence ratio in the rich direction occurs, the NOx remains very low. However, the Continental NOx sensor output increases, while NOx remains low. This is likely due to NH_3 formation within the NSCR catalyst under rich operating conditions (DeFoort, Olsen, and Wilson 2004). Through post processing of baseline test data it was determined that at 60% load (48KW electric power), the optimal target AFR was 17.053. This value yielded a combination of the highest reduction efficiencies of all exhaust gas species of interest.

4.4 Load Sweep (Steady State and Transient)

The next test was steady state and transient load variation. Steady state testing was performed in the same manner as the equivalence ratio sweep. Engine load settings of 20, 40, 60, and 80% were chosen for both steady state and transient load testing. Emissions reduction efficiency (%) was calculated by recording and comparing pre and post catalyst concentrations. Reduction efficiency for NOx, CO, THC, and VOC's with respect to engine load is displayed in Figure 4-4.

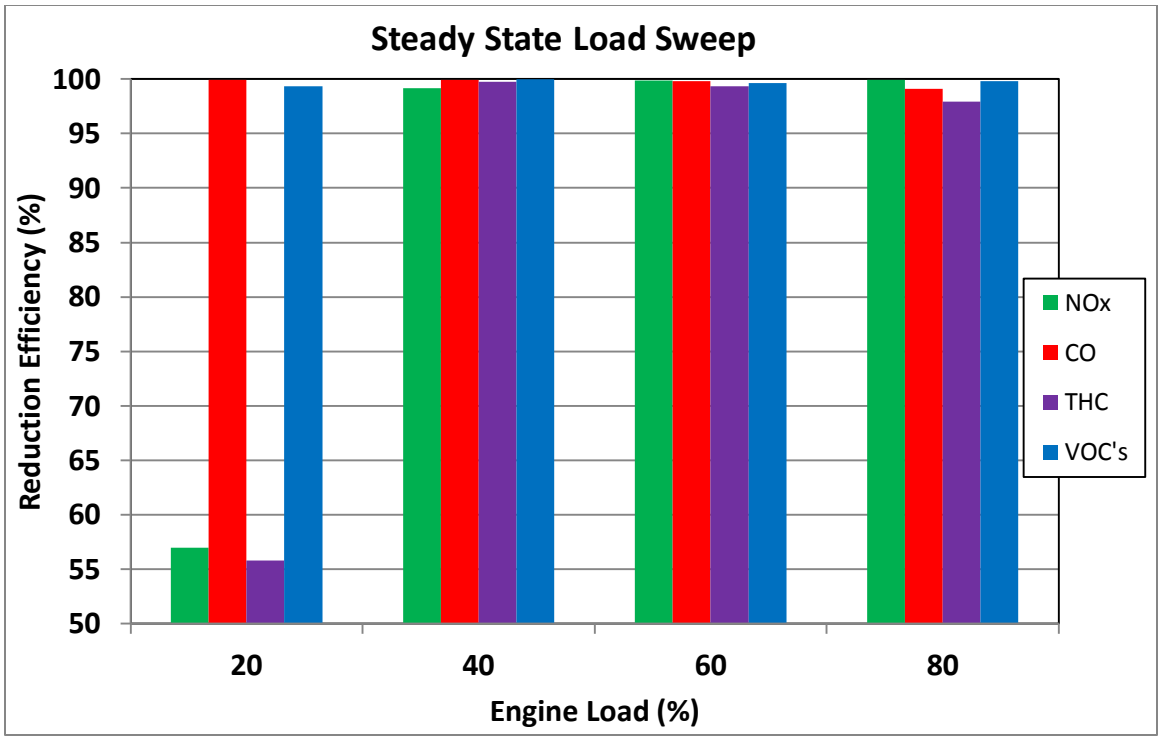

Figure 4-4: Exhaust emissions reduction efficiency with respect to engine load, using lambda feedback

Performance degradation occurs at 20 and 80% load. At 20% load the catalyst temperature decreases, resulting in lower reduction efficiencies and higher emissions concentrations. The data shows that a minor target AFR shift would increase the reduction efficiencies where degradation occurs. NOx sensor feedback control has the potential to make the required AFR adjustment in order to achieve this.

Transient load testing was performed which involved making numerous engine load steps via the generator controls. The ability for the fuel delivery system and catalyst to compensate for load transients is evaluated. As discussed in Section 3.8, the CCC EGC2 settings were optimized in order to achieve this.

The results from the load variation tests indicated that temperature plays a large role in the NSCR catalyst systems ability to achieve high emissions reduction. The higher the load, the higher the catalyst temperature will be. The effects of post catalyst temperature with respect to emissions reduction efficiency using a constant target AFR with lambda feedback control is displayed in Figure 4-5. Temperature and emissions reduction % was acquired from the steady state load sweep data. Although the system was operating at steady state during this test, pre catalyst emissions were continuously varying as well as the actual AFR via lambda feedback.

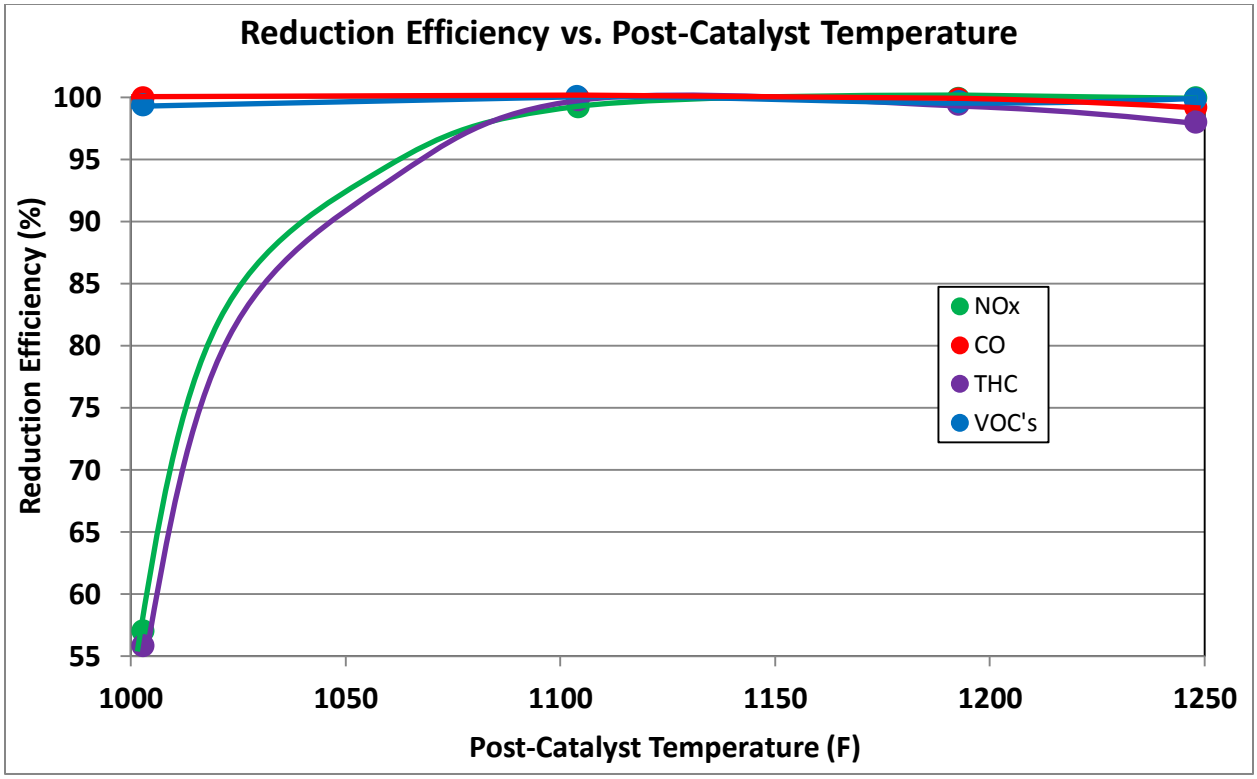

Figure 4-5: Exhaust emissions reduction efficiency with respect to post catalyst temperature

Figure 4-6 shows the transient load test results. When the test was initiated at 0% load, catalyst temperatures were low. As the load was increased the catalyst temperature followed.

The species concentration decreased and emissions reduction efficiency of the catalyst increased. As the load was stepped down from its maximum load of 80%, the emissions reduction efficiency remained higher than that of the corresponding increasing load step.

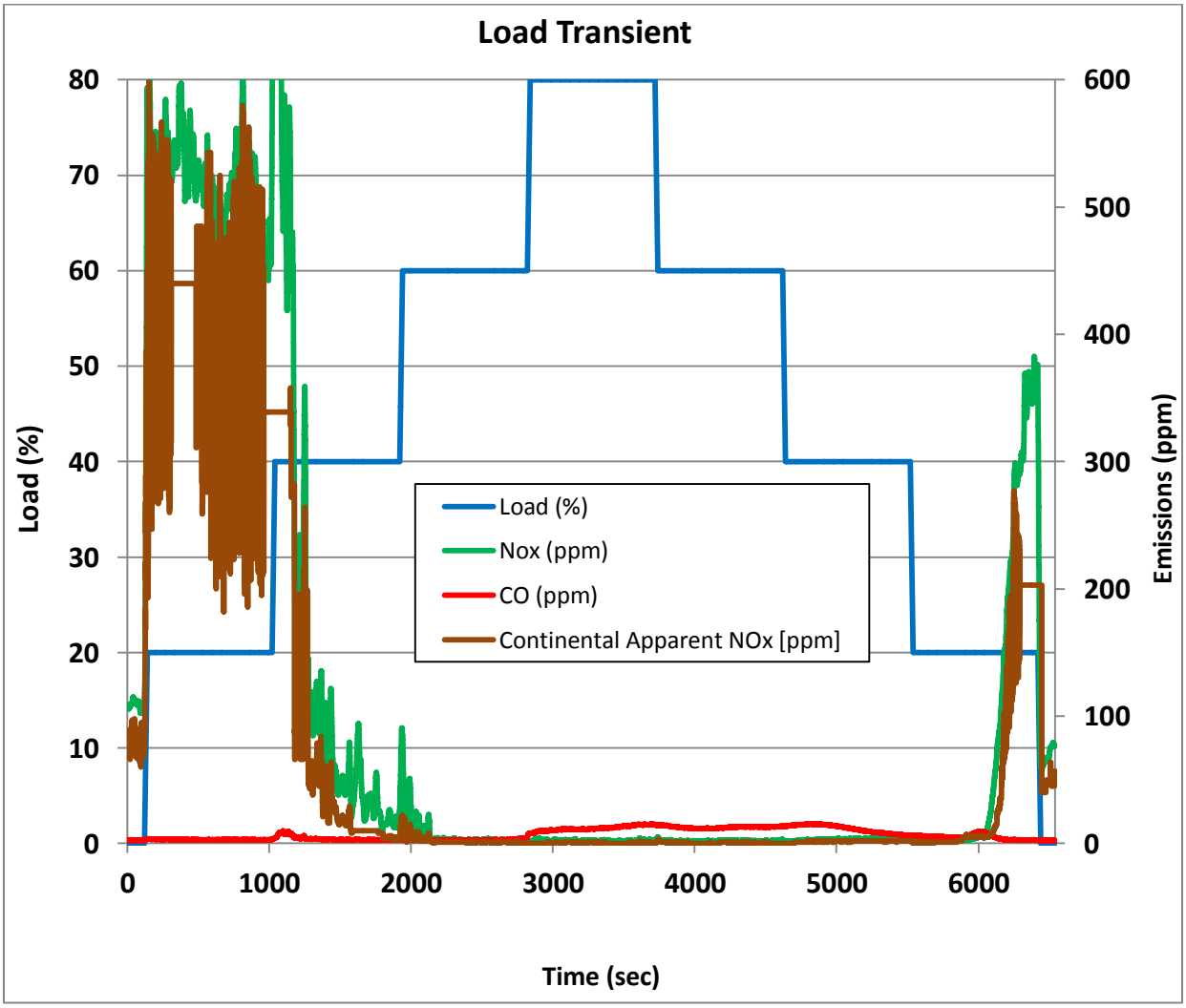

Figure 4-6: Exhaust emissions concentration (ppm) for load transient

This is due to the catalyst retaining heat from the higher load run previously. The time period between each load change is not long enough for catalyst temperatures to reach steady

state before the next load change is performed. Pre and post catalyst temperatures throughout the transient load test can be observed in Figure 4-7.

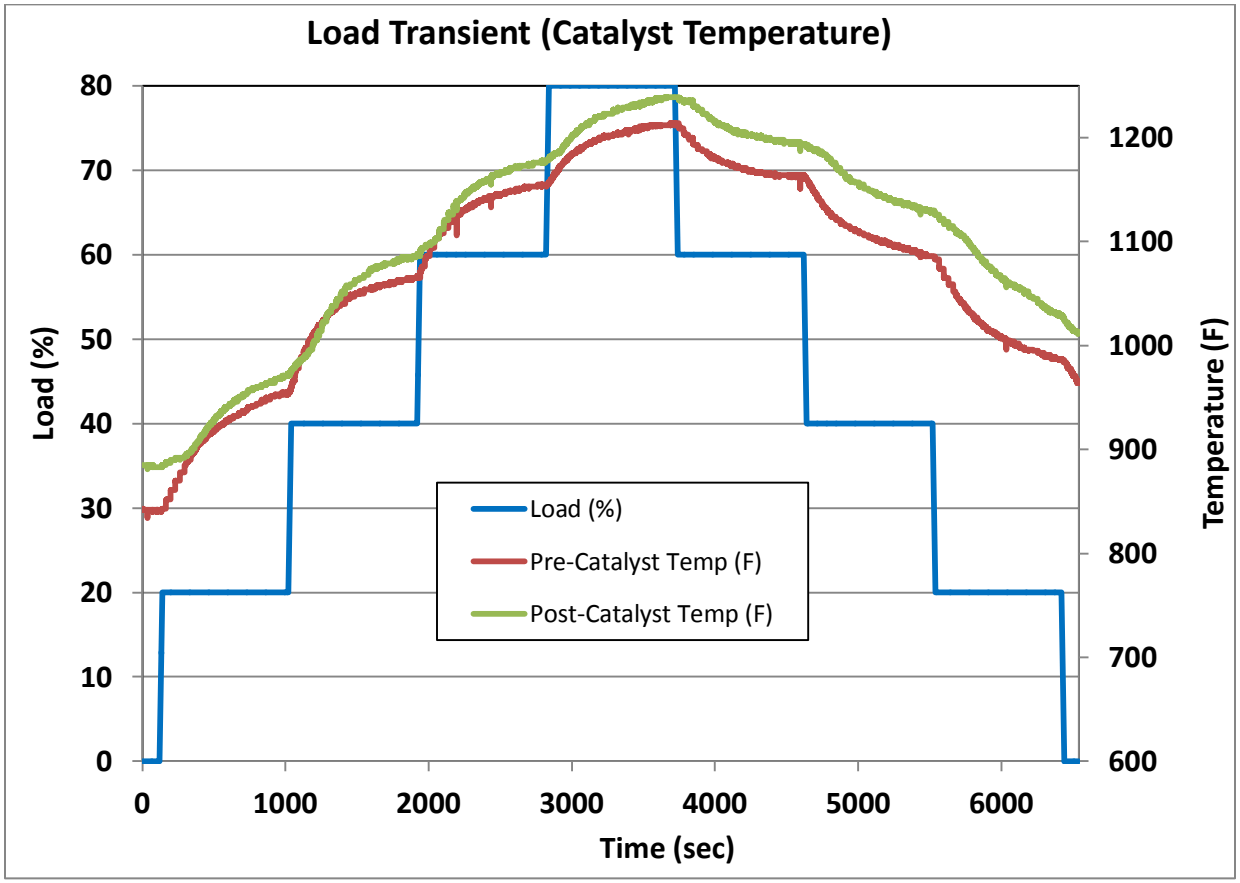

Figure 4-7: Pre and post catalyst temperatures for load transient

4.5 Transient Propane Injection

Propane blending was introduced with the intention to assess the CCC EGC2 and DCL catalyst ability to accurately control fuel delivery and reduce exhaust emissions, respectively. The target flow rates in relation to the actual concentration (molar %) acquired from the fuel

analysis via the GC data is shown in Table 4-3. This data was acquired during steady state engine operation with constant target propane flow rates.

Table 4-3: Propane blending target flow rate (SCFH), actual molar concentration (%), and calculated stoichiometric AFR

Propane Blending (Concentration)	
Target (SCFH)	**Actual (molar %)**
0	0.94
25	4.96
50	10.14
75	16.82
100	30.15

As the target propane flow rate was increased, the calculated stoichiometric AFR decreased in magnitude. Propane has a stoichiometric AFR value greater than that of typical natural gas, therefore as the propane concentration increases, a rich AFR condition is introduced if the AFR is not allowed to be adjusted.

At 60 seconds into the test procedure, propane blending was instantaneously turned on to a target flow rate of 100 SCFH. After 5 minutes, the propane blending was turned off and the engine was allowed to run for an additional 5 minutes. The resulting emissions as well as the NOx sensor's response are displayed in Figure 4-8.

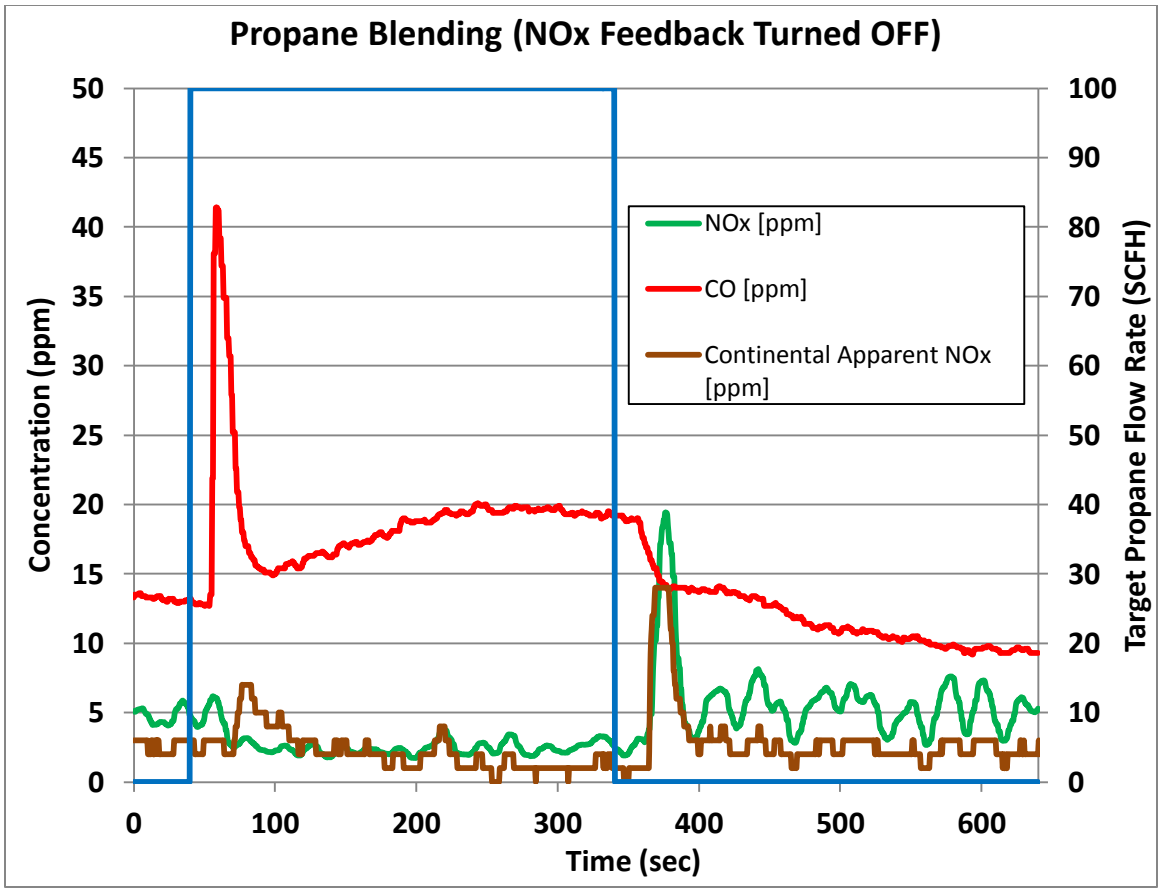

Figure 4-8: Propane blending transient with lambda feedback control

When the lambda feedback reports a need for more or less fuel to achieve the desired target AFR, the fuel pressure is electronically adjusted within the carburetor to compensate for this. For both the steady state and transient propane blending tests, the fuel pressure range entered into the CCC Valve Viewer software was immediately reached at all target propane flow rates. To correct this, the fuel pressure range had to be widened within the software. This was performed prior to repeating the transient propane blending tests discussed within this text. Another issue with the ability of the CCC EGC2 to correctly adjust AFR when doing a fuel

composition shift is that the venture located internal to the carburetor is designed for natural gas fuel which has approximately 1% molar propane concentration.

4.6 Exhaust Back Pressure Transient

The exhaust back pressure transient was developed to create an instantaneous amount of back pressure across the exhaust sensors and the catalyst. Initial testing revealed that steady state operation of the engine at high exhaust back pressures increased the exhaust gas and engine temperatures significantly. Risk of overheating the engine and interrupting testing as well as damaging the catalyst was a concern. In order to perform this test at the 4 possible exhaust back pressure (psig) settings, a transient test protocol was developed. The higher the pressure, the shorter period of time the engine could be operated.

The exhaust back pressure test consisted of the following sequence: (a) operate engine at 0 psig for 1 minute, (b) instantaneously adjusted to 10 psig for 1 minute, (c) 0 psig for 2 minutes to allow cool down, (d) 9 psig for 1 minute, (e) 0 psig for 2 minutes, (f) 5 psig for 2 minutes, (g) 0 psig for 2 minutes, and (h) 1 psig for 5 minutes. The exhaust back pressure transient profile, NOx and CO emissions concentrations, and NOx sensors response is displayed in Figure 4-9.

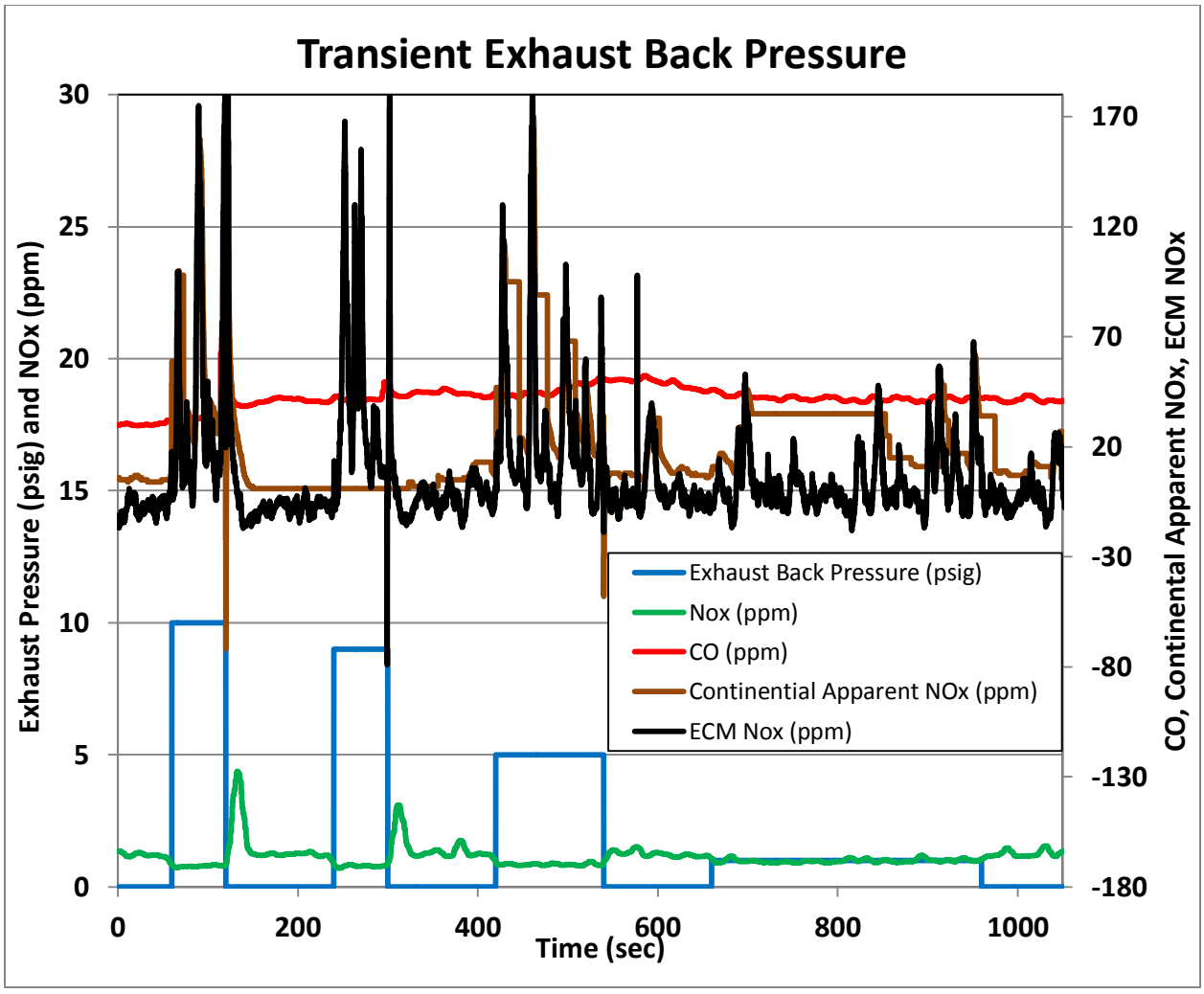

Figure 4-9: Exhaust back pressure transient

The effects of the exhaust back pressure valve were insignificant. NOx and CO concentrations were nearly unaffected and both NOx sensors did not reveal anything in particular. It was decided that the exhaust back pressure test would be removed from future testing using NOx sensor feedback control, since the standard AFR control system was able to maintain catalyst reduction efficiencies. Refer to Appendix II for tabularized data and additional figures from baseline testing.

5. NSCR Control with NOx Sensor Feedback

The minimization control algorithm was developed through multiple iterations. A series of preliminary tests were performed prior to the final testing using NOx sensor feedback fuel control. This consisted of optimizing the control algorithm by adding control variables and going through an iterative testing process to determine the values that made the algorithm behave appropriately under various engine operating conditions.

5.1 Control Algorithm Development

NOx sensor feedback fuel control was implemented utilizing a minimization control algorithm that was programmed into LabVIEW. Various control parameters were chosen to be adjustable by the user via a graphical user interface within LabVIEW, and are described in Table 5-1. The Continental NOx sensor returns a value every 50ms or at a rate of 20Hz. It was determined that a write rate of 10 seconds worked well, which corresponds to 200 samples being taken upon each iteration. Manual lambda setpoint was used initially to see how the control algorithm could drive the NOx sensor output to a minimum from both lean and rich burn operating points. Adaptive lambda increment size coupled with NOx output range was required to minimize the time taken to drive the NOx sensor to a minimum as well as ensure that over shoot was limited. The lean multiplier (LM) and rich multiplier (RM) are gains applied to the lambda increment size based on whether the AFR was moving lean or rich, respectively.

Figure 5-1 displays the Continental NOx sensors apparent NOx concentration (ppm) with respect to lambda.

Table 5-1: Control algorithm variables

Control Variable	Operation
Write Rate (Hz)	Determines the sampling rate or # of samples to be compared
Manual Lambda Setpoint	Allows an offset from Target AFR entered in CCC Valve Viewer software
Adaptive Lambda Increment Size	Implemented array determines step size with respect to NOx sensor concentration (ppm)
NOx Output Range	NOx sensor concentration (ppm) ranges allowing variable lambda increment size
Lean Multiplier (LM)	Gain value applied to lambda increment size, for positive lambda step
Rich Multiplier (RM)	Gain value applied to lambda increment size, for negative lambda step

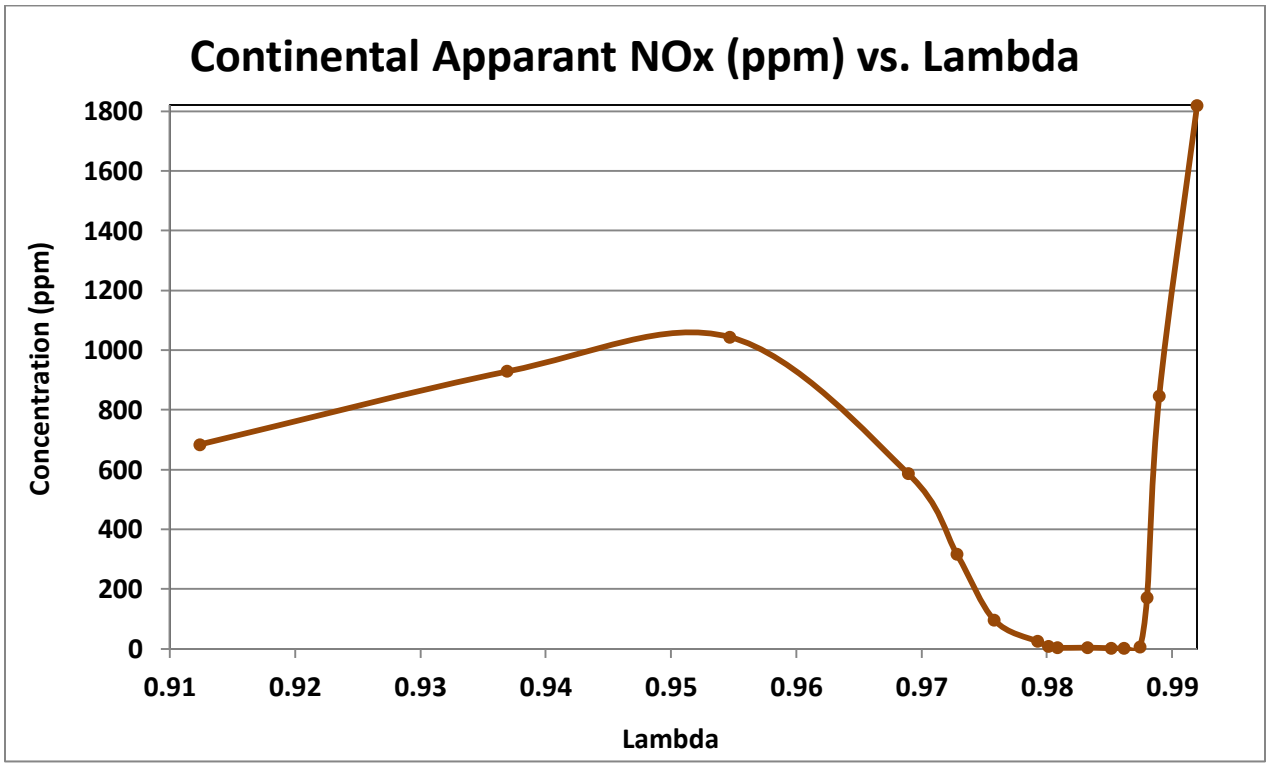

Figure 5-1: Continental NOx sensor behavior with respect to lambda

The minimization control algorithm logic is displayed in Figure 5-2. A sample of NOx sensor values based on the sampling rate specified are taken and then averaged. An additional sample is acquired and averaged immediately after and then compared to the previous. If the latter sample is lower in magnitude, then a lambda increment size is executed in the same direction as the previously performed step. The step size is determined based on the adaptive increment lookup table which was developed as a 7 point array that relates the lambda step size to the NOx sensor concentration (ppm).

If the latter sample is larger in magnitude, this represents a step taken in the wrong direction upon which the algorithm will execute a lambda increment step in the opposite direction. The algorithm has no regard to which side of the equivalence ratio curve the engine is operating on (rich or lean). A positive or negative lambda increment step size is determined from the previous step taken and whether this yielded an increase or decrease in NOx sensor concentration. When the lambda step taken is a positive value, the LM is applied to the step size. When the lambda step taken is negative, the RM gain is applied. The difference in magnitudes was determined through an iterative testing process prior to final testing using NOx sensor feedback control. A value of 1.3 for the LM and 0.7 for the RM was used during final testing. Due to the non-symmetry of the NOx sensor output curve with respect to equivalence ratio, the target minimum had to be approached with separate magnitudes depending on the direction of travel as shown in Figure 5-1.

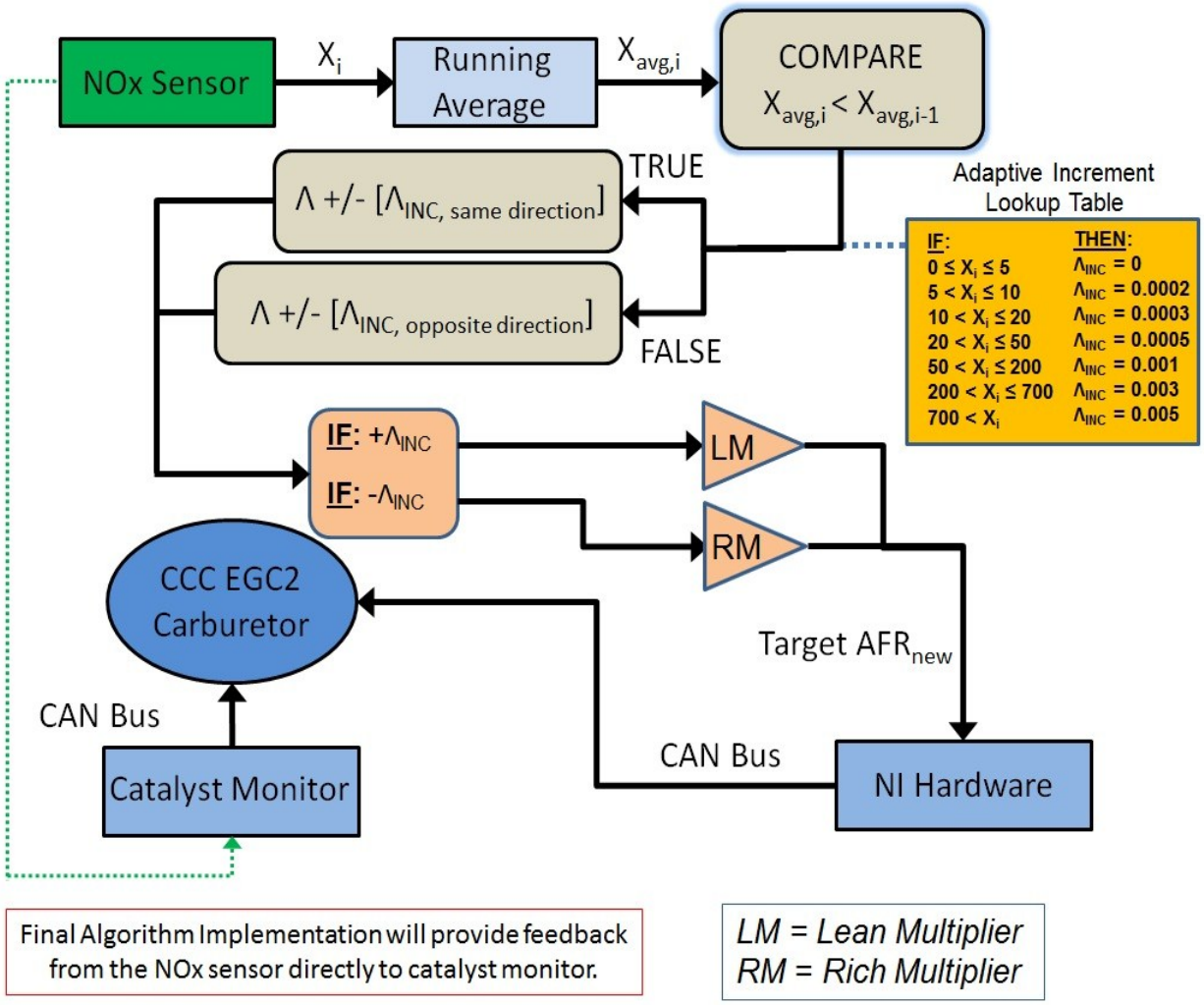

Figure 5-2: Minimization control algorithm flow chart and logic for NOx sensor feedback control

During testing, the NOx sensor feedback and lambda increment step size was communicated through the CAN Bus wired into the NI-9853 hardware.

5.2 Test Results

Final testing utilizing NOx sensor feedback fuel control consisted of multiple steady state and transient tests. Tests were performed initially in order to see if the control algorithm could

drive the NOx sensor concentration to a minimum. During this process, turning dithering off appeared to drive the NOx sensor to a minimum slightly faster. Using the manual lambda set point control variable, the system was initialized at a rich and lean starting point and then NOx sensor closed loop operation was activated. Figure 5-3 and Figure 5-4 displays the ability of the control algorithm to drive the NOx sensor concentration (ppm) to a minimum value and maintain it. The corresponding AFR via the ECM AFRecorder 4800R is displayed as well.

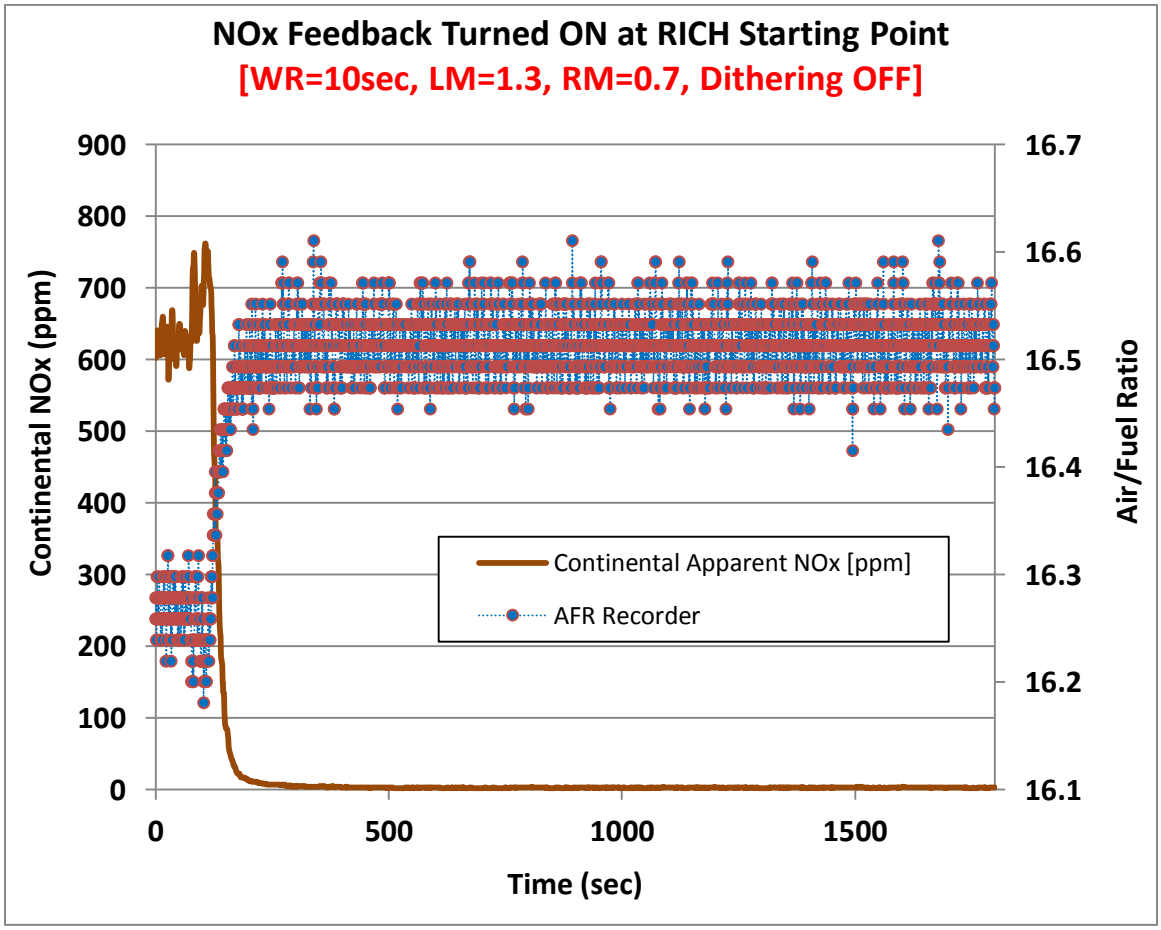

Figure 5-3: NOx sensor closed loop operation turned on at rich starting point

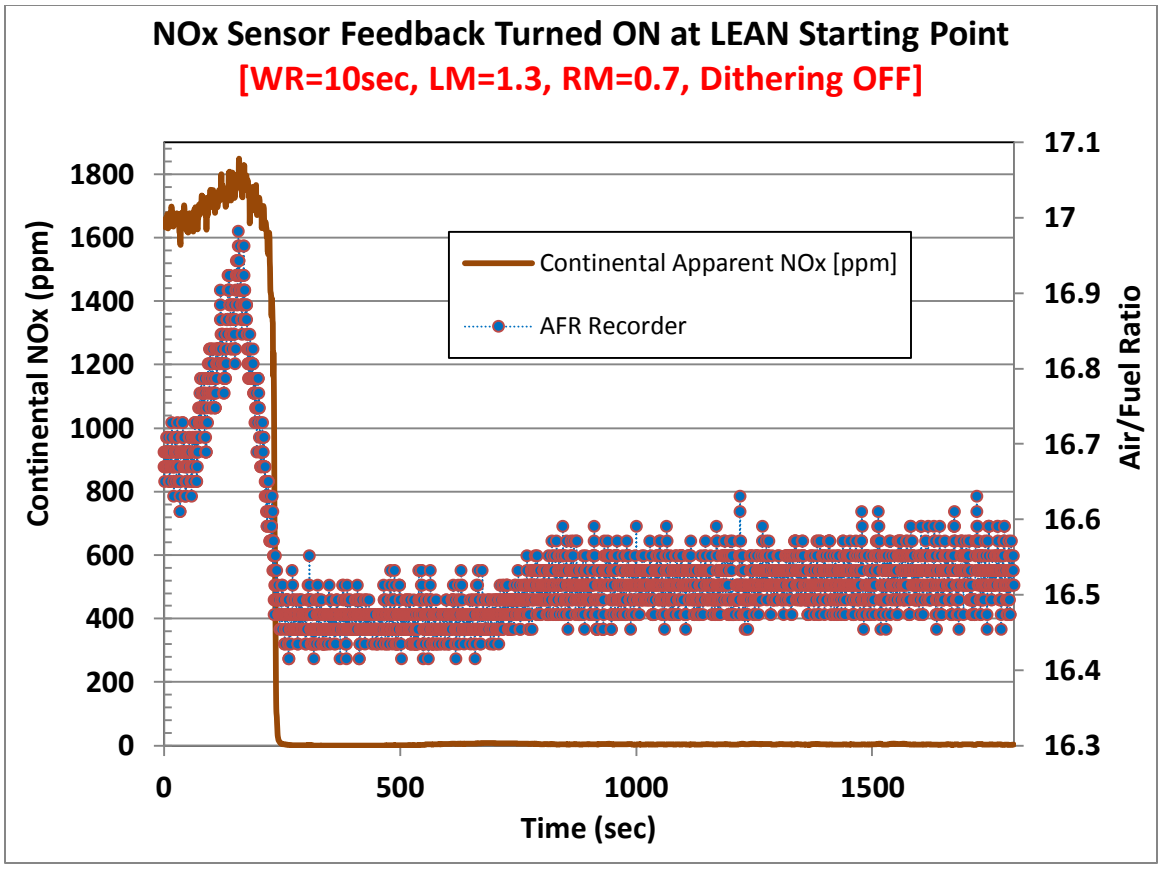

Figure 5-4: NOx sensor closed loop operation turned on at lean starting point

The chemical delay within the NSCR system as the equivalence ratio sweeps from one side of the NOx sensor minimum to the other was investigated. Figure 5-5 and Figure 5-6 displays these trends. The system was initialized at a lean burn starting point using the manual lambda set point, allowed to run for 60 seconds and then manually adjusted rich with NOx feedback disabled. The test was repeated but at a rich starting point and manually adjusting the lambda set point lean. This time delay makes it difficult for the system to handle transients without overshoot. The reaction rates of NH_3, O_2, and NO as well as the Pt and Rh concentration in the NSCR catalyst system plays a large role (Heck and Farrauto 2009). If the

sampling rate is extended to compensate then the response time to drive the NOx sensor back to a minimum is increased as well. Sweeping from lean to rich took the NOx sensor a time period of approximately 2.5 minutes to reach steady state concentrations. Sweeping from rich to lean took approximately 8 minutes. NH_3 production in the NSCR catalyst system takes significantly less time than purging the NH_3 from the catalyst by introducing a chemical reaction with NOx that is produced by the engine operating lean burn. Engine exhaust emissions were observed prior to the NOx sensor response.

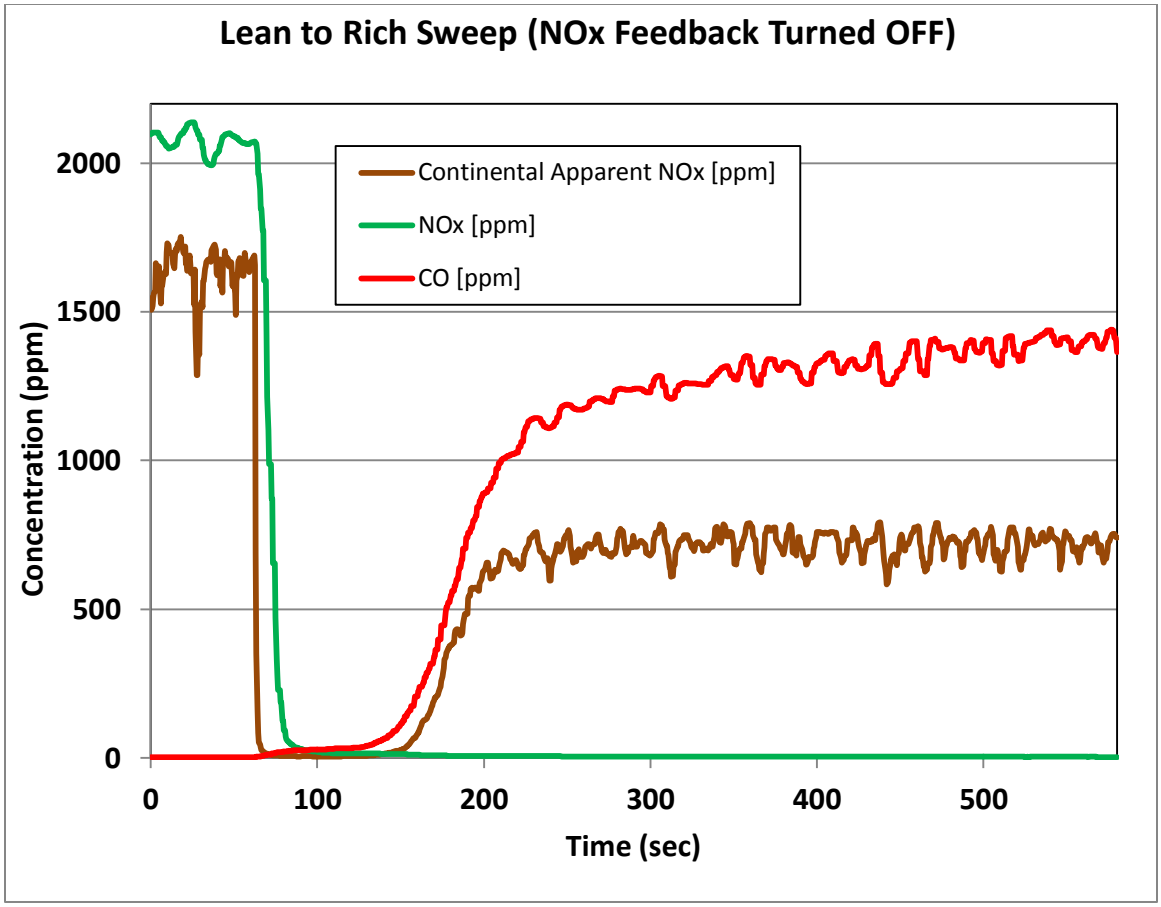

Figure 5-5: NOx sensor and exhaust emissions response for manual lean to rich sweep

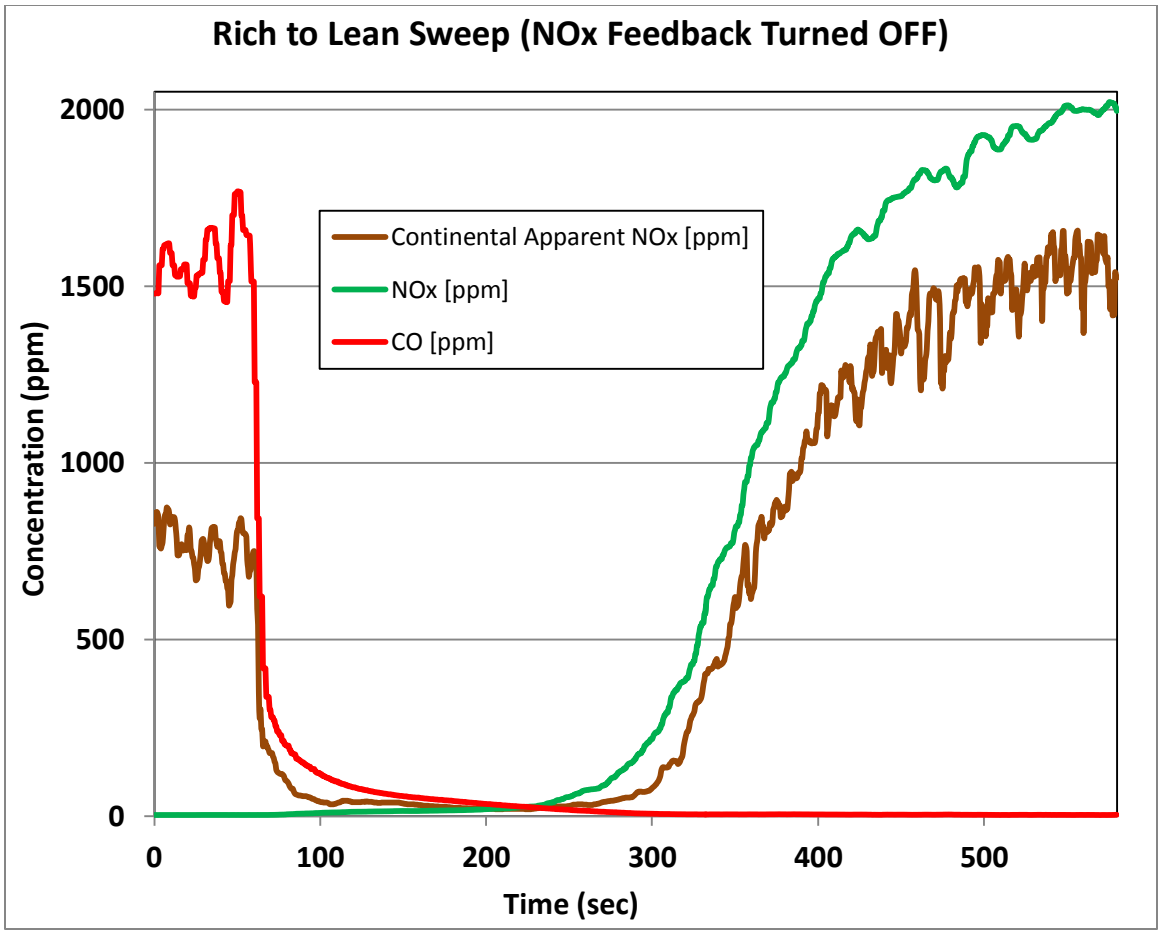

Figure 5-6: NOx sensor and exhaust emissions response for manual rich to lean sweep

Steady state load testing was repeated from baseline testing by operating the engine at 20, 40, 60, and 80% load settings and acquiring 5 minute averaged pre and post catalyst concentrations. The results of the load sweep with closed loop NOx sensor fuel control are displayed in Figure 5-7. Initially closed loop NOx control was enabled before testing proceeded. Before each load setting was recorded, the control algorithm was allowed to make the required lambda adjustment until the NOx sensor concentration was driven to a minimum.

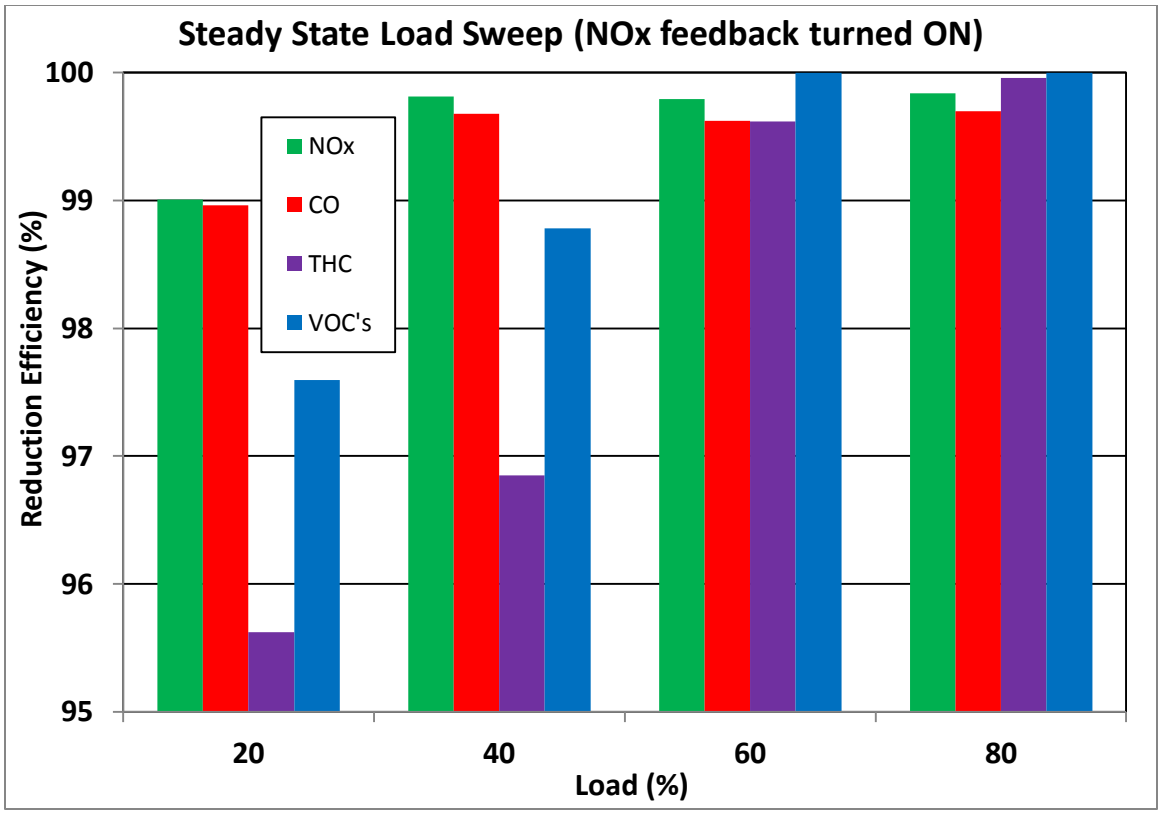

Figure 5-7: Exhaust emissions reduction efficiency with respect to engine load, with NOx sensor feedback control

The improvement using NOx feedback control is significant in comparison to baseline testing using only lambda feedback control. Table 5-2 displays the exhaust emissions concentration with respect to brake specific power (g/bkW-hr) for NOx, CO, and VOC's for both baseline testing using lambda feedback and final testing using NOx sensor feedback control. The highlighted cells represent the emissions concentration that meet or exceed CARB 2007 emissions standards. The NSCR catalyst reduction efficiency % improvement between lambda feedback and NOx feedback control is displayed as well.

Table 5-2: Post catalyst BSE (g/bkW-hr) and reduction efficiency (%) for steady state load sweep. Comparison of lambda versus NOx sensor feedback control is displayed, as well as reduction efficiency improvement (%)

		Post Catalyst Concentration (g/bkW-hr)		
	Load (%)	NOx	CO	VOC's
CARB 2007	----------	0.032	0.045	0.009
Lambda Feedback	20	3.432	0.013	0.003
	40	0.114	0.013	0.003
	60	0.023	0.024	0.003
	80	0.015	0.077	0.002
NOx Feedback	20	0.065	0.053	0.006
	40	0.022	0.040	0.003
	60	0.028	0.034	0
	80	0.026	0.025	0
		Emissions Reduction Efficiency (%)		
Lambda Feedback	20	56.990	99.900	99.310
	40	99.170	99.900	100.000
	60	99.860	99.780	99.610
	80	99.920	99.130	99.800
NOx Feedback	20	99.006	98.964	97.597
	40	99.812	99.681	98.784
	60	99.795	99.624	100
	80	99.837	99.699	100
Reduction Efficiency % Improvement	20	42.02	-0.94	-1.71
	40	0.64	-0.22	-1.22
	60	-0.06	-0.16	0.39
	80	-0.08	0.57	0.20

At lower loads, the required lambda increment in the rich direction made by the NOx feedback control improve NOx concentration significantly and was able to meet CARB 2007 NOx standards. At high load (80%) the required lambda increment in the lean direction was performed by the NOx feedback control and yielded a significant improvement in CO concentration, meeting the CARB 2007 CO standards. Limits for VOC's were met with both

lambda feedback and NOx sensor feedback control testing at all loads. The summed total of reduction efficiency % Improvement for the steady state load sweep test is 39.43 %.

The transient load test was repeated from baseline testing. Figure 5-8 displays the results. NOx concentration at lower loads was improved significantly. When the engine load was increased on the first half of the test, the NOx sensor control system experienced overshoot. The lambda increment was initially decreased (rich) when NOx sensor concentration spiked at the 20% load step. The system reacted to this and then took a positive lambda step (lean) too far, causing CO concentration to increase. It continued to oscillate until about half way through the test and then maintained a minimum NOx sensor feedback concentration. Average exhaust emissions reduction over the course of the test were not significantly reduced. The system did demonstrate the ability to recover from the initial transients and drive the NOx sensor to a minimum though.

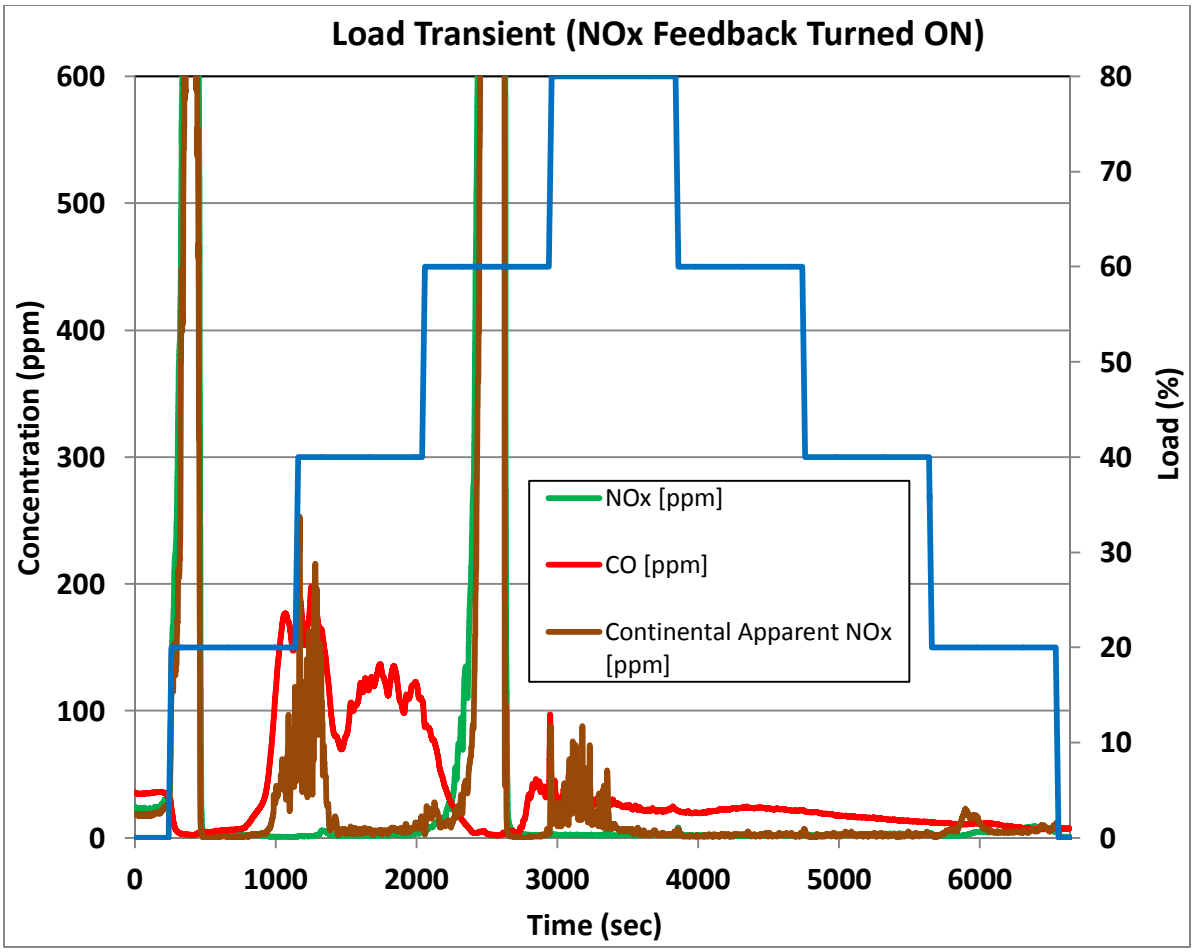

Figure 5-8: Load transient with closed loop NOx sensor feedback

Transient propane blending was repeated from baseline testing. The results are shown in Figure 5-9. Average exhaust emissions concentrations using NOx sensor feedback fuel control were not significantly improved over baseline testing using lambda feedback control. Exhaust emissions were driven to approximately the same concentration values at the end of the test. The system demonstrated the ability to recover from the fuel composition transient and minimize the NOx sensor concentration.

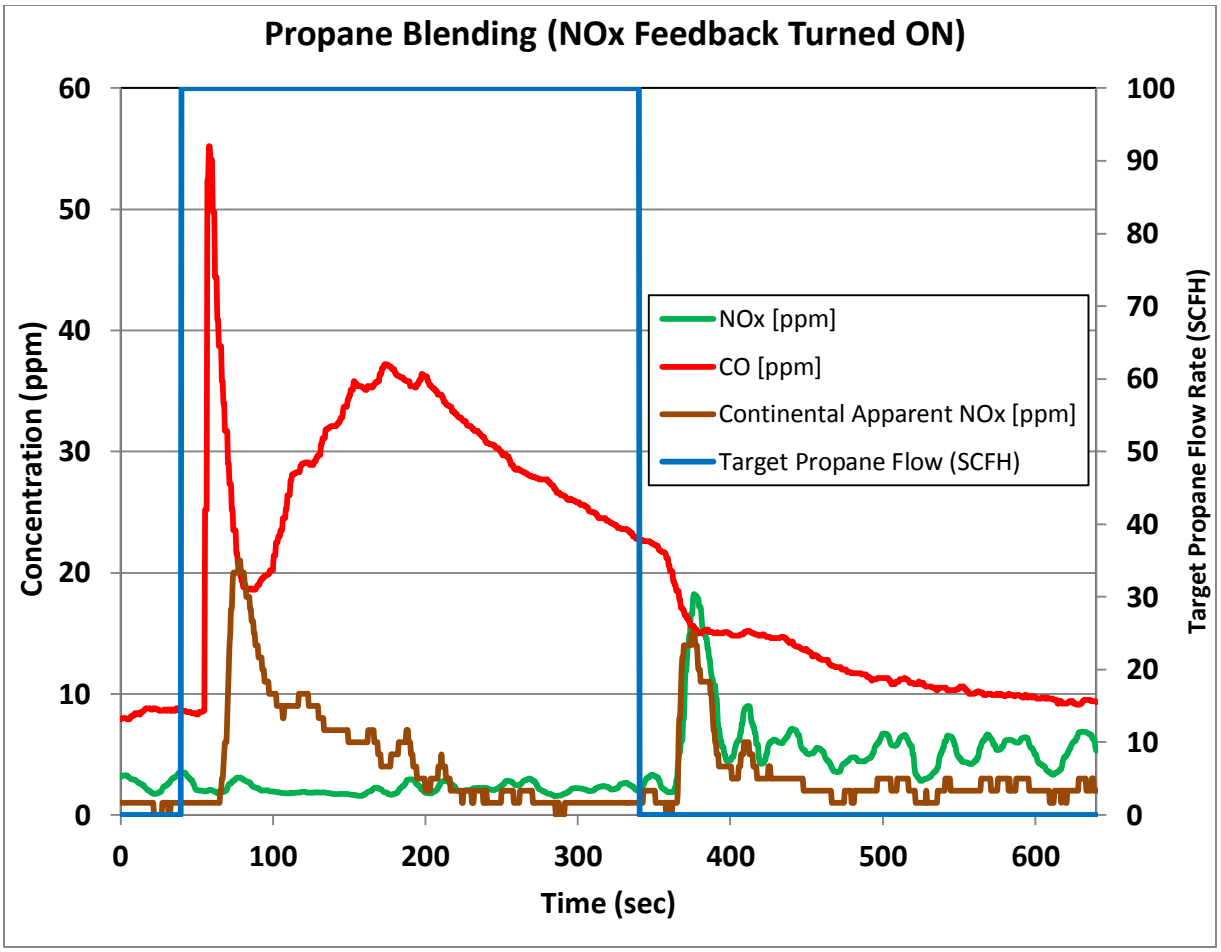

Figure 5-9: Transient propane blending with closed loop NOx sensor feedback

6. Summary and Conclusions

This work was intended to evaluate if utilizing a post catalyst NOx sensor for closed loop fuel control for NSCR catalysts was feasible. For proper NSCR catalyst system operation and high exhaust emissions reduction efficiency to occur, equivalence ratio must be precisely controlled. The engine platform utilized was a Cummins-Onan 100kW Generator Set, model GGHD 60HZ, which incorporates a 7.5 liter SI natural gas ICE. The engine was reconfigured for testing utilizing an electronic carburetor with lambda feedback, NSCR catalyst assembly, instrumentation, and required data acquisition system. A thorough test plan was developed and performed using lambda sensor feedback control as baseline for comparison. A control algorithm to drive the NOx sensor concentration to a minimum was developed in LabVIEW. Final testing with the minimization control algorithm using NOx sensor closed loop fuel control was performed following algorithm refinement and optimization.

An equivalence ratio sweep performed during baseline testing displayed the precision fuel control required to maintain high emissions reduction efficiency of CO, NOx, and VOC's in a NSCR system. Target equivalence ratio control must be maintained to approximately plus/minus 0.5%. Steady state testing at 20, 40, 60, and 80% load revealed that the AFR needs to be shifted at each setting due to the change in catalyst temperature. The required magnitude was approximately 0.002 lambda between each load, with the AFR adjusted more rich at lower loads. Final testing using NOx sensor feedback control improved the reduction

efficiency significantly at lower loads to that of baseline testing using only lambda sensor feedback. The load transient showed significant improvement at lower loads using NOx sensor feedback by shifting the AFR, reducing NOx concentration. Improvement for the fuel composition transient (propane blending) was not observed. The system recovered in a similar manner and drove NOx and CO concentrations as well as the NOx sensor output to minimum values of nearly identical magnitudes.

The motivation for this work was without regard to the chemical delay that occurs within the NSCR catalyst system when sweeping from one side of the NOx sensor minimum to the other. The reaction rates of NH_3, O_2, and NO as well as the Pt and Rh concentration in the NSCR catalyst system plays a large role (Heck and Farrauto 2009). This large time delay results in system overshoot unless the sampling rate is extended significantly. Sweeping from lean to rich took the NOx sensor a time period of approximately 2.5 minutes to reach steady state concentrations. Sweeping from rich to lean took approximately 8 minutes. Producing NH_3 in the NSCR catalyst system takes significantly less time than purging the NH_3 from the catalyst by introducing a chemical reaction with NOx that is produced by the engine operating lean burn. This is feasible for long term steady state engine operation, however, will not compensate for a transient condition within a reasonable time.

6.1 Recommendations for Future Work

Given the opportunity to continue this project and improve upon closed loop NOx sensor fuel control, various approaches could compliment the system. If more time permitted, more optimization of the existing control parameter values could be carried out. Further

development of the existing control algorithm could be done. The adaptive increment array could be expanded to include more points, making the rate at which the lambda set point needs to be adjusted based on NOx sensor concentration (ppm) more precise. Other control mechanisms could be investigated and implemented as well.

Currently the minimization control algorithm implemented is simply a proportional controller with a nonlinear gain. It does not have an integral or derivative gain incorporated, causing overshoot to occur. The same control logic where 2 samples are continuously averaged and then compared could remain the same as well as the adaptive lambda increment array. However, rather than having only a non symmetric proportional gain (LM and RM) based on which side of the NOx sensor response curve the engine is operating on, an integral and derivative gain could be implemented as well. By incorporating a Proportional Integral Derivative (PID) gain control, the system could be improved upon. The proportional gain depends on the current error, the integral term depending on the accumulation of past errors, and the derivative term predicting future errors. The addition of the integral gain would help maintain steady state operation where random oscillations occur due to instability.

The addition of a pre-catalyst NOx sensor could provide better control. The additional NOx sensor could distinguish which side of the spectrum the system is operating on. The post catalyst NOx sensor would operate as displayed through the results of this project and the pre catalyst NOx sensor would be there only to measure under lean burn operation. During rich burn, the pre catalyst sensor would remain at a minimum due to low engine out NOx and no NH_3 production. If the system experienced overshoot in the lean direction, the pre catalyst NOx sensor would acknowledge this much sooner than the post catalyst sensor. The concentration

differential of the 2 sensors would represent which side of the curve the engine is operating on. Implementing the additional pre catalyst NOx sensor could allow for the sampling rate to operate faster and transient response times could be maintained without overshoot.

The final step is to implement the minimization control algorithm into the CCC Catalyst Monitor. The Continental NOx sensor, CCC EGC2 and Catalyst Monitor are all on the CAN Bus, allowing lambda increment adjustments to take place without the use of LabVIEW.

REFERENCES

Amadu, Sule, and Daniel Olsen. 2008. “Operating Characteristics of an NSCR Catalyst on an 80 kW Cummins-Onan Genset.”

BASF Corporation. “Lean NOx Trap.” http://www.catalysts.basf.com/p02/USWeb-Internet/catalysts/e/content/microsites/catalysts/prods-inds/mobile-emissions/lnt.

Bosch. 2006. “Bosch Lambda Sensor.” http://www.bosch-lambdasonde.de/en/downloads/bosch_lambdasonden_no1.pdf.

CEPA ARB. 2007. “Energy - Distributed Generation Program”. Government. *California Environmental Protection Agency Air Resources Board*. http://www.arb.ca.gov/energy/dg/dg.htm.

Cheney, Ward, and David Kincaid. 1994. *Numerical Mathematics and Computing*. 3rd ed. Brooks/Cole Publishing Company.

Cho, Haeng Muk, and Bang-Quan He. 2007. “Spark Ignition Natural Gas engines—A Review.” *Energy Conversion and Management* 48 (2) (February): 608–618. doi:10.1016/j.enconman.2006.05.023.

Continental. 2008. “Continental NOx Sensor Technical”. Siemens VDO Automotive AG.

Continental Controls Corporation. 2008. “Electronic Gas Carburetors EGC2/EGC4.” www.continentalcontrols.com.

Continental Controls Corporation. 2010. “Catalyst Monitor and Datalogging.” www.continentalcontrols.com.

DeFoort, Morgan, Daniel Olsen, and Brian Wilson. 2004. “The Effect of Air-fuel Ratio Control Strategies on Nitrogen Compound Formation in Three-way Catalysts.” *International Journal of Engine Research* 5 (1) (February 1).

Energy and Environmental Analysis. 2008. “Technology Characterization: Reciprocating Engines.”

Engine Control and Monitoring. 2008. “NOx 5210(g) Single/Dual NOx Analyzer Instruction Manual.”

Gerald, Curtis, and Patrick Wheatley. 2004. *Applied Numerical Analysis*. 7th ed. Addison-Wesley.

Gonnet, Gaston. 2002. “1.5.2 Brent’s Method (Golden Section Search in One Dimension).” *Scientific Computation*. http://linneus20.ethz.ch:8080/1_5_2.html.

Heck, Ronald, and Robert Farrauto. 2009. *Catalytic Air Pollution Control: Commercial Technology*. 3rd ed. John Wiley & Sons Inc.

Heywood, John. 1998. *Internal Combustion Engine Fundamentals*. McGraw Hill.

Inagaki, Hiroshi, Takafumi Oshima, Shigeru Miyata, and Noriaki Kondo. 1998. *NOx Meter Utilizing ZrO2 Pumping Cell*. Warrendale, PA: SAE International. http://papers.sae.org/980266.

DCL International. 2009. “Catalytic Converters & Silencers for Stationary Engines Below 700hp.” http://www.dcl-inc.com/threewaycatalyst/12.

Johnson Matthey Catalysts. “Johnson Matthey Catalysts.” http://www.jmcatalysts.com/.

Korakianitis, T. 2009. “Natural-gas Fueled Spark-ignition (SI) and Compression-ignition (CI) Engine Performance and Emissions.” *Science Direct* (August 21). http://www.sciencedirect.com/science/article/pii/S0360128510000377.

Marquis, Brent. 2001. “A Semiconducting Metal Oxide Sensor Array for the Detection of NOx and NH3 10.1016/S0925-4005(01)00680-3 : Sensors and Actuators B: Chemical | ScienceDirect.com.” http://www.sciencedirect.com/science/article/pii/S0925400501006803.

Navarro, Xavier. 2008. “Renault Announces New NOx Trap Features in New Diesel Catalytic Converter.” *Autobloggreen*. http://green.autoblog.com/2008/06/26/renault-announces-new-nox-trap-features-in-new-diesel-catalytic/.

NGK. 2012. “NGK - NOx Sensor.” http://www.ngkeurope.com/en/products-technologies/lambda-sensors/lambda-sensor-technologies/special-sensors/nox-sensor/.

Nuss-Warren, Sarah, and Keith Hohn. 2011. “Final Report: Cost-Effective Reciprocating Engine Emissions Control and Monitoring for E&P Field and Gathering Engines.”

Onan Corporation. 2001a. “GGHD Spec Sheet”. Cummins Onan.

Onan Corporation. 2001b. “GGHD Alternator Data Sheet”. Cummins Onan.

Pulkrabek, Willard. 2004. *Engineering Fundamentals of the Internal Combustion Engine*. 2nd ed. Pearson Education, Inc.

Schmitt, Josh. 2010. “Selective Catalytic Reduction: Testing, Numeric Modeling, and Control Strategies.” (Master’s Thesis). Colorado State University, Fort Collins, CO.

US EPA. 2011. “Rule and Implementation Information for Oil & Natural Gas Production.” *United States Environmental Protection Agency*. http://www.epa.gov/ttn/atw/oilgas/oilgaspg.html.

Vronay Engineering Services Corp. 2011. *Performance Evaluation of a State-of-the-Art Air/Fuel Ratio Control System and an NSCR Catalyst on a Spark-Ignited Natural Gas Fueled Engine Operating at Fontana Wood Preserving Fontana California*.

Vronay, John, Ranson Roser, John Pratapas, Serguei Zelepouga, and Hilary Grimes. 2010. *Task 2.4 SENSOR SCREENING TEST REPORT Task 5 EMISSION SYSTEM TEST PLAN & EMISSION SYSTEM DEVELOPMENT REPORT*.

Woo, Leta. 2010. "NOx Sensor Development" June 10, Lawrence Livermore National Laboratory.

Appendix I– Experimental Setup and Hardware

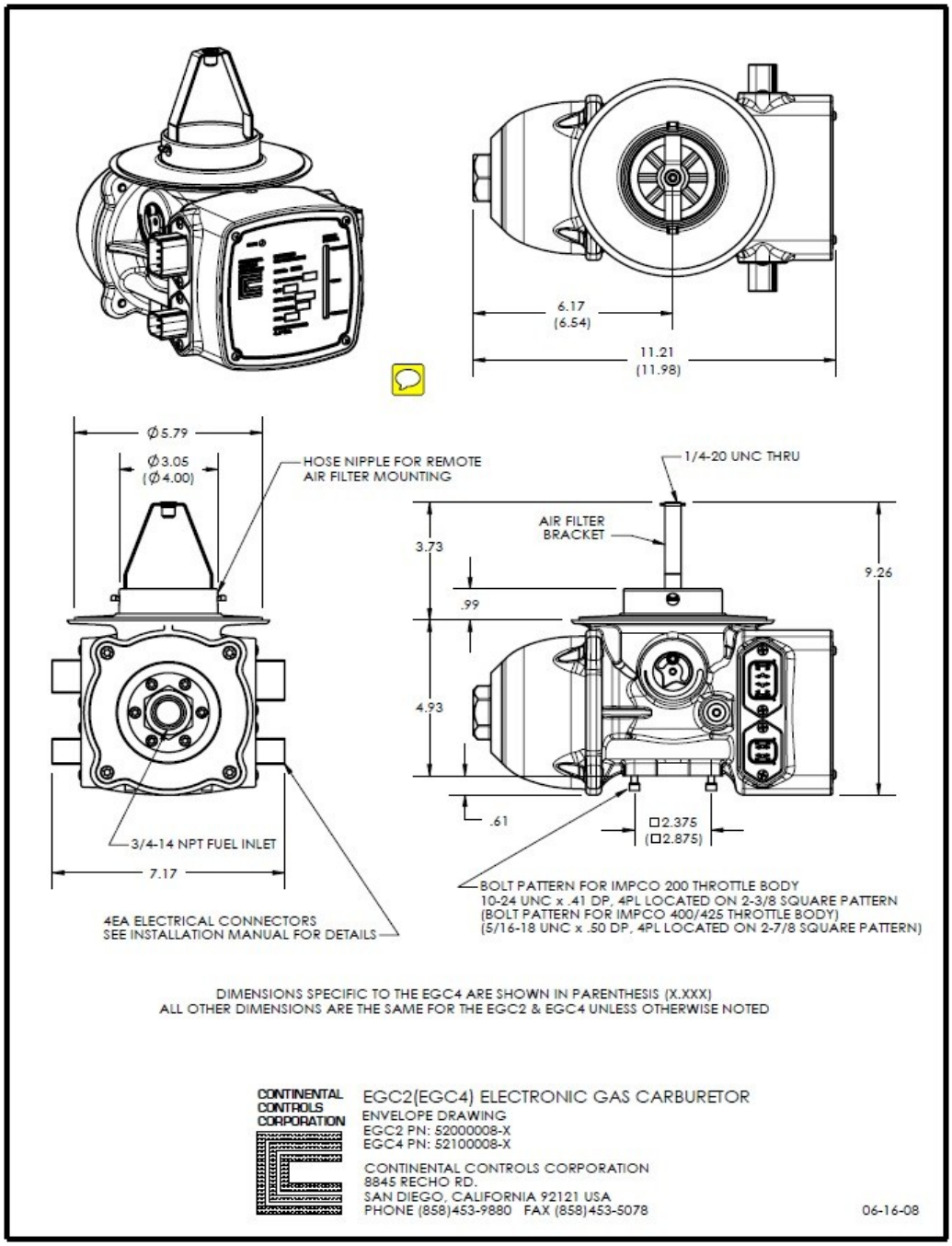

REVISIONS			
LTR	DESCRIPTION	DATE	APPRVD
–	PRELIMINARY RELEASE	1.21.98	S.G.
–	PRODUCTION RELEASE	9.19.00	S.G.
A	REVISED PER ECO 1772	7.01.04	S.G.

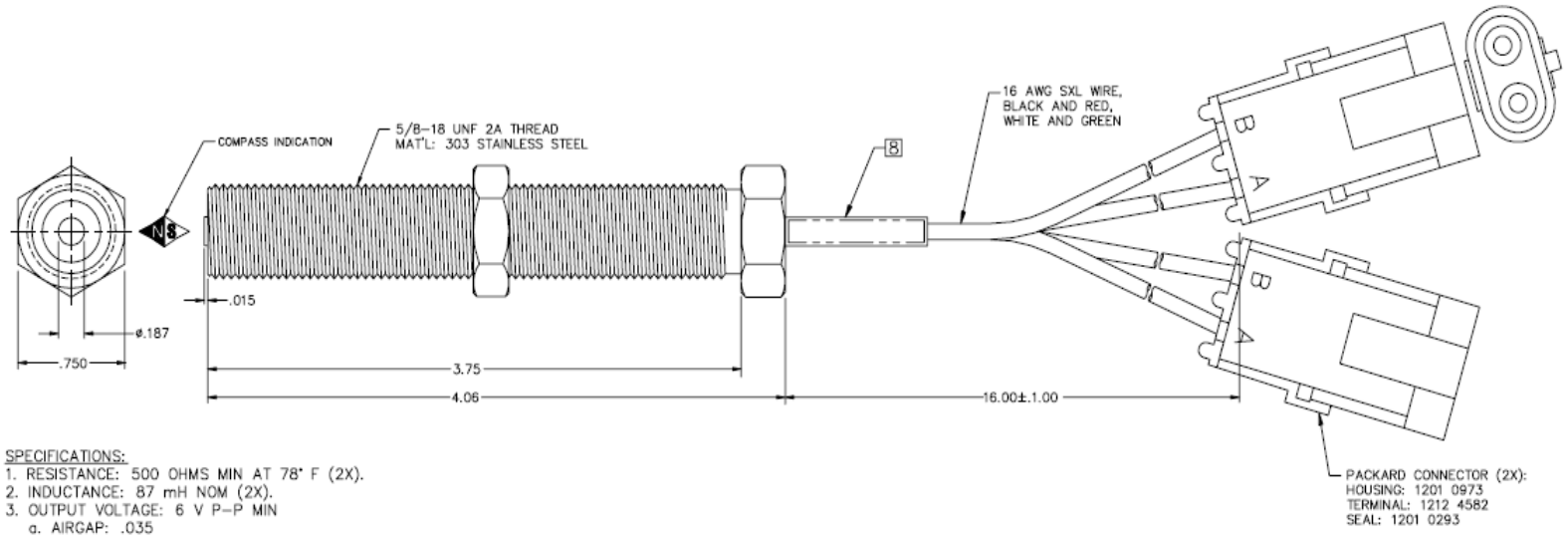

SPECIFICATIONS:

1. RESISTANCE: 500 OHMS MIN AT 78° F (2X).
2. INDUCTANCE: 87 mH NOM (2X).
3. OUTPUT VOLTAGE: 6 V P–P MIN
   a. AIRGAP: .035
   b. TEST WHEEL: 8 PITCH GEAR
   c. SURFACE SPEED: 200 I.P.S.
   d. LOAD: NONE.
4. POLARITY: WHITE AND RED LEADS ("A") NEGATIVE WITH RESPECT TO BLACK AND GREEN LEADS ("B") WITH THE APPROACH OF A FERROUS TARGET.
5. TEMPERATURE RANGE: –65° F TO 225° F (OPERATING).
   –100° F TO 225° F (STORAGE).
6. HIGH POT: 500V ±15V RMS MIN. LEAD WIRES TO CASE.
7. LEAD WIRES MUST EACH WITHSTAND A 2 LB PULL TEST.
8. MARK SHRINK TUBING "CUSTOMER P/N & REV. LETTER", "MSC P/N & REV. LETTER" AND DATE CODE (MM–YYYY)" WITH BLACK INK AND COVER LABEL WITH CLEAR SHRINK TUBING.

NEXT ASSY	USED ON
APPLICATION	

UNLESS OTHERWISE SPECIFIED DIMENSIONS ARE IN INCHES
TOLERANCES ARE:
FRACTIONS: DECIMALS: ANGLES:
± 1/64 .XX ± .01 ± 1/2°
.XXX ± .005

MATERIAL

FINISH

DO NOT SCALE DRAWING

CONTRACT NO.

APPROVALS	DATE
DRAWN A.P.W.	1.21.98
CHECKED S.G.	1.21.98
APPRVD S.G.	1.21.98

MAGNETIC SENSORS CORPORATION
1365 N. McCAN STREET
ANAHEIM, CA 92806

V.R. SPEED SENSOR

SIZE	CODE INDENT	DRAWING NO.
B	0LVP6	403001–20

SCALE: NONE | SK10626 | SHEET 1 OF 1

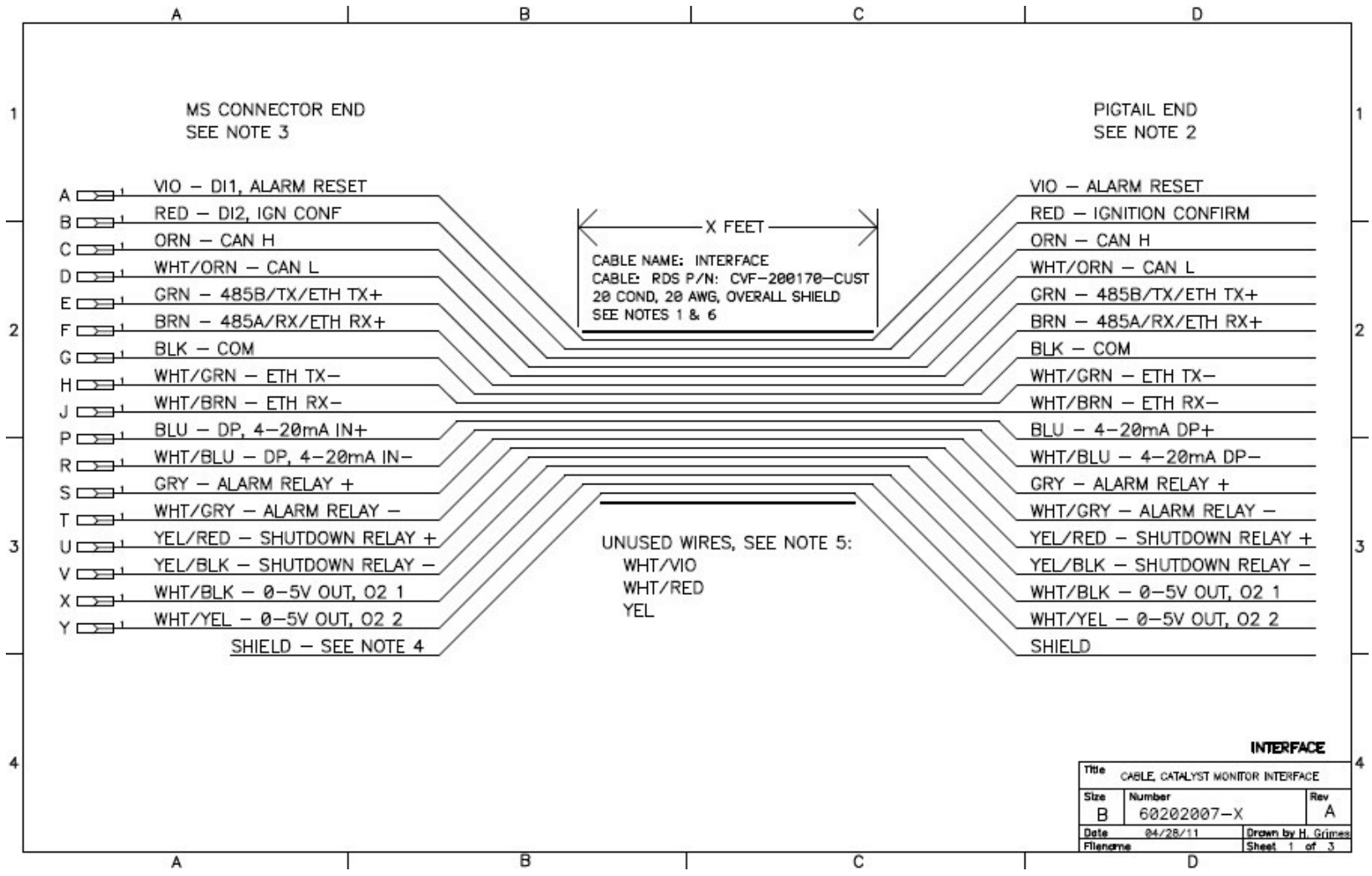
MS CONNECTOR END
SEE NOTE 3
PIGTAIL END
SEE NOTE 2
A VIO – DI1, ALARM RESET
B RED – DI2, IGN CONF
C ORN – CAN H
D WHT/ORN – CAN L
E GRN – 485B/TX/ETH TX+
F BRN – 485A/RX/ETH RX+
G BLK – COM
H WHT/GRN – ETH TX–
J WHT/BRN – ETH RX–
P BLU – DP, 4–20mA IN+
R WHT/BLU – DP, 4–20mA IN–
S GRY – ALARM RELAY +
T WHT/GRY – ALARM RELAY –
U YEL/RED – SHUTDOWN RELAY +
V YEL/BLK – SHUTDOWN RELAY –
X WHT/BLK – 0–5V OUT, O2 1
Y WHT/YEL – 0–5V OUT, O2 2
SHIELD – SEE NOTE 4
X FEET
CABLE NAME: INTERFACE
CABLE: RDS P/N: CVF–200170–CUST
20 COND, 20 AWG, OVERALL SHIELD
SEE NOTES 1 & 6
UNUSED WIRES, SEE NOTE 5:
WHT/VIO
WHT/RED
YEL
VIO – ALARM RESET
RED – IGNITION CONFIRM
ORN – CAN H
WHT/ORN – CAN L
GRN – 485B/TX/ETH TX+
BRN – 485A/RX/ETH RX+
BLK – COM
WHT/GRN – ETH TX–
WHT/BRN – ETH RX–
BLU – 4–20mA DP+
WHT/BLU – 4–20mA DP–
GRY – ALARM RELAY +
WHT/GRY – ALARM RELAY –
YEL/RED – SHUTDOWN RELAY +
YEL/BLK – SHUTDOWN RELAY –
WHT/BLK – 0–5V OUT, O2 1
WHT/YEL – 0–5V OUT, O2 2
SHIELD
INTERFACE
Title CABLE, CATALYST MONITOR INTERFACE
Size B
Number 60202007–X
Rev A
Date 04/28/11
Drawn by H. Grimes
Filename
Sheet 1 of 3

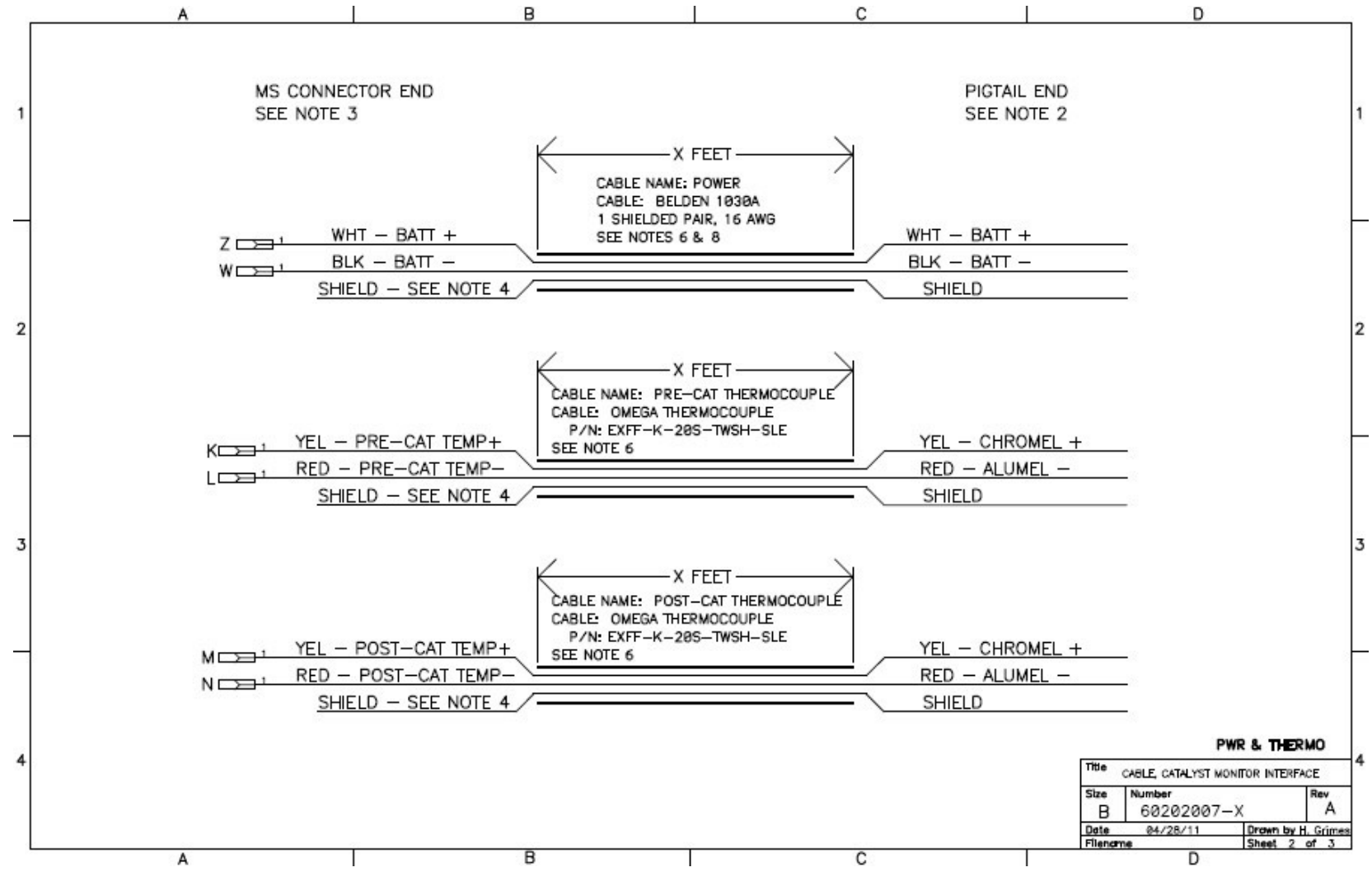
MS CONNECTOR END
SEE NOTE 3
PIGTAIL END
SEE NOTE 2
X FEET
CABLE NAME: POWER
CABLE: BELDEN 1030A
1 SHIELDED PAIR, 16 AWG
SEE NOTES 6 & 8
Z
W
WHT – BATT +
BLK – BATT –
SHIELD – SEE NOTE 4
WHT – BATT +
BLK – BATT –
SHIELD
X FEET
CABLE NAME: PRE–CAT THERMOCOUPLE
CABLE: OMEGA THERMOCOUPLE
P/N: EXFF–K–20S–TWSH–SLE
SEE NOTE 6
K
L
YEL – PRE–CAT TEMP+
RED – PRE–CAT TEMP–
SHIELD – SEE NOTE 4
YEL – CHROMEL +
RED – ALUMEL –
SHIELD
X FEET
CABLE NAME: POST–CAT THERMOCOUPLE
CABLE: OMEGA THERMOCOUPLE
P/N: EXFF–K–20S–TWSH–SLE
SEE NOTE 6
M
N
YEL – POST–CAT TEMP+
RED – POST–CAT TEMP–
SHIELD – SEE NOTE 4
YEL – CHROMEL +
RED – ALUMEL –
SHIELD
PWR & THERMO
Title
CABLE, CATALYST MONITOR INTERFACE
Size
B
Number
60202007–X
Rev
A
Date
04/28/11
Drawn by H. Grimes
Filename
Sheet 2 of 3

DCL INTERNATIONAL RESERVES THE RIGHT TO REVISE THE INTERNAL DESIGN WITHOUT NOTICE

PRELIMINARY /CONCEPT DRAWING

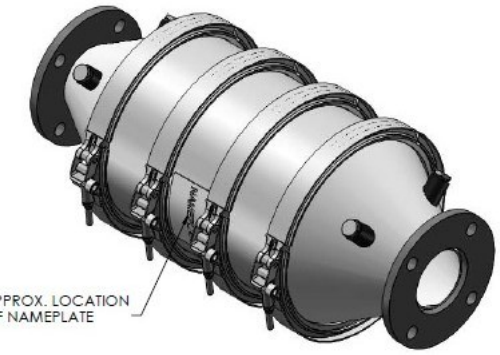

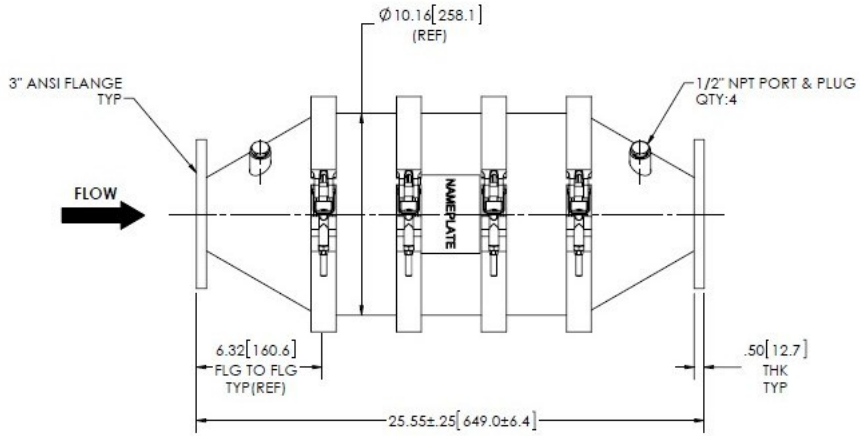

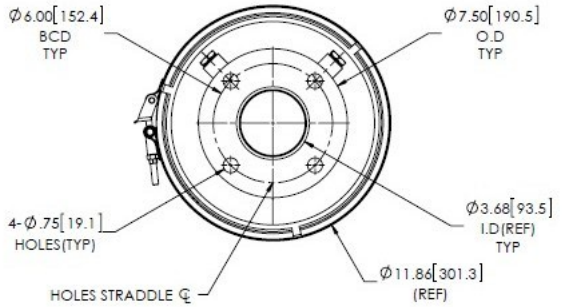

TOTAL WEIGHT: AROUND ~75 LBS

NO	REVISION	DRAWN BY	DATE	CHK'D BY
0	INITIAL RELEASE	MY	11/04/25	Michael

DCL International Inc.

UNLESS OTHERWISE NOTED
1. REMOVE ALL BURRS AND SHARP EDGES
2. DIMENSIONS ARE IN INCHES
3. [ ] DIMENSIONS ARE IN MILLIMETRE
TOLERANCES
X ±.2 [±5
.XX ±.10 [.X] ±2.5
.XXX ±.060 [.XX] ±1.50
ANGULAR TOLERANCE ±2°
THIRD ANGLE PROJECTION

TITLE:		ORIG. P/N:
DC12-3 CATALYST ASM		
APPLICATION:		ENGINE:
DATE: 11/04/25	DRAWN BY: MY	CHECKED BY:
PAPER SIZE:	SCALE: 1:5	FILE NAME: DC12-3_110525

PART NO.: DC12-3_110525

EO-5027

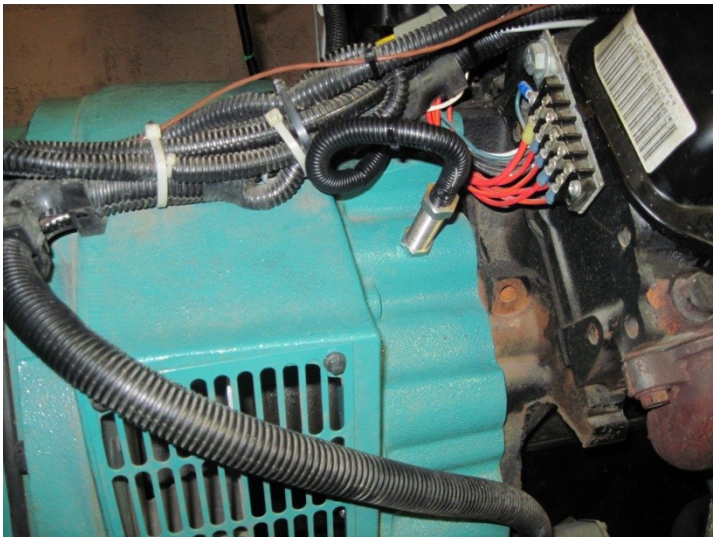

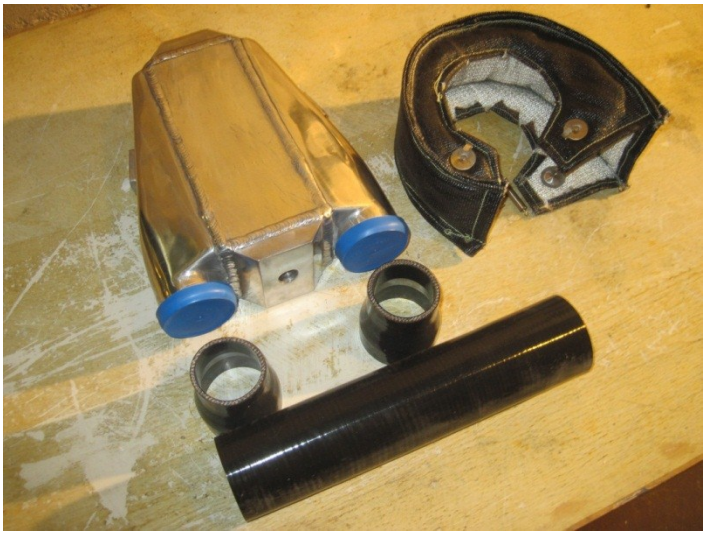

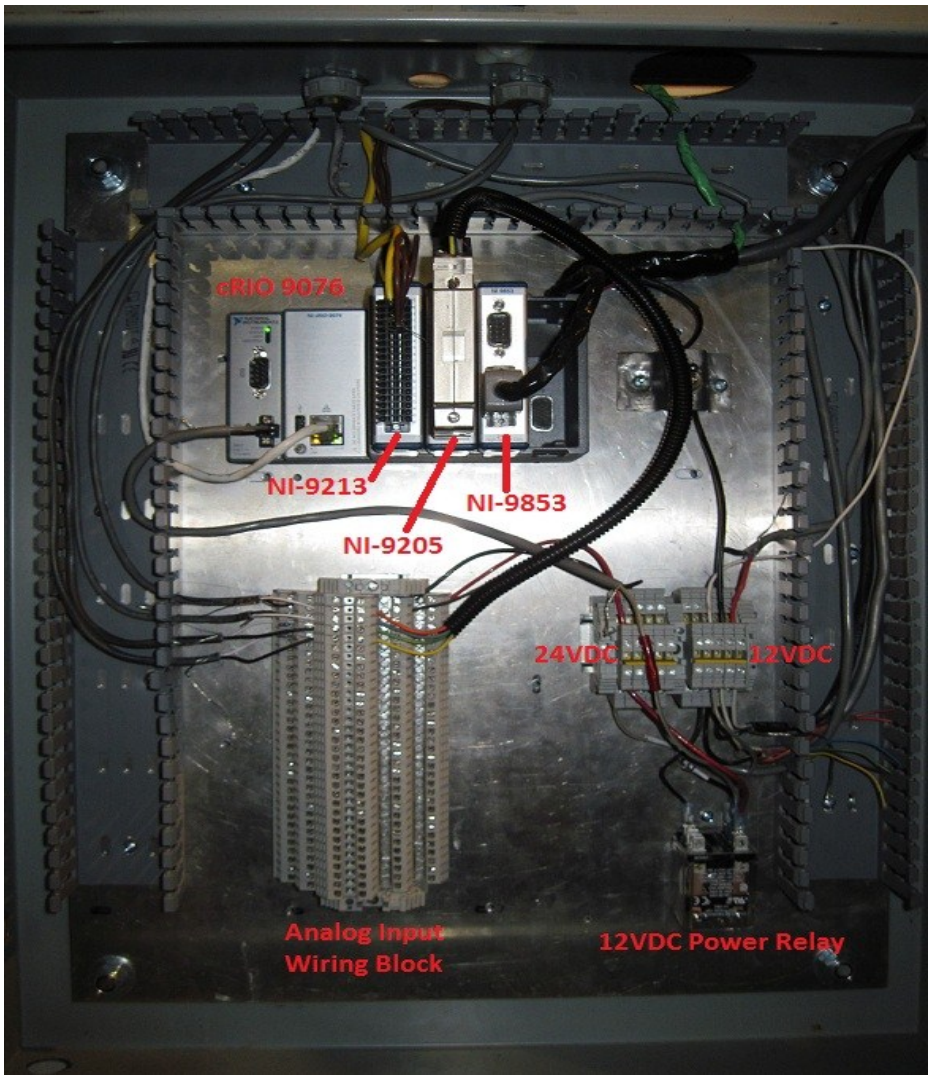
cRIO 9076
NI-9213
NI-9205
NI-9853
24VDC
12VDC
Analog Input
Wiring Block
12VDC Power Relay

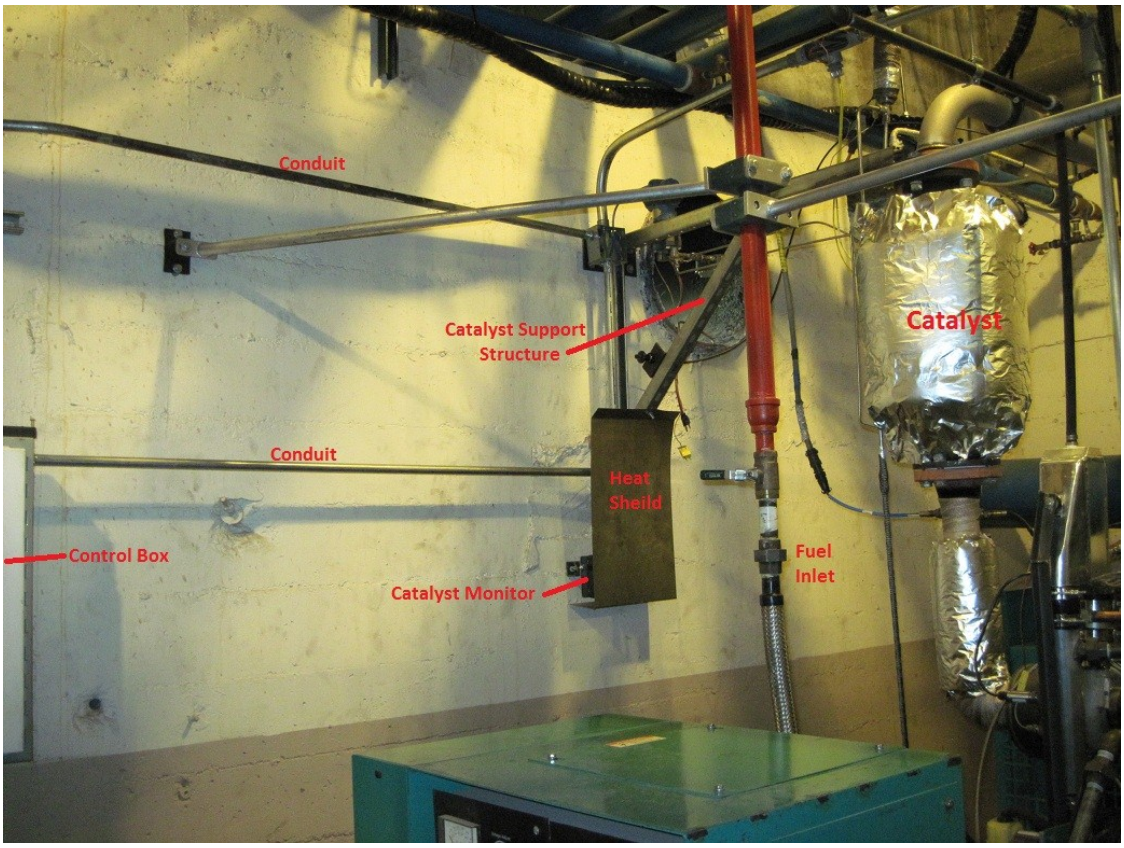
Conduit
Catalyst Support Structure
Catalyst
Conduit
Heat Sheild
Control Box
Fuel Inlet
Catalyst Monitor

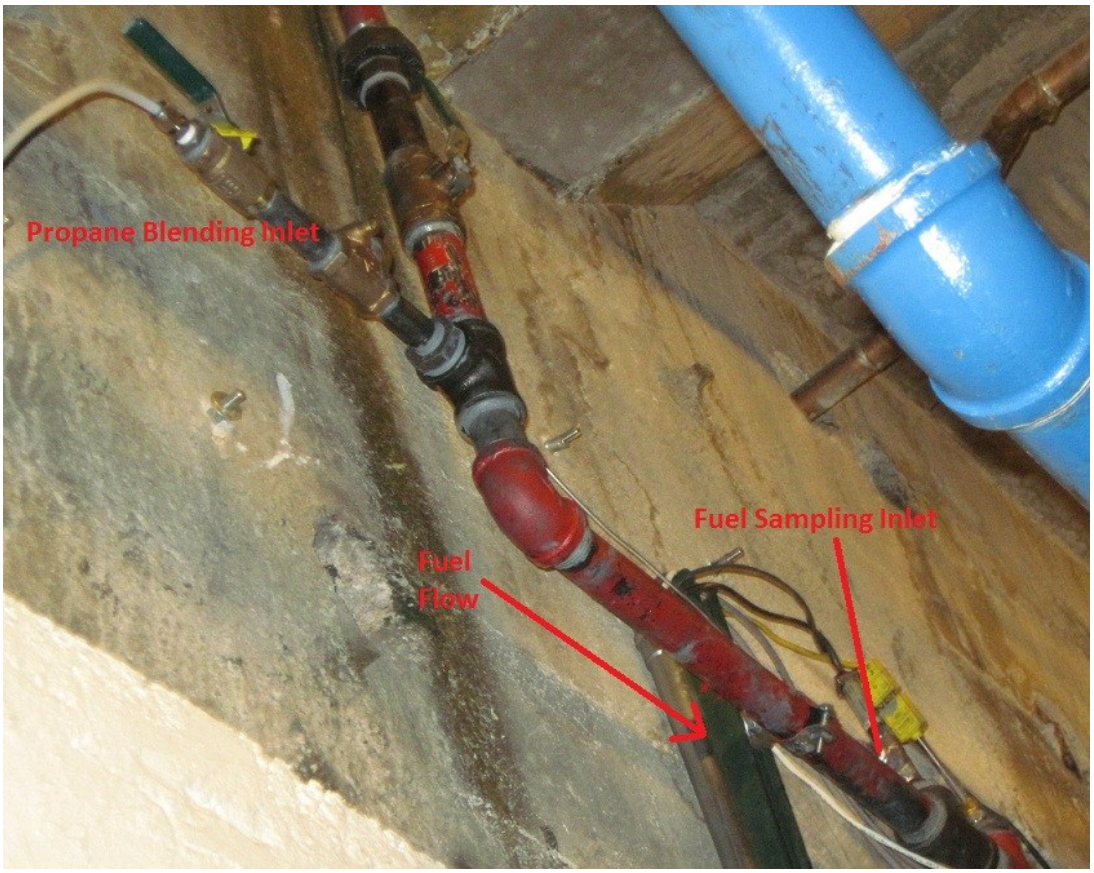
Propane Blending Inlet
Fuel Sampling Inlet
Fuel
Flow

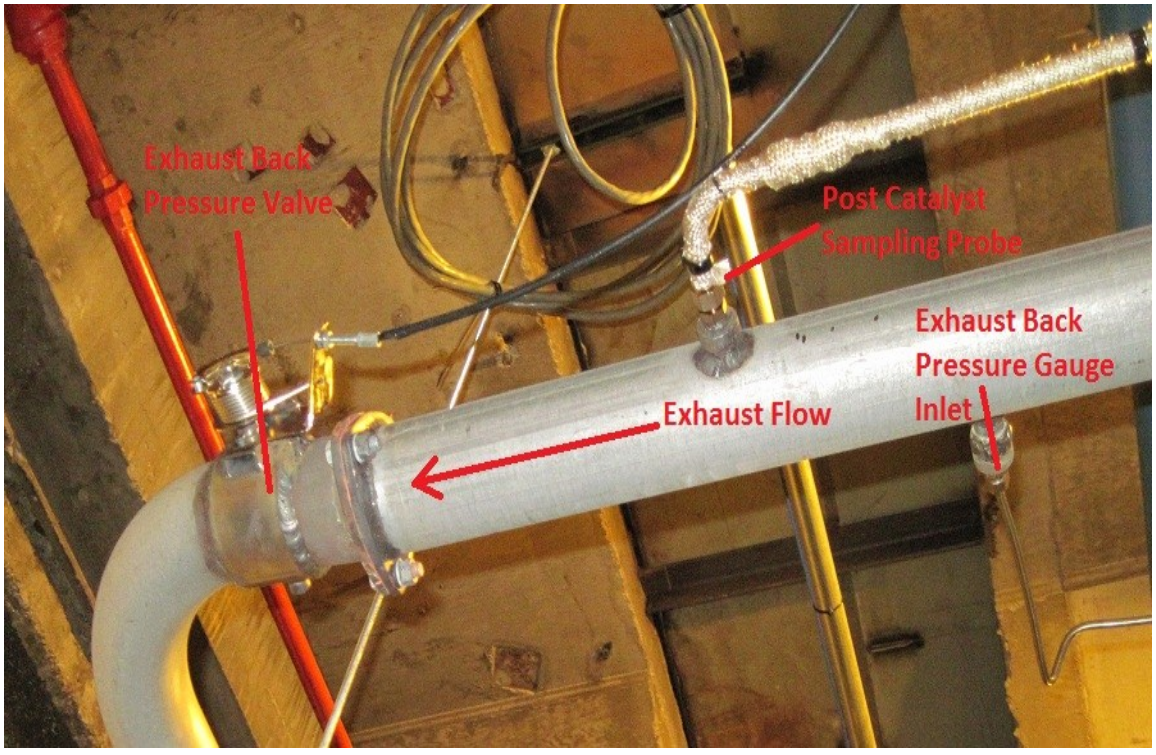
Exhaust Back
Pressure Valve
Post Catalyst
Sampling Probe
Exhaust Back
Pressure Gauge
Inlet
Exhaust Flow

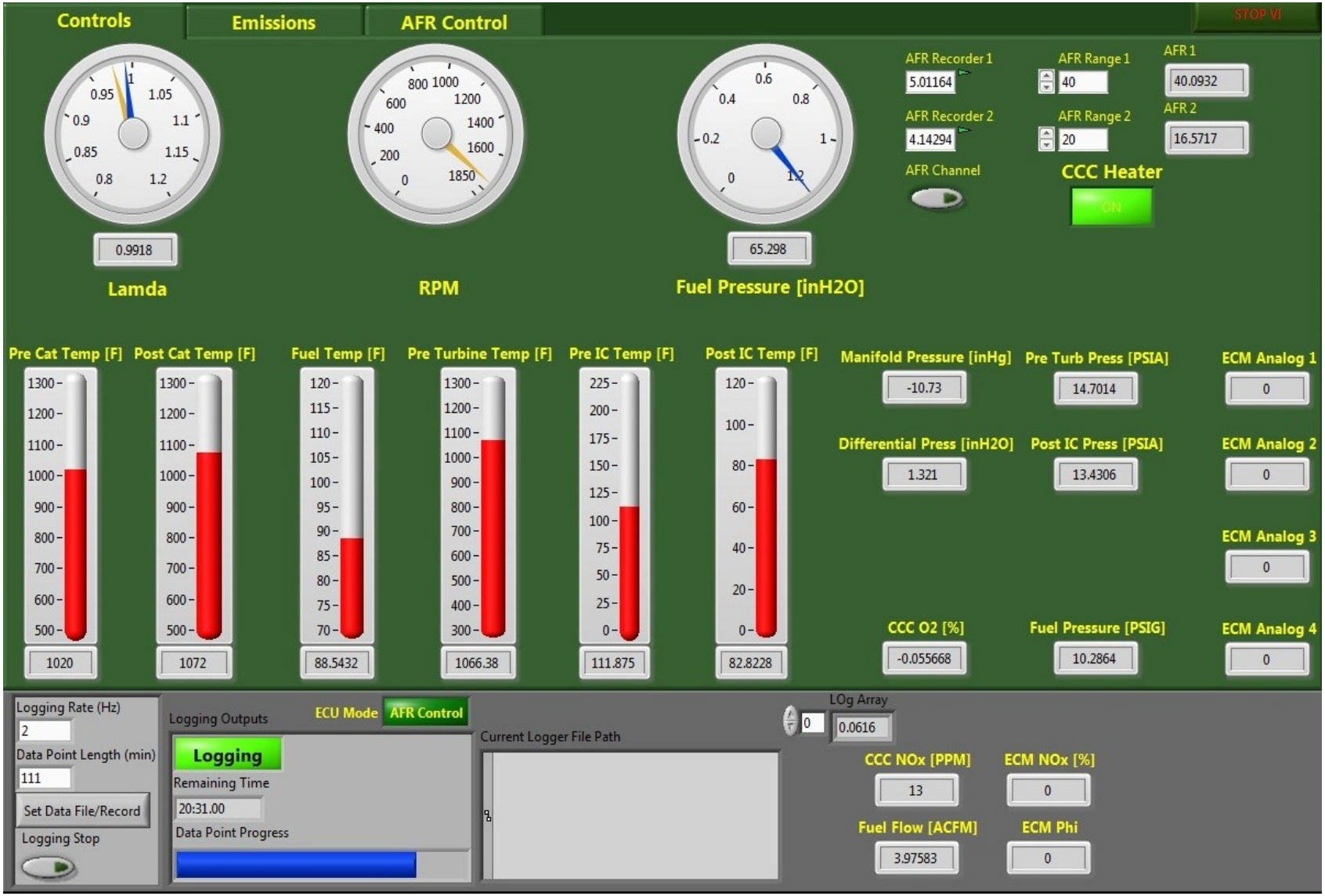
Controls
Emissions
AFR Control
STOP VI
0.9918
Lamda
RPM
65.298
Fuel Pressure [inH2O]
AFR Recorder 1
5.01164
AFR Range 1
40
AFR 1
40.0932
AFR Recorder 2
4.14294
AFR Range 2
20
AFR 2
16.5717
AFR Channel
CCC Heater
ON
Pre Cat Temp [F]
Post Cat Temp [F]
Fuel Temp [F]
Pre Turbine Temp [F]
Pre IC Temp [F]
Post IC Temp [F]
1020
1072
88.5432
1066.38
111.875
82.8228
Manifold Pressure [inHg]
-10.73
Pre Turb Press [PSIA]
14.7014
ECM Analog 1
0
Differential Press [inH2O]
1.321
Post IC Press [PSIA]
13.4306
ECM Analog 2
0
ECM Analog 3
0
CCC O2 [%]
-0.055668
Fuel Pressure [PSIG]
10.2864
ECM Analog 4
0
Logging Rate (Hz)
2
Data Point Length (min)
111
Set Data File/Record
Logging Stop
Logging Outputs
ECU Mode
AFR Control
Logging
Remaining Time
20:31.00
Data Point Progress
Current Logger File Path
LOg Array
0
0.0616
CCC NOx [PPM]
13
ECM NOx [%]
0
Fuel Flow [ACFM]
3.97583
ECM Phi
0


Controls
Emissions
AFR Control
STOP VI
NOx
CO2
CO
NO
0
NO2
0
NOx
0
RT Value
0.76
Range #
4
Range Limit
2000
RT Mode
NOx
Over-range
Auto-Range
OFF
CO2 %
11.98
Range #
4
Range Limit
20
Auto-Range
Over-Range
CO ppm
16
Range #
3
Range Limit
2000
Auto-Range
OFF
Over-Range
THC
THC ppm
67.88
Range #
3
Range Limit
2000
Auto-Range
OFF
Over-Range
O2 Raw
0.0533091
O2 Range
6
O2 Offset
0
CEMS O2 [%]
0.0639709
Emissions
PPM Emissiosn
% Emissiosns
Time
2031546
2032569
THC
NOx
O2
CO2
CO
Logging Rate (Hz)
2
Data Point Length (min)
111
Set Data File/Record
Logging Stop
Logging Outputs
ECU Mode
AFR Control
Logging
Remaining Time
21:11.50
Data Point Progress
Current Logger File Path
LOg Array
0
0.0609
CCC NOx [PPM]
7
ECM NOx [%]
0
Fuel Flow [ACFM]
3.89307
ECM Phi
0

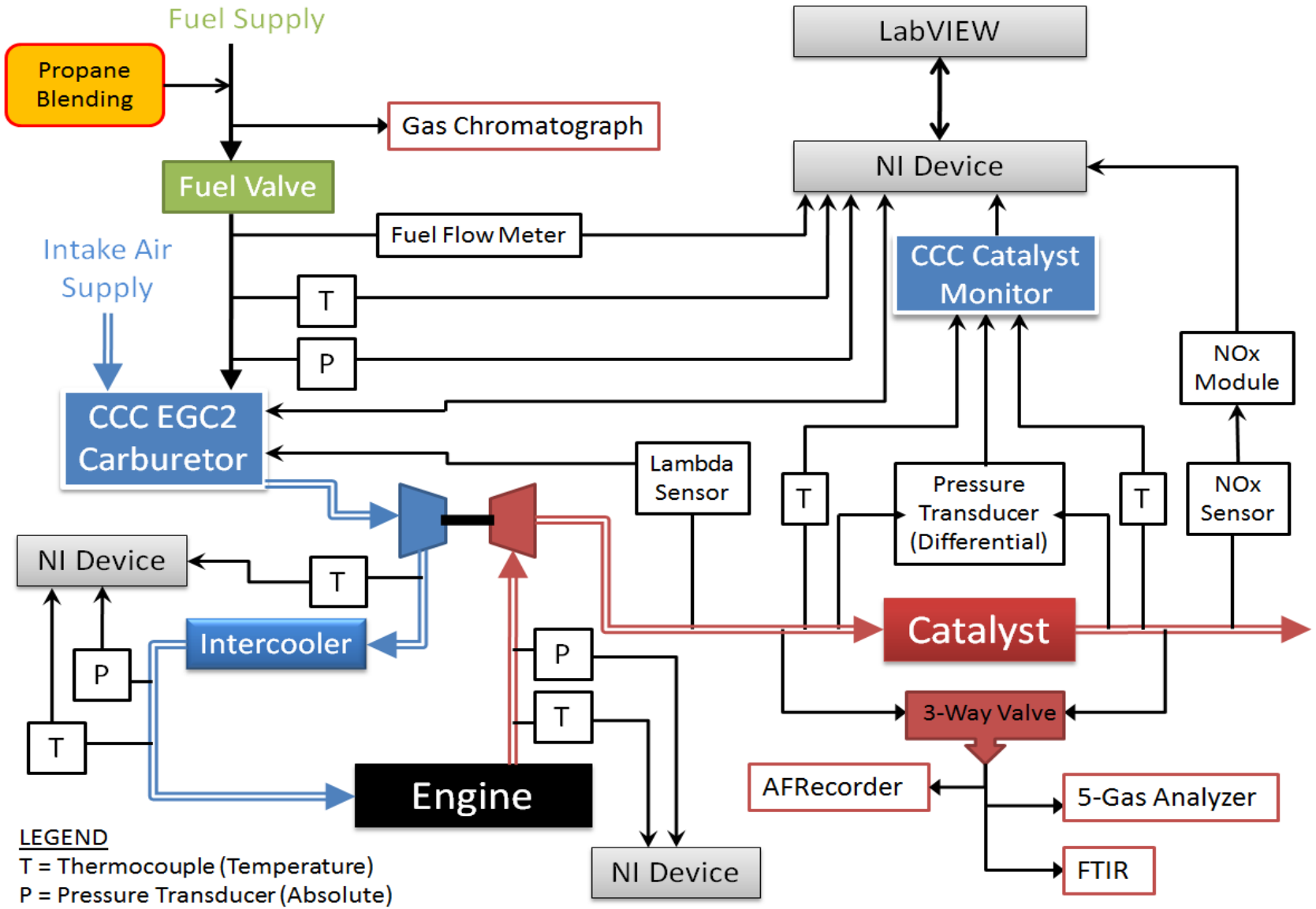
Fuel Supply
Propane Blending
Gas Chromatograph
Fuel Valve
Fuel Flow Meter
Intake Air Supply
T
P
CCC EGC2 Carburetor
Lambda Sensor
NI Device
T
Intercooler
P
T
Engine
P
T
NI Device
LabVIEW
NI Device
CCC Catalyst Monitor
NOx Module
T
Pressure Transducer (Differential)
T
NOx Sensor
Catalyst
3-Way Valve
AFRecorder
5-Gas Analyzer
FTIR
LEGEND
T = Thermocouple (Temperature)
P = Pressure Transducer (Absolute)

Appendix II– Baseline Testing

	Pre Catalyst (ppm)			
Equivalence Ratio	**NOx**	**CO**	**THC**	**VOC's**
1.008073484	2331.512	1211.24459	676.9895	75.8641
1.011153306	2208.057	1834.66389	721.0178	74.0769
1.012147031	2176.757	1986.27787	728.6063	74.3731
1.012742405	2171.387	2133.97504	728.923	78.3975
1.014033741	2073.592	2208.23627	767.7506	63.005
1.015065823	2071.622	2341.00666	774.7662	61.3765
1.0170312	2082.768	2481.64226	793.1145	61.2342
1.019535024	2144.034	2645.46589	753.7403	71.5277
1.020281244	2123.446	2792.45258	757.2829	72.7322
1.021162426	2083.181	2976.63062	761.1027	73.031
1.024807292	2039.449	3780.98003	779.8408	74.3437
1.027924549	1993.544	4827.6406	769.8697	82.8671
1.032067094	1933.68	5811.6173	787.5745	67.394
1.047483112	1413.015	8123.69218	794.1815	47.0432
1.06731942	1179.303	10107.1614	825.8722	64.307
1.096046405	839.7786	11323.401	868.9165	70.1659

	Post Catalyst (ppm)				
Equivalence Ratio	NOx	CO	THC	VOC's	Continental NOx Sensor
1.008073484	2307.942	2.32579035	288.39	16.3306	1817.55574
1.011153306	1149.216	6.75574043	61.49652	3.794	845.1797005
1.012147031	255.8864	2.97420965	7.058241	0	171.7054908
1.012742405	13.43616	5.26955075	3.003022	0	5.18968386
1.014033741	3.267171	15.1951747	35.55555	2.1179	1.590682196
1.015065823	2.141547	21.9410982	116.514	7.1738	1.818635607
1.0170312	1.365724	26.3116473	183.5578	10.3984	3.955074875
1.019535024	2.063428	15.5174709	265.2875	15.2748	3.227953411
1.020281244	1.515923	22.4222962	373.9967	17.2237	8.410981697
1.021162426	1.708769	38.4830283	460.3155	20.2851	24.27953411
1.024807292	1.64599	211.608486	705.9705	26.0046	96.57570715
1.027924549	3.061697	915.571048	793.185	40.9495	315.5424293
1.032067094	3.221498	1691.66556	796.8913	55.3748	586.3544093
1.047483112	2.580116	4205.79368	830.7073	73.1937	1043.787022
1.06731942	2.010849	7342.57737	832.1203	85.3651	928.4409318
1.096046405	1.393195	9894.0599	871.0928	109.7294	683.9134775

	Reduction Efficiency (%)			
Equivalence Ratio	NOx	CO	THC	VOC's
1.008073484	1.010934	99.8079834	57.40111	78.47388
1.011153306	47.95353	99.6317723	91.47087	94.8783
1.012147031	88.2446	99.8502622	99.03127	100
1.012742405	99.38122	99.7530641	99.58802	100
1.014033741	99.84244	99.3118864	95.36887	96.63852
1.015065823	99.89662	99.0627494	84.96139	88.31181
1.0170312	99.93443	98.9397486	76.85607	83.01864
1.019535024	99.90376	99.4134315	64.80385	78.64492
1.020281244	99.92861	99.1970393	50.61335	76.31902
1.021162426	99.91797	98.7071614	39.51992	72.22399
1.024807292	99.91929	94.4033429	9.472474	65.02111
1.027924549	99.84642	81.0348134	0	50.58413
1.032067094	99.8334	70.891656	0	17.83423
1.047483112	99.8174	48.2280522	0	0
1.06731942	99.82949	27.3527246	0	0
1.096046405	99.8341	12.6228957	0	0

	Reduction Efficiency (%)			
Load (%)	NOx	CO	VOC's	THC
20	56.99	99.90	99.31	55.81
40	99.17	99.90	100	99.76
60	99.86	99.78	99.61	99.36
80	99.92	99.13	99.8	97.92

Load (%)	Pre-Cat Temp (F)	Post-Cat Temp (F)
20	975	1003
40	1073	1104
60	1162	1193
80	1219	1248

	Reduction Efficiency (%)		
Load (%)	VOC's	CH2O	CH4
20	99.31	80.01	41.22
40	100	60.47	67.53
60	99.61	75.7	99.16
80	99.8	28.33	97.36

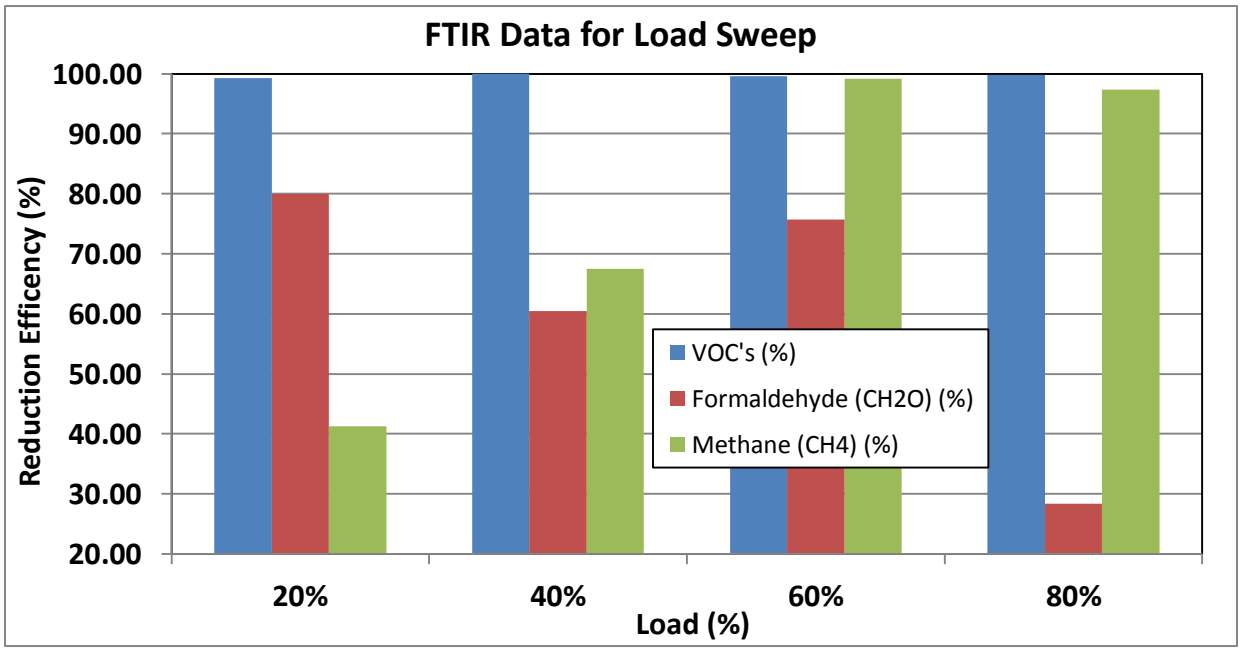

Combustion Stoichiometry						Analysis Date:		10/17/2011		A/Fstoic =	16.379097		0.948	Btu/kJ		
Fuel											MW of Elements					
Constit.	Raw %	Norm %	mol fract	mass fract	MW	MW*mol fr	C content	H content	O content	N content	C	12.011	LHV, kJ/kg	mf*LHV	Cp, kJ/kg-K	Cv, kJ/kg-K
CH4	89.83	90.19	0.901908	0.81685	16.0426	14.46894	0.901908	3.6076305	0	0	H	1.0079	50016	40855.56621	2.2537	1.7354
C2H6	6.99	7.02	0.070181	0.119137	30.0694	2.110292	0.140361	0.4210843	0	0	N	14.0067	47489	5657.715241	1.7662	1.4897
C3H8	0.82	0.82	0.00823	0.020496	44.0962	0.363041	0.024699	0.0658635	0	0	O	15.9994	46357	950.1156318	1.6794	1.4909
C4H10	0.11	0.11	0.00110	0.003624	58.123	0.064192	0.004418	0.0110442	0	0			45742	165.7684892	1.7164	1.5734
C5H12		0.00	0.00000	0	72.1498	0	0	0	0	0			45355	0	1.9764	1.88
C6H14		0.00	0.00000	0	86.1766	0	0	0	0	0			45105	0	1.6642	1.5489
CO		0.00	0.00000	0	28.0104	0	0	0	0	0			10100	0	1.0404	0.744
H2	0.08	0.08	0.00080	9.14E-05	2.0158	0.001619	0	0.0016064	0	0			120000	10.96894342	14.307	10.183
N2	0.48	0.48	0.004819	0.007622	28.0134	0.135004	0	0	0	0.009638554			0	0	1.039	0.743
O2	0	0.00	0	0	31.9988	0	0	0	0	0			0	0	0.918	0.658
CO2	1.29	1.30	0.012952	0.03218	44.0098	0.570006	0.012952	0	0.025904	0			0	0	0.846	0.657
H2O		0.00	0	0	18.0152	0	0	0	0	0			0	0	1.8723	1.4108
Sums-->	99.6	100	1	1		17.7131	1.084337	4.1072289	0.025904	0.009638554		LHV_fuel	47640.1345	kJ/kg	2.128446677	1.659035
												=	928.022561	Btu/SCF	Ave gamma=	1.283

MWave =	17.7131	rho =	0.724232	kg/m^3 =	0.020548	kg/ft^3

Following Ferguson and Kirkpatrick

All Constituents		Combustibles Only			All Constituents			Combustables	
					Urban and Sharp, 1994			Urban and Sharp, 1994	
α =	1.084337	α =	1.09077	H/C --->	y =	3.787777778	H/C --->	y =	3.833567613
β =	4.107229	β =	4.181539	O/C --->	z =	0.023888889	O/C --->	z =	0
γ =	0.025904	γ =	0	N/C --->	f =	0.008888889	N/C --->	f =	0
δ =	0.009639	δ =	0		A =	1.935		A =	1.958391903
a_s =	2.098193	a_s =	2.136155		A/Fs =	16.37909719		A/Fs =	17.05801178
A/F_s =	16.26686	A/F_s =	16.94114						

Mol fract sum Comb =	98.22289157

Appendix III– NSCR Control with NOx Sensor Feedback

	Pre Catalyst (ppm)		
Load (%)	**NOx**	**CO**	**THC**
20	878.19	3244.83	635.40
40	1597.42	2739.68	691.86
60	2049.38	2225.21	734.89
80	2434.96	2097.80	717.03

	Post Catalyst (ppm)			
Load (%)	**NOx**	**CO**	**THC**	**Continental NOx Sensor**
20	8.73	33.63	27.82	4.52
40	3.00	8.73	21.79	0.67
60	4.19	8.36	2.78	1.47
80	3.97	6.32	0.28	1.31

	Reduction Efficiency			
Load (%)	**NOx**	**CO**	**THC**	**VOC's**
20	99.01	98.96	95.62	97.59682888
40	99.81	99.68	96.85	98.78395769
60	99.80	99.62	99.62	100
80	99.84	99.70	99.96	100